



**HAL**  
open science

# Towards an Energy Planning Strategy for Autonomous Driving of an Over-actuated Road Vehicle

Ismail Bensekrane

► **To cite this version:**

Ismail Bensekrane. Towards an Energy Planning Strategy for Autonomous Driving of an Over-actuated Road Vehicle. Automatic. Université de Lille, 2019. English. NNT: . tel-04465263

**HAL Id: tel-04465263**

**<https://hal.science/tel-04465263>**

Submitted on 19 Feb 2024

**HAL** is a multi-disciplinary open access archive for the deposit and dissemination of scientific research documents, whether they are published or not. The documents may come from teaching and research institutions in France or abroad, or from public or private research centers.

L'archive ouverte pluridisciplinaire **HAL**, est destinée au dépôt et à la diffusion de documents scientifiques de niveau recherche, publiés ou non, émanant des établissements d'enseignement et de recherche français ou étrangers, des laboratoires publics ou privés.

# Towards an Energy Planning Strategy for Autonomous Driving of an Over-actuated Road Vehicle

**PhD THESIS**

to obtain the title of

**Doctor from Université de Lille**

**Specialty : ROBOTICS**

Defended by

Ismail BENSEKRANE

prepared at

CRISTAL CNRS-UMR 9189

defended on July 11, 2019

at Polytech Lille

## **Jury**

<i>Reviewers :</i>	Pr. Sergey DRAKUNOV	- Embry-Riddle University, Florida (USA)
	Pr. Mohamed BENBOUZID	- University of Brest (France)
<i>Examiners :</i>	Pr. Eric KERRIGAN	- Imperial College London (UK)
	Dr. Veronique CEREZEO	- Ifsttar Centre of Nantes (France)
	Dr. Mohamed BOUTELDJA	- Cerema, Bron Site (France)
<i>Supervisor :</i>	Pr. Rochdi MERZOUKI	- University of Lille (France)

# Vers une Stratégie de Planification Energétique pour la Conduite Autonome d'un Véhicule Routier Sur-actionnée

## THÈSE

soumise à l'Université de Lille pour le degré de

## Doctorat

Spécialité : ROBOTIQUE

par

Ismail BENSEKRANE

préparée au laboratoire  
CRISTAL CNRS-UMR 9189

soutenue le 11 Juillet 2019  
à Polytech Lille

## Jury

<i>Reviewers :</i>	Pr. Sergey DRAKUNOV	- Embry-Riddle University, Florida (USA)
	Pr. Mohamed BENBOUZID	- Université de Brest (France)
<i>Examiners :</i>	Pr. Eric KERRIGAN	- Imperial College London (UK)
	Dr. Veronique CEREZEO	- Ifsttar Centre de Nantes (France)
	Dr. Mohamed BOUTELDJA	- Cerema, Site de Bron (France)
<i>Supervisor :</i>	Pr. Rochdi MERZOUKI	- Université de Lille (France)

---

# Towards an Energy Planning Strategy for Autonomous Driving of an Over-actuated Road Vehicle

## Abstract

In this thesis, an energy planning for over-actuated unmanned road vehicles (URVs) with redundant steering configurations is proposed. In fact, indicators on the road profile geometry, the redundancy of actuation, the optimal velocity profile and the driving modes are identified for each segment of the URV's trajectory. Thus, a power consumption estimation model of an over-actuated autonomous driving vehicle is developed. Two methods for power consumption modeling are considered. The first method is based on an analytic model of power consumption, taking into account the degree of steerability, the degree of mobility and the degree of actuation redundancy. The second method used for power consumption modeling is based on data-learning qualitative method, namely: Adaptive Neuro Fuzzy Inference System (ANFIS). The latter has been considered in case of the presence of unknown dynamic parameters of the URV and uncertainties of interaction with the environment. Validation of the estimation of the power consumption has been applied on a real autonomous vehicle called RobuCar. Energy planning strategy has been built using two approaches, discrete and continuous. The discrete approach depends on the construction of an energy digraph with all feasible configurations taking into account kinematic and dynamic constraints based on a 3D grid map setup, according to the velocity, the arc-length, and the driving mode. In this weighted directed graph, the edges describe the consumed energy by the URV along a segment of a trajectory. An optimization algorithm is applied on the digraph to get a global optimal solution combining the driving mode, the power consumption and the velocity profile of the URV. The continuous approach is based on a multi-criteria optimization strategy using genetic algorithms (NSGA-II). Then a real road path is considered and modelled by using two smooth geometrical combinations: the first one uses lines, clothoids and arcs, and the second one uses lines and Pythagorean Hodograph (PH) curves. The energy planning strategy is then applied to the generated paths. Also, a directed graph is built to synthesis the optimal velocity profile that minimizes the overall energy consumption while accounting for all driving modes. Results are compared with those given by the dynamic programming method for global offline optimization.

**Keywords:** Energy Planning, Power consumption, Redundancy, Over-actuated, Autonomous driving.

---

# Vers une Stratégie de Planification Énergétique pour la Conduite Autonome d'un Véhicule Routier Sur-actionné

## Résumé

Dans cette thèse, une planification énergétique pour les véhicules routiers sans conducteur (URV), suractionnés avec une direction redondante est proposée. En effet, des indicateurs sur la géométrie de la route, la redondance des actionnements, le profil de la vitesse optimale et le mode de conduite sont identifiés pour chaque segment de la trajectoire de l'URV. Ainsi, un modèle d'estimation de la consommation d'énergie d'un URV sur-actionné est développé. Deux méthodes de modélisation de la consommation d'énergie sont considérées. La première méthode est basée sur un modèle analytique de consommation d'énergie prenant en compte le degré de steerabilité, le degré de mobilité et le degré de redondance dans l'actionnement. La deuxième méthode utilisée pour la modélisation de la consommation d'énergie repose sur la méthode qualitative d'apprentissage des données, à savoir: le système d'inférence neuro-floue adaptatif (ANFIS). Cette dernière a été considérée pour répondre à la présence des incertitudes paramétriques de l'URV et aux incertitudes sur son interaction avec l'environnement. La validation de l'estimation de la consommation énergétique a été appliquée à un véhicule autonome réel appelé RobuCar. La stratégie de la planification énergétique a été élaborée selon deux approches: discrète et continue. L'approche discrète repose sur la construction d'un digraphe d'énergie avec toutes les configurations possibles, tenant compte des contraintes cinématiques et dynamiques basées sur une grille 3D, selon: la vitesse, la longueur de l'arc, le mode de conduite. Dans ce graphe orienté et pondéré, les arêtes décrivent l'énergie consommée par l'URV le long d'un segment de la trajectoire. Un algorithme d'optimisation est appliqué sur le digraphe pour obtenir une solution globale optimale combinant le mode de conduite, la consommation électrique et le profil de vitesse de l'URV. L'approche continue repose sur une stratégie d'optimisation multicritères utilisant des algorithmes génétiques (NSGA-II). Ensuite, un chemin réel est considéré et modélisé, en utilisant deux types de courbes constituée d'un ensemble de géométries lisses: la première est lignes, clothoïdes et arcs, et la seconde regroupe des lignes et courbes de Hodograph de Pythagore. La stratégie de planification énergétique est ensuite appliquée aux chemins générés. En outre, un graph orienté est construit pour synthétiser le profil de vitesse optimale qui minimise la consommation énergétique globale tout en prenant en compte tous les modes de conduite. Les résultats sont comparés à ceux donnés par la méthode de programmation dynamique pour une optimisation globale hors ligne.

**Mots clés:** Panification énergétique, Consommation d'énergie, Redondance, Sur-actionné, Conduite autonome.

---

*This thesis is dedicated to my parents, Habib Bensekrane and Yamina Djaber, my wife, and my family for their love, endless support and encouragement.*

## Acknowledgments

Firstly, I would like to express my sincere gratitude to my supervisor Prof. Rochdi Merzouki for his continuous support for my Ph.D. study and related research, for his patience, motivation, and immense knowledge. His guidance helped me in all the time of research and writing of this thesis. I could not have imagined having a better advisor and mentor for my Ph.D. study.

Besides my advisor, I would like to thank the reviewers of my thesis Prof. Pr. Sergey Drakunov and Prof. Mohamed Benbouzid for their insightful comments and encouragement.

I would like to thank Prof. Taha Chettibi, Prof. Yacine Amara, and Prof. Abdelwahab Bazoula, at Ecole Polytechnic Militaire, Algeria for their suggestions and assistance to perform the present work.

A special thank to Pushpendra Kumar for his help and support, and for extended discussions on my research.

I thank my fellow labmates, Othman Lakhal, Abdelkader Belarouci, Vincent Coelen, Mahdi Ouzghala, Adel Termeche, Manarshhjet Singh, Achille Melingui for the stimulating discussions, working together before deadlines, coffee breaks, and for all the fun we have had in the last three years. I would also like to extend my thanks to the technicians of the laboratory, Michel Pollart and Olivier Scrive, their assistance with all types of technical problems.

Also, I thank my indian friends Devadas Bhat, Tanushree Kane, Himani Garg, Piyush Jain, Sepal Daliwale, and Shilpa Sonar. I enjoyed their company throughout my Ph.D. Many thanks to Inderjeet Singh for being with me as friend and labmate during all the time at Lille. These four years of togetherness show a great bond of friendship.

I also need to thank my wonderful friends from outside France, Ahmed Allam, Omar Meroufel, Benlefki Abderraouf, Amine Boustil, Billel Kellalib for their continuous support and long talks on the phone.

At last, my greatest thank is for my parents, my wife, and my family, for their love and encouragements during all the intense time of my studies and during my dissertation. They never forget to send me their love everyday. Without their support and their care, I would not have been able to perform this big workload and to succeed in my education.

# Contents

<b>List of Abbreviations</b>	<b>1</b>
<b>1 General Introduction</b>	<b>5</b>
1.1 Framework and context of the thesis . . . . .	5
1.2 General Introduction . . . . .	6
1.3 Thesis objective . . . . .	8
1.4 Problem Statement . . . . .	8
1.5 Contribution . . . . .	9
1.6 Disseminated Results . . . . .	11
1.7 Manuscript organization . . . . .	12
<b>2 Power Management of Autonomous Road Vehicles</b>	<b>13</b>
2.1 Introduction . . . . .	13
2.2 Kinematic Properties of Unmanned Road Vehicles (URVs) . . . . .	14
2.2.1 Degree of freedom . . . . .	16
2.2.2 Degree of mobility . . . . .	16
2.2.3 Degree of steerability . . . . .	17
2.2.4 Degree of manoeuverability . . . . .	17
2.2.5 Holonomy Constraint . . . . .	18
2.2.6 Omni-directional Property . . . . .	18
2.3 Power Consumption and Energy Management of URVs . . . . .	19
2.3.1 Energy Consumption of URVs: . . . . .	20
2.4 Optimal autonomous driving of URVs . . . . .	30
2.4.1 URV path planning problem . . . . .	30
2.4.2 Trajectory optimization problem of URVs . . . . .	33
2.4.3 URV routing problem . . . . .	36
2.4.4 URV task assignment problem . . . . .	37
2.4.5 URV energy planning . . . . .	43
2.5 Conclusion . . . . .	44
<b>3 Power Consumption Modeling for Over-actuated URVs</b>	<b>45</b>
3.1 Introduction . . . . .	45
3.2 Quantitative approach of power consumption modeling estimation . . . . .	46
3.3 Qualitative approach of power consumption modeling estimation . . . . .	51
3.3.1 ANFIS architecture . . . . .	51
3.3.2 Estimation of Power Consumption . . . . .	53
3.4 Road profile . . . . .	54
3.5 Experimental results and Model validation . . . . .	54
3.6 Conclusion . . . . .	64



<b>4</b>	<b>Discrete Approach of Energy Planning Methodology</b>	<b>65</b>
4.1	Introduction . . . . .	65
4.1.1	Main contributions . . . . .	66
4.1.2	Problem formulation . . . . .	66
4.2	Discrete Energy Planning for Autonomous Navigation of the URV . . . . .	67
4.2.1	Pre-Processing Phase: Power Consumption Estimation . . . . .	67
4.2.2	Optimization Phase: Energy planning . . . . .	68
4.3	Results and discussion . . . . .	73
4.4	Conclusion . . . . .	79
<b>5</b>	<b>Continuous Approach of Energy Planning Methodology</b>	<b>81</b>
5.1	Introduction . . . . .	81
5.1.1	Related Work . . . . .	82
5.1.2	Main contributions . . . . .	83
5.2	Path Smoothing . . . . .	85
5.2.1	Road Profile . . . . .	85
5.2.2	Method 1: . . . . .	86
5.2.3	Method 2: . . . . .	86
5.3	Energy Planning . . . . .	88
5.3.1	Vector of Objectives and constraints . . . . .	88
5.3.2	Energy optimization methodology . . . . .	89
5.4	Experimental data-based results with virtual point control for an indoor TOMR . . . . .	92
5.5	Robot Modeling . . . . .	92
5.6	Velocity planning using kinetic energy planning . . . . .	94
5.7	Virtual Point Following Methodology . . . . .	95
5.7.1	Energy Model of Robotino . . . . .	97
5.8	Experimental Results And discussion . . . . .	97
5.8.1	Description of holonomic robot Robotino . . . . .	97
5.8.2	Constant kinetic energy approach . . . . .	97
5.8.3	Multi-criteria optimization . . . . .	98
5.9	Experimental data-based results for an outdoor over-actuated URV . . . . .	100
5.10	Conclusion . . . . .	110
<b>6</b>	<b>Conclusion and Prospective</b>	<b>113</b>
6.1	Summary of Conclusions . . . . .	113
6.2	Future works . . . . .	115
<b>A</b>	<b>Experimental Validation</b>	<b>117</b>
A.1	SCANeR <sup>TM</sup> Studio . . . . .	117
A.1.1	Massive simulation . . . . .	119
A.1.2	Vehicle Dynamics . . . . .	120
A.2	RobuCAR Motor Characterization . . . . .	120
A.2.1	Technical specifications . . . . .	121

---

A.2.2 Test bench for motor characterization . . . . .	121
<b>Bibliography</b>	<b>127</b>

# List of Figures

1.1	Organization of the works developed within the group MOCIS . . . . .	6
1.2	Different driving modes (steering configurations) of one considered UAV with $m = 6$ . . . . .	10
2.1	Configuration of Fixed Standard Wheel . . . . .	15
2.2	Configuration of Steered Standard Wheel . . . . .	15
2.3	Configuration of Castor Wheel . . . . .	16
2.4	Configuration of Swedish Wheel . . . . .	17
2.5	Energy Utilization for URVs [Xiao 2014] . . . . .	21
2.6	Steering type of Vehicle [Jazar 2017] . . . . .	22
2.7	Power Vs Radius Bars . . . . .	23
2.8	Sensors in URV [Takeda 2011] . . . . .	23
2.9	Influence of Different URV Parameters on Total Required Battery Energy to Accomplish a 2km Traverse [Hou 2019]. . . . .	24
2.10	Percentage of Power Consumption for URVs [Hou 2019]. . . . .	25
2.11	Nomad URV. . . . .	25
2.12	Nomad URV Configurations. [Shamah 1999] . . . . .	26
2.13	Power consumption for Nomad Vehicle [Shamah 1999] . . . . .	27
2.14	Khepera robot [Parasuraman 2014] . . . . .	27
2.15	Tracked vehicles . . . . .	28
2.16	Wheeled mobile robots . . . . .	28
2.17	GIATAMX10RC URV with multiple configurations [Maclaurin 2008] . . . . .	29
2.18	RomoRobot URV [Brembeck 2012] . . . . .	30
2.19	Optimal Autonomous Driving . . . . .	31
2.20	Family Tree of Path Planning Methods . . . . .	32
2.21	Components Of Optimal Control . . . . .	34
2.22	MRTA schemes . . . . .	37
2.23	Optimization Techniques . . . . .	39
2.24	All EMS [Zhang 2015] . . . . .	41
3.1	URV schematic diagram in Dual configuration . . . . .	46
3.2	ANFIS architecture. . . . .	52
3.3	Flowchart for the estimation of the power consumption. . . . .	54
3.4	Trajectory from the Campus of University of Lille . . . . .	55
3.5	Curvature of the trajectory . . . . .	56
3.6	RobuCAR . . . . .	56
3.7	Comparison between SCANeR model and Experimental path with curvature profile for Dual4 driving mode. . . . .	57
3.8	Comparison between experimental and simulated angular velocities for each wheel. . . . .	57

3.9	Comparison between experimental and simulated longitudinal acceleration for each wheel. . . . .	58
3.10	Comparison between experimental and simulated steering angles for each wheel. . . . .	58
3.11	Comparison between experimental and simulated lateral acceleration for each wheel. . . . .	59
3.12	Comparison between (a) battery voltage, (b) battery current, and (c) Power consumption of Real Vehicle and simulated model in SCANeR™	60
3.13	Comparison of the power consumption of URV using ANFIS and experiment with (a) Skid4 and (b) Skid2 configurations. . . . .	61
3.14	Comparison of the power consumption of URV using ANFIS and experiment with (a) Single4 and (b) Single2 configurations. . . . .	62
3.15	Comparison of the power consumption of URV using ANFIS and experiment with (a) Dual4 and (b) Dual2 configurations. . . . .	63
4.1	methodology for URV energy planning. . . . .	68
4.2	Energy planning schema. . . . .	70
4.3	Real and filtered curvature. . . . .	70
4.4	Real and filtered trajectory. . . . .	71
4.5	Energy digraph in 3D grid. . . . .	71
4.6	Driving pattern during sampling intervals. . . . .	72
4.7	Optimal velocity profile for the campus trajectory ( $t < 40min$ ). . . . .	74
4.8	Optimal mode distribution for the campus trajectory ( $t < 40min$ ) (zoom in at sharp turn). . . . .	74
4.9	Percentage of modes use before correction in campus trajectory with traveling time ( $t < 40min$ ). . . . .	75
4.10	Percentage of modes use after correction in campus trajectory with traveling time ( $t < 40min$ ). . . . .	75
4.11	Post-processing with correction in mode distribution at sharp turn. . . . .	76
4.12	Optimal velocity profile for campus trajectory with traveling time ( $t < 30min$ ). . . . .	76
4.13	Optimal driving modes for campus trajectory with traveling time ( $t < 30min$ ). . . . .	77
4.14	Optimal velocity profile and for campus trajectory with traveling time ( $t < 20min$ ). . . . .	77
4.15	Optimal driving modes for campus trajectory with traveling time ( $t < 20min$ ). . . . .	78
5.1	Different driving modes of RobuCAR . . . . .	83
5.2	The proposed methodology for power consumption estimation and energy planning. . . . .	84
5.3	Campus trajectory of the University of Lille . . . . .	85
5.4	The filtered and real curvature . . . . .	85
5.5	Basic conditions to generate a PH curve . . . . .	87

5.6	The filtered and real curvature . . . . .	87
5.7	Energy optimization methodology. . . . .	89
5.8	Generation of Pareto Fronts of velocity profiles . . . . .	90
5.9	Generation of motion profile candidate . . . . .	90
5.11	Example for superposition of velocity profiles . . . . .	91
5.10	Selection of objective point from Pareto front . . . . .	91
5.12	Example of digraph . . . . .	92
5.13	Three-wheeled omnidirectional mobile robot structure . . . . .	93
5.14	Robotino3 mobile robot . . . . .	98
5.15	Experimental environment . . . . .	98
5.16	Comparison of Robotino path with reference path . . . . .	99
5.17	Comparison of power consumption of Robotino with estimated model . . . . .	99
5.18	Comparison of Robotino velocity with reference velocity . . . . .	100
5.19	Comparison of Robotino path with the reference path . . . . .	100
5.20	Comparison of power consumption of Robotino with the estimated model . . . . .	101
5.21	Comparison of Robotino velocity with the reference velocity . . . . .	101
5.22	Pareto front for method 1 smoothing for Dual2. . . . .	102
5.23	Pareto front for method 1 smoothing for Dual4. . . . .	103
5.24	Pareto front for method 1 smoothing for Single2. . . . .	103
5.25	Pareto front for method 1 smoothing for Single4. . . . .	104
5.26	Pareto front for method 2 smoothing for Dual2. . . . .	104
5.27	Pareto front for method 2 smoothing for Dual4. . . . .	105
5.28	Pareto front for method 2 smoothing for Single2. . . . .	105
5.29	Pareto front for method 2 smoothing for Single4. . . . .	106
5.30	Superposition of optimal velocity profiles for different driving modes with smoothing Method 1. . . . .	106
5.31	Superposition of optimal velocity profiles for different driving modes with smoothing Method 2. . . . .	107
5.32	Optimal velocity profile and optimal distribution of driving modes for Method 1. . . . .	107
5.33	Optimal velocity profile and optimal distribution of driving modes for Method 2. . . . .	108
5.34	Optimal velocity profile and optimal distribution of driving modes for discrete DP method presented in [Bensekrane 2018]. . . . .	108
5.35	Comparison of Experimental and ANFIS power consumption for optimal distribution of driving modes for Method 1. . . . .	109
5.36	Comparison of Experimental and ANFIS power consumption for optimal distribution of driving modes for Method 2. . . . .	110
A.1	Simulation of RobuCAR in Campus of Lille University . . . . .	118
A.2	Environment modeling and vehicle sensing . . . . .	118
A.3	Different lighting for driving . . . . .	119
A.4	CALLAS & PROSPER for vehicle dynamics . . . . .	120

A.5 RobuCAR motor on the test bench . . . . .	122
A.6 Load variation test bench . . . . .	122
A.7 Acquisition setup for the motor characterization . . . . .	122
A.8 Map efficiency with free load . . . . .	123
A.9 Map efficiency with 10% load . . . . .	123
A.10 Map efficiency with 20% load . . . . .	124
A.11 Map efficiency with 30% load . . . . .	124
A.12 Map efficiency with 40% load . . . . .	125
A.13 Map efficiency with 50% load . . . . .	125

# List of Tables

1.1	Parameters describing URV driving configurations for $m = 6$ . . . . .	10
3.1	Mean errors in power estimation . . . . .	64
4.1	Constraints of driving mode for each type of road segment. . . . .	70
4.2	Comparison of energy consumption with traveling time ( $t < 40min$ ) . . . . .	78
4.3	Time consumed for the different steps in the algorithm ( $t < 40min$ ) . . . . .	79
5.1	Parameters describing driving modes of RobuCAR . . . . .	84
5.2	Comparison of energy consumption . . . . .	109
5.3	Comparison of energy consumption . . . . .	110

# List of Abbreviations

A-PMP	approximate Pontryagin's Minimum Principle
ADEA	Adaptive Differential Evolution Algorithm
ANFIS	Adaptive Neuro-Fuzzy Inference System
BA	Bees Algorithm
CA	Control Allocation
CRISAL	Centre de Recherche en Informatique, Signal et Automatique de Lille
CVRP	Capacited Vehicle Routing Problem
DDP	Deterministic Dynamic Programming
DOF	Degree of Freedom
DOM	Degree of Mobility
DOMS	Degree of Maneuverability
DOS	Degree of Steerability
DP	Dynamic Programming
EA	Evolutionary Algorithm
ECMS	Edge Cloud Management Controller
EM	Energy Management
EOM	Equations of Motion
ES	Extremum Seeking
FDP	Fast Dynamic Programming
GA	Genetic Algorithms
GPS	Global Positioning System
GT	Game Theory
HEV	Hybrid Electrical Vehicles
IA	Instantaneous Assignment
IDP	Iterative Dynamic Programming



IPOPT	Interior Point OPTimizer
MOCIS	Méthodes et Outils pour la Conception Intégrée des Systèmes
MPC	Model Predictive Control
MR	Multi-Robot
MRTA	Multi-Robot Task Assignment
MT	Multi-Task
NDP	Neuro-dynamic Programming
NLP	Nonlinear Programming
NN	Neural Network
NSGA	Nondominated Sorting Genetic Algorithm
NSGA-II	Non-dominated Sorting Genetic Algorithm-II
OC	Optimal Control
OEM	Optimal Energy Management
PA	Power Allocation
PCOA	Parallel Chaos Optimization Algorithm
PH	Pythagorean Hodograph
PMP	Pontryagin's Minimum Principle
PP	Path Planning
PSO	particle swarm optimization
QP	Quadratic Programming
RGA	Real-valued Genetic Algorithm
RRT	Exploring Random Trees
SA	Simulated Annealing
SEUMRE	Space Exploration and Unimodal Region Elimination
SOC	State of Charge
SQP	Sequential Quadratic Programming
SR	Single Robot

ST	Single Task
SVM	support vector machine
TA	Time extended Assignment
TD	Temporal Difference
TO	Trajectory Optimization
TOMR	Three-wheeled Omnidirectional Mobile Robota
TOP	Trajectory Optimization Problem
URV	Unmanned Road vehicle
URVTAP)	URV Task Assignment Problem
VRP	Vehicle Routing Problem

# General Introduction

---

## Contents

---

<b>1.1</b>	<b>Framework and context of the thesis</b> . . . . .	<b>5</b>
<b>1.2</b>	<b>General Introduction</b> . . . . .	<b>6</b>
<b>1.3</b>	<b>Thesis objective</b> . . . . .	<b>8</b>
<b>1.4</b>	<b>Problem Statement</b> . . . . .	<b>8</b>
<b>1.5</b>	<b>Contribution</b> . . . . .	<b>9</b>
<b>1.6</b>	<b>Disseminated Results</b> . . . . .	<b>11</b>
<b>1.7</b>	<b>Manuscript organization</b> . . . . .	<b>12</b>

---

## 1.1 Framework and context of the thesis

This PhD thesis has been prepared within the research group Méthodes et Outils pour la Conception Intégrée de Systèmes (MOCIS)<sup>1</sup>, of the Centre de Recherche en Informatique, Signal et Automatique de Lille (CRISAL) (UMR CNRS 9189)<sup>2</sup>.

The CRISAL research objectives affect the growth of fundamental, methodological, and technological research in the areas dealing with automatic control, computer engineering, and signal processing. The present work was designed under the guidance of Rochdi Merzouki, Professor at Polytech Lille - University of Lille. The research group MOCIS has vast experience with the combined design of systems, about modelling, structural analysis, control and diagnosis through the practice of unifying graphical tools. Fig. 1.1 explains the topological organization of this group. This integrated design can concentrate on the microscopic system, model representing an elementary robot as a physical system, or to the high-level macroscopic system, including other robots, environment, communication between robot to robot or robot to the environment. Such class of organizational architecture is planned with the idea of System of Systems (SoS). In this context, various research works have been realized over the last 10 years. In this work, we concentrate on energy planning for physical systems in transportation and robotics.

---

<sup>1</sup><https://www.cristal.univ-lille.fr/?rubrique27&eid=24>

<sup>2</sup><https://www.cristal.univ-lille.fr/>

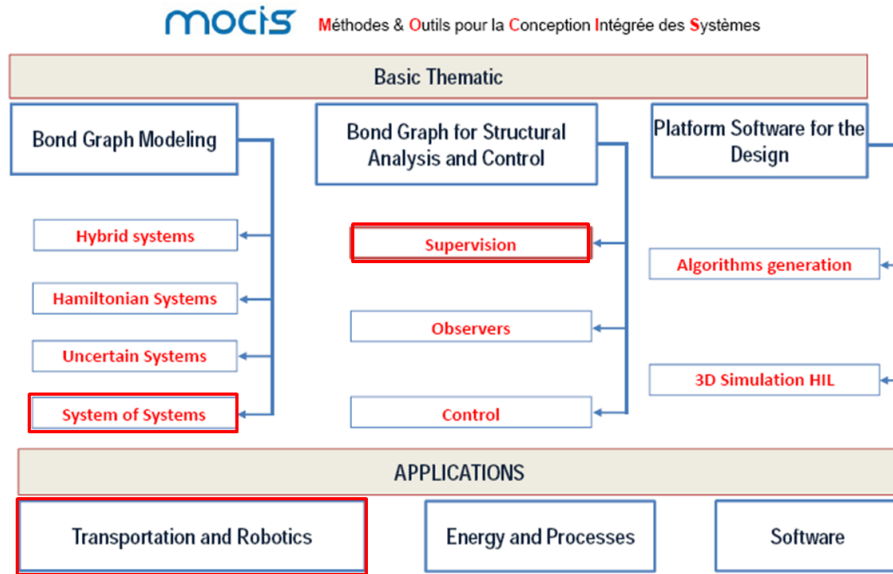


Figure 1.1: Organization of the works developed within the group MOCIS

## 1.2 General Introduction

In the last decade, autonomous vehicles have been increasingly utilized in many sectors, including the industry and planetary research. These vehicles provide a reduction of emissions in big cities and allow to conduct autonomous operations in unfamiliar and confined spaces. These vehicles, due to their operational autonomy, facilitate the execution of repetitive or programmed tasks efficiently and safely. For the specifications of tasks repetition and environmental safety (human or material), the manufacturers are innovating the technology of unmanned road vehicles (URV)s, studied, redundant in actuation and ready to ensure the continuation of achievement of tasks in normal and imperfect situations. This redundancy of inputs has been already utilized for aircraft systems. Thus, in this thesis work, research on a class of over-actuated and over-instrumented URV has been designed. Notwithstanding the benefits of intelligent autonomous vehicles, energy dependence is one of the principal problems facing the manufacturers. This returned back the researchers to enhance the autonomous control and navigation of the URV in the function of the available driving energy efficiently. Many energy supply systems have been developed over time. Thermal engines are more efficient in energy autonomy, but emit a lot of  $CO_2$ . Hybrid vehicles are a technology that succeeds thermal motorization and it is a blend of an electric motor and the engine using an alternator and a battery system for saving energy. Many manufacturers have utilized this technology that can be defined as an intermediate to a fully electric engine to reduce emissions of  $CO_2$  in an urban environment ultimately.

Electric vehicles are the new age of motorized vehicles, where automotive man-

Manufacturers have actively invested because they are more sustainable and practice green energy. However, the warehouse of the electrical energy is done by the batteries, where their fabrication stays problematic in terms of respect of the environment. One specification correlated to the battery design is that it needs a very long life-cycle, offering to make optimal management of the energy resources. Thus, the execution indicator of the batteries struggles about their optimal cycles for the charging and discharging. The best current battery technology is the lithium ion-based.

Power planning or energy management of electric vehicles is established to start analyzing from the last decade. Nowadays, energy autonomy of electric vehicles needs on-board power resources such as batteries. So, the operational execution of autonomous systems is based principally on the autonomy of the power supply. Many studies have been performed whose purpose is to increase the autonomy of on-board power systems so that it is sustainable in the time. These studies concentrate on the development of storage technologies; or of course, energy management and optimization while managing existing resources. Energetic systems that we address as part of this thesis define a class of mobile rolling and over-actuated vehicles, with redundancy in traction and steering actuation, which enables managing their mobility in various driving situations. In the literature, on-board energy optimization research has been conducted in terms of transportation kinematics, trajectory optimization, control/command optimization, and power management. For all these research activities, it is assumed that the power storage on-board is also optimal.

Optimal Energy Management (OEM) of autonomous systems combines between multiple methods of optimization implemented to the path planning, the trajectory planning, the tasks allocation, and the routing. The objective of the OEM is to find the optimal velocity profile and control/command that consumes the minimum of energy on an identified road profile. The OEM needs a set of information affecting the power consumption of vehicles, where its distribution requires the modeling of:

- Charging capability of the batteries,
- Kinematics and dynamics of the URVs,
- 3-D path or curvature profile,
- Velocity profile

The OEM is generally applied for the online driving of autonomous vehicles. therefore, it is essential to have a baseline of energy consumption along the traveled path. Thus, **energy planning is a methodology allowing identifying an optimal distribution of the energy**, those autonomous vehicles can use as a reference, to manage its driving modes and energy consumption automatically. This is the main contribution to this Ph.D. thesis.

### 1.3 Thesis objective

The objective of this thesis is to propose an offline methodology for optimal distribution of energy in the case of autonomous and over-actuated vehicles, in the presence of normal or faulty situations. This is called **energy planning**, which defines an offline optimal allocation of the power before the vehicle travel, allowing then, the online management of the energy, in terms of optimal control distribution. **Our objective from this thesis work is to extend the existing technique of effort-based "Control Allocation - CA" to the dual of flow and effort-based "Power Allocation - PA"**. The aim is to master the energy management in different driving modes. The energy planning will allow estimating the mobility and manoeuvrability required by the over-actuated URV to achieve its mission for a given trajectory and the driving in the normal and degraded situations.

### 1.4 Problem Statement

Let us consider the second order dynamic equation of an URV expressed in vehicle coordinated can be given as follows:

$$\hat{M}(q)\ddot{q} + H(\dot{q}, q)\dot{q} + G(q) = \tau \quad (1.1)$$

where,  $q$  is the generalized position vector which represents position or angle,  $\dot{q}$  is a generalized velocity vector which represents linear or angular velocity of the URV,  $\hat{M}(q)$  is the inertia matrix,  $H(\dot{q}, q)$  is a matrix of centrifugal and Coriolis effects,  $G(q)$  is the gravitational matrix, and  $\tau$  is the generalized vector of the external efforts.

Thus, the power consumption of the URV can be estimated as follows:

$$\hat{P} = \dot{q}^T \tau \quad (1.2)$$

From equations 1.1 and 1.2, the power consumption can be written as follows:

$$\begin{aligned} \hat{P} &= \dot{q}^T [\hat{M}(q)\ddot{q} + H(\dot{q}, q)\dot{q} + G(q)] \\ &= \dot{q}^T \hat{M}(q)\ddot{q} + \dot{q}^T H(\dot{q}, q)\dot{q} + \dot{q}^T G(q) \end{aligned} \quad (1.3)$$

The problem of energy planning can be stated as an optimization problem and given by its discrete form as follows:

$$\min_{V_{i,k}, M_{i,m}} J = \sum_{i=1}^n \hat{P}_{i,k}(t_i, V_{i,k}, A_{i,k}, C_i, M_{i,m}) \times (\Delta t_i) \quad (1.4)$$

subject-to

$$\begin{aligned}
 t_i &< t_{max} \\
 V_{min} &\leq V_{i,k} \leq V_{max} \\
 A_{min} &\leq A_{i,k} \leq A_{max}
 \end{aligned}
 \tag{1.4a}$$

Where,  $V_{i,k}$ ,  $A_{i,k}$  represent respectively the  $k^{th}$  velocity and the acceleration profiles, defined for the  $i^{th}$  road segment.  $M_{i,m}$  is the  $m^{th}$  driving modes for the  $i^{th}$  road segment and  $\hat{P}_{i,k}$  is the  $k^{th}$  consumed power by the URV for the  $i^{th}$  road segment. The parameters  $t_i$  and  $C_i$  represent respectively the traveling time and the curvature of the  $i^{th}$  road segment.  $m$  depends of the number of independent steering system and actuated wheels.

Upper and lower limits restrict the velocity and acceleration profiles of the centre of gravity.  $J$  denotes the evaluation function of energy consumption of the URV along  $n$  road segment.

In this thesis work, it is considered a generic class of URVs which are redundant in actuation (over-actuated URV), with independent traction wheels and independent steering systems. Such URV is a vehicle-like robot with 3 Degree of Freedom (DoF) and can have different steering configurations of driving modes, characterized by a degree of steerability  $\delta s$  and a degree of redundancy  $\delta_R$ , which are dependent, as shown in Fig. 1.2, where:

- The dual configuration ( $\delta s = 2$ ) has two steering actuation for the front and rear wheels.
- The single configuration ( $\delta s = 1$ ) has only one steering actuation for the front wheels.
- The skid configuration ( $\delta s = 0$ ) has no steering actuation, where the vehicle orientation is obtained from the difference of the velocity, obtained from the traction wheels.

The active wheels (actuated) are filled with black , and the white colour represents the passive wheels (non actuated). The description of all the configurations of the URV is given in Table 1.1.

## 1.5 Contribution

In this thesis work, we proposed a methodology to support for energy planning. **The proposed methodology will allow the URVs to identify an optimal**

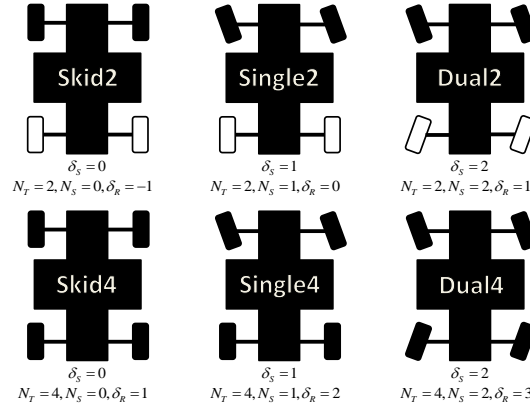


Figure 1.2: Different driving modes (steering configurations) of one considered UAV with  $m = 6$ .

Table 1.1: Parameters describing URV driving configurations for  $m = 6$ .

	Traction actuators	Steering actuators
Skid4 ( $\delta_s = 0, \delta_R = 1$ )	4	0
Single4 ( $\delta_s = 1, \delta_R = 2$ )	4	1
Dual4 ( $\delta_s = 2, \delta_R = 3$ )	4	2
Skid2 ( $\delta_s = 0, \delta_R = -1$ )	2	0
Single2 ( $\delta_s = 1, \delta_R = 0$ )	2	1
Dual2 ( $\delta_s = 2, \delta_R = 1$ )	2	2

**couple of power allocation and driving modes along a defined trajectory.**

This energy planning is assumed to be executed offline before the URV starts operating. This methodology aim is to ensure the power availability to the URV before it begins realizing its mission (routing, path planning, task allocation, trajectory planning). This planning energy should respect the dynamic constraints (vehicle load, interaction with the ground): the kinematic constraints (driving modes of the vehicle) and the road geometry (curvature profile).

- The Power consumption estimation of an over-actuated URV is developed using two approaches:
  - A qualitative approach based on the data-learning method.
  - A quantitative approach based on the generalization of Newton-Euler formulation to multiple driving modes.
- Energy planning for over-actuated URVs is proposed using discrete and continuous methods. It determines the optimal velocity profile and the corresponding driving mode for every segment of the trajectory, considering into account the road curvature and the kinematic parameters of the URV.



- Simulations and Experimental results are applied on a real URV called Robucar, in presence with decentralized driving modes ( $m = 6$ ).

## 1.6 Disseminated Results

The obtained results are disseminated through the following publications:

### Journals

- Bensekrane, I., Kumar, P., Melingui, A., Coelen, V., Amara, Y., Chettibi, T. & Merzouki, R. Energy Planning for Autonomous Navigation of an Over-actuated Road Vehicle", *IEEE/ITS Intelligent transportation system*,2019. **Accepted with Minor Revision**
- Bensekrane, I., Kumar, P., Melingui, A., Chettibi, T., Singh, I., Singh, M. & Merzouki, R., "Energy Planning for Autonomous Driving of an Unmanned Road Vehicle on Smooth Paths", *IEEE/TVT Transactions on Vehicular Technology*, 2019. **Under Revision**
- Kumar, P., Bensekrane, I., Merzouki, R., "Estimation of Power Consumption of Wheeled Mobile Robots with Multiple Kinematics: A Bond Graph Approach", *IEEE/ASME Transactions on Mechatronics*, 2019. **Under Revision**

### International conferences

- Bensekrane, I., Kumar, P., Amara, Y., & Merzouki, R. (2017, December). Towards adaptive power consumption estimation for over-actuated unmanned vehicles. In *2017 IEEE International Conference on Robotics and Biomimetics (ROBIO)* (pp. 92-97). *IEEE*.
- Datouo, R., Motto, F. B., Zobo, B. E., Melingui, A., Bensekrane, I., & Merzouki, R. (2017, December). Optimal motion planning for minimizing the energy consumption of wheeled mobile robots. In *2017 IEEE International Conference on Robotics and Biomimetics (ROBIO)* (pp. 2179-2184). *IEEE*.
- Bensekrane, I., Kumar, P., Melingui, A., Coelen, V., Amara, Y., & Merzouki, R. (2018, August) Energy Planning for Unmanned Over-actuated Road Vehicle. In *2018 IEEE Vehicle Power and Propulsion Conference (VPPC)*. *IEEE*.
- Kumar, P., Bensekrane, I., Singh, M., & Merzouki, R. (2018, October) Bond Graph-based Power Consumption Estimation of a Non-holonomic Wheeled Mobile Robot with Multiple Driving Modes. In *2018 IEEE International Conference on Systems and Control (ICSC)*. *IEEE*.
- P. Kumar, I. Bensekrane and R. Merzouki. (2018, December) "Modeling of the Multi-domain Steering System with Hybrid Dynamics for an Over-actuated Autonomous Vehicle," *IEEE International Conference on Robotics and Biomimetics (ROBIO)*, (pp. 2514-2519). *IEEE*.

## 1.7 Manuscript organization

The document is organized in the following six chapters:

- The second chapter presents a literature review in the area of power consumption modelling and the energy management of manned and unmanned vehicles. This chapter allows making a scientific positioning of the energy planning methodology, proposed in this work, relative to different approaches used in energy management methodology.
- The third chapter presents the power consumption modeling of an over-actuated URV. The power consumption is estimated with quantitative and qualitative approaches. In the quantitative, the power consumption is formulated according to geometrical criteria, kinematics and dynamic parameters, and the different driving modes. In the qualitative approach, a learning data based method is discussed. The inputs of this model are the curvature of the road path, the velocity profile, and the acceleration of the URV. The qualitative based-approach is considered for taking into account the quantitative modeling uncertainties.
- The fourth chapter summarizes deals with the discrete based approach for energy planning. This approach is developed based on a discrete model and curvature filtering of the road path. An energy digraph is then constructed based on the path segmentation. The latter is utilized with different methods for graph search as dynamic programming, Dijkstra and  $A^*$ . These algorithms provide a global optimal solution of a couple of the velocity profile and the driving mode in each segment of the filtered road path. Finally, the comparison of the performances of power consumption of a real URV, according to the travel time is discussed.
- In the fifth chapter, a continuous energy planning is proposed for an over-actuated URV based on a multi-criteria optimization methodology utilizing the genetic algorithm (NSGA-II). The aim is to approximate the road path profile by a succession of continuous curves. A real road path of University of Lille campus is considered and modelled by utilizing two smooth geometrical combinations: the first one is lines, clothoids, and arcs, and the second one is lines and Pythagorean Hodograph (PH) curves. The energy planning methodology is then applied to the generated paths. In the proposed methodology, a target point is selected from the Pareto front in order to set-up the best velocity profile for each driving mode. Also, a directed graph is built to synthesis the optimal velocity profile, that minimizes the overall energy consumption while accounting for the driving modes.
- Finally, the sixth chapter summarizes the conclusions of the main contributions and the perspective of this work for the online case and its generalization to various autonomous systems.

# Power Management of Autonomous Road Vehicles

---

## Contents

---

<b>2.1</b>	<b>Introduction</b>	<b>13</b>
<b>2.2</b>	<b>Kinematic Properties of Unmanned Road Vehicles (URVs)</b>	<b>14</b>
2.2.1	Degree of freedom	16
2.2.2	Degree of mobility	16
2.2.3	Degree of steerability	17
2.2.4	Degree of manoeuvrability	17
2.2.5	Holonomy Constraint	18
2.2.6	Omni-directional Property	18
<b>2.3</b>	<b>Power Consumption and Energy Management of URVs</b>	<b>19</b>
2.3.1	Energy Consumption of URVs:	20
<b>2.4</b>	<b>Optimal autonomous driving of URVs</b>	<b>30</b>
2.4.1	URV path planning problem	30
2.4.2	Trajectory optimization problem of URVs	33
2.4.3	URV routing problem	36
2.4.4	URV task assignment problem	37
2.4.5	URV energy planning	43
<b>2.5</b>	<b>Conclusion</b>	<b>44</b>

---

## 2.1 Introduction

This chapter discusses with the literature review on power management for Unmanned Road Vehicles (URVs). These denote the targeted autonomous systems, analysed in this work. This state of the art is essential for the positioning of the scientific contributions produced in this PhD thesis work. First, the kinematic properties of the URVs are presented. This includes the definitions of: degree of freedom, degree of mobility, degree of steerability and degree of manoeuvrability, holonomy and omni-directional motions. These properties are helpful for autonomous road vehicle design. Knowing that the power consumption of the URVs is estimated based on the kinematics of the vehicle and the dynamic of the interaction with the

ground. More the vehicle has an actuation, more it consumes power. Therefore, having multiple actuators allow to make a tolerant control and maintain the autonomous navigation of the URV. *Thus, the energy planning for URVs is an optimization problem, where the objective is to identify the best driving configuration with appropriate kinematics, offering less power consumption.*

## 2.2 Kinematic Properties of Unmanned Road Vehicles (URVs)

URVs are rapidly expanding in the automotive industry. Various research works are developed in this area to overcome the problems of modelling and control of URVs. Most of the URVs are generally redundant in actuation and sensors. This has an advantage to facilitate the monitoring and avoid the blocking situations in case of presence of faults. Over-actuated URVs can have many driving configurations according to their kinematic properties. Five properties of vehicle like-robots are defined, according to their kinematics, namely: the degree of mobility, the degree of steerability, the degree of manoeuvrability, the holonomy and the omnidirectionality [Campion 1996], [Siegwart 2011]. The mobility of the URVs is not directly dependent on the number of wheels but on the types of wheels: conventional or omnidirectional, steerable or fixed. The frame of a URV can be equipped with these four types of wheels, each giving rise to a set of generalized coordinates. The classification of the different kinds of wheels is detailed below [Campion 1996]:

- **Fixed Standard Wheel:** Such wheel is also named conventional or non-steerable wheels. Its orientation angle is not varying and so, it has no steering rotation axis (Fig.2.1):

$Q$ : is a fixed point in the chassis and is defined with the polar coordinate  $(l, \alpha)$  in the frame  $[P, \vec{i}, \vec{j}]$  as follows:  $l = \|\overrightarrow{PQ}\|$ ,

$$\alpha = (\vec{i}, \overrightarrow{PQ})$$

$S$  is the center of the wheel.  $\beta$  is the angle between  $\overrightarrow{PQ}$  and the normal oriented to the plane of the wheel.

$d$  is the norm of  $\overrightarrow{QS}$  projection on the horizontal plan.

$h$  is the norm of  $\overrightarrow{QS}$  projection on a vertical axis.

$\phi$  is the rotation angle of the wheel.

- **Steered Standard Wheel:** Steerable wheel means that its orientation angle is modifying and its steering rotation axis is defined by two points: the centre of the wheel and the ground contact. In this type of wheel, the steering system is actuated (Fig.2.2).
- **Castor Wheel:** Castor wheel is also steerable, but its steering rotation axis

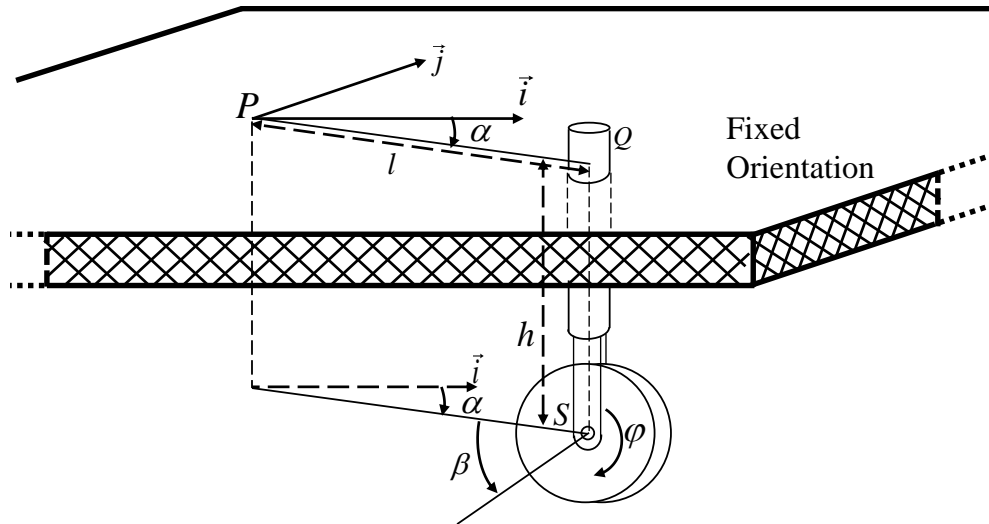


Figure 2.1: Configuration of Fixed Standard Wheel

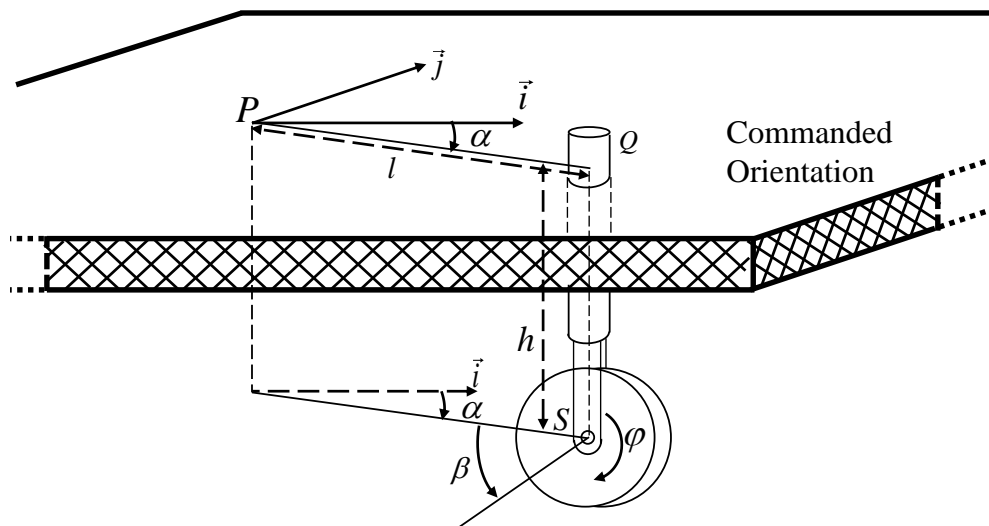


Figure 2.2: Configuration of Steered Standard Wheel

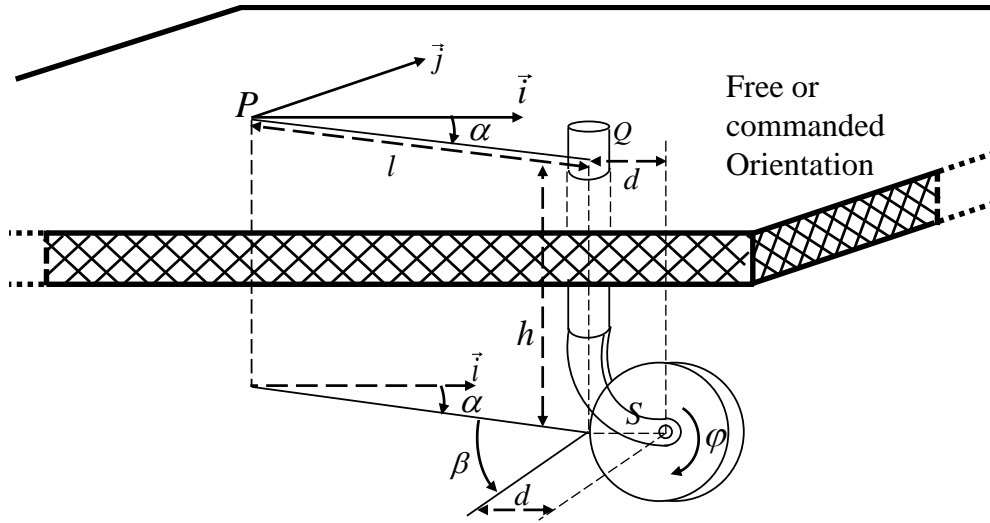


Figure 2.3: Configuration of Castor Wheel

does not cross through the ground contact point. Furthermore, the steering system is not driven by an actuator, where the motion is free (Fig.2.3).

- **Swedish Wheel:** Swedish wheel is composed of one established standard wheel and a set of small rollers connected to its circumference. The axis of the small rollers are not parallel to those of the established standard wheel, and their orientation angles are typically about 45 degrees or 90 degrees. This type of wheel do not steer rotation axis, but it can move omni-directionally (Fig.2.4).  $\gamma$  is the angle between the plane of the omni-directional wheel and the perpendicular to the direction of free evolution.

### 2.2.1 Degree of freedom

The degrees of freedom (DoF) of the URV can be represented as the whole of the independent parameters needed to define its pose in the considered workspace. The most common workspace is a plane in which the URV can go with two translation motions (longitudinal and lateral) along two principal axes; and one rotation motion (yaw) about the axis perpendicular to the plane. Therefore, total DoF is:

$$DoF = 3 \quad (2.1)$$

### 2.2.2 Degree of mobility

The degree of mobility (DoM) of the URV is a sum of the number of DoF that it can achieve through rotation of the wheels without steering [Siegwart 2011]. It can be defined by:

$$DoM = 3 - \text{rank}[C] \quad (2.2)$$

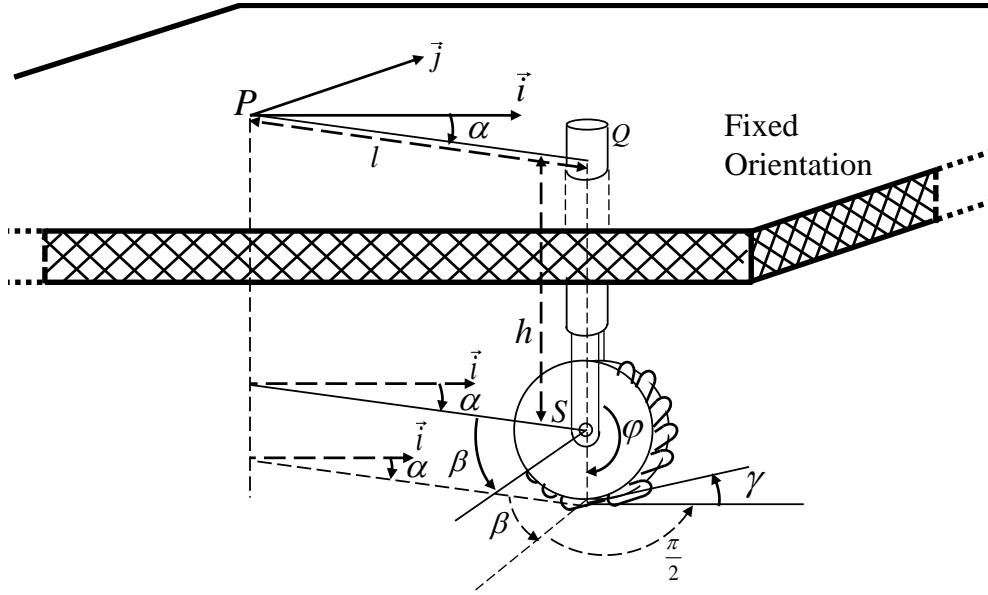


Figure 2.4: Configuration of Swedish Wheel

The range of DoM is compromised between  $[0 \ 3]$ , where  $C$  is the constraint matrix, described as follows:

$$C = \begin{bmatrix} C_f \\ C_s \end{bmatrix} \quad (2.3)$$

$C_f$  is a constant matrix of orthogonal motions to the effective direction for all fixed wheels, and  $C_s$  is a variable matrix of orthogonal motion to the effective direction for all steerable wheels.  $C_s$  varies with time as a function of steering angles of the wheels, noted  $\beta(t)$ .

$$C_s = [\cos(\alpha + \beta) \quad \sin(\alpha + \beta) \quad l \sin \beta] \quad (2.4)$$

### 2.2.3 Degree of steerability

The degree of steerability (DoS) of the URV is a measure of the number of independently controllable steering systems. It can be defined by:

$$DoS = \text{rank} [C_s] \quad (2.5)$$

The range of DoS varies in between  $[0 \ 2]$ .

### 2.2.4 Degree of manoeuvrability

The degree of manoeuvrability (DoMS) of the URV is a measure of the overall DoF that the URV can achieve through rotation of the wheels around their centers. It can be defined by:

$$DoMS = DoM + DoS \quad (2.6)$$

The range of DoMS is defined in between  $[0 \ 3]$

### 2.2.5 Holonomy Constraint



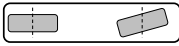

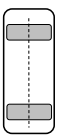

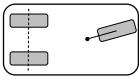

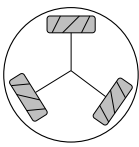

A URV is holonomic if all the kinematic constraints of the URV body are holonomic. A holonomic kinematic constraint can be expressed as an explicit function of position and time. The URV is holonomic if and only if:

$$DoM = DoF \tag{2.7}$$

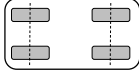

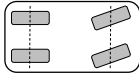

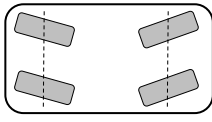


### 2.2.6 Omni-directional Property

An omni-directional URV can have mobility in all the directions of the DoF. Therefore, an omni-directional URV has a DoM equals to three:

$$DoM = DoF = 3 \tag{2.8}$$

S.N	Types of URV	Kinematic Properties				Applications
		DoF	DoM	DoS	DoMS	
1	One wheel robot 	3	2	0	2	Unicycle 
2	Two wheel robot (with steering) 	3	1	1	2	Honda self-balancing bike 
3	Two wheeled robot with differential-drive 	3	2	0	2	Segway 
4	Three/four wheeled robot with differential-drive 	3	2	0	2	Khepera robot 
5	Three swedish wheeled robot 	3	3	0	3	Robotino 



S.N	Types of URV	Kinematic Properties				Applications
		DoF	DoM	DoS	DoMS	
6	Four wheeled robot with skid steering 	3	1	0	1	Robucar with skid configuration 
7	Four wheeled robot with front steering wheels 	3	1	1	2	Robucar with single configuration 
8	Four wheeled robot with front and rear steering wheels 	3	1	2	3	Robucar with dual configuration  Robutainer 

## 2.3 Power Consumption and Energy Management of URVs

The URV is undergoing a necessary shift in expansion and dimension. It has broad participation in the industry and the daily lives of humans. Their involvement is to make life easier, to save time, and to make repetitive tasks in complex conditions. Most of these URVs are powered with electric sources like batteries. Nowadays, the energy management of the autonomy of the URVs has become a real challenge, in order to optimize the overall energy consumption.

Modelling the energy consumption of the URVs [Liu 2012] allows analyzing the influence of operating modes of the vehicle on its energy consumption, and provides the best strategy of energy management [Xu 2016].

To optimize the energy consumption of the URVs, some contributions have adopted different methods, based on the optimization of the trajectory [Verstraten 2016], [Lu 2000], the optimization of the control [Martín 2008], [Haidegger 2012], or the optimization of the vehicle design [Vrkalovic 2017].

### 2.3.1 Energy Consumption of URVs:

URVs Power consumption can be the source of three main components [Kim 2008]: propulsion, steering and embedded technologies (2.5). In this Figure, rectangle boxes symbolize components of the URV, while the ellipses indicate the component energy consumption. Energy is drawn from the battery pack at the starting stage of the chain. The battery's left energy is called "Residual Battery Energy" [Xiao 2014].

#### 2.3.1.1 Power consumption from the propulsion

The overall battery energy of the URV is used to drive the actuators, while the rest of the energy is used to power the embedded electronics [Vantsevich 2007]. The "Power Electronics Loss" consists mainly of heat loss and the fan power cooling. The actuators also consume the energy at the bearings due to resistance losses in windings, core losses and mechanical losses [Aarniovuori 2018]. Almost the electrical power is transformed into mechanical power, where the internal resistance in the gears, the bearings, etc..., are considered as internal friction. This mechanical-based power loss depends on the type of drive train, the lubrication, etc. The external friction also called external efforts, consume the important part of the battery energy. These efforts represent the multi-domain dynamics of the interaction between the wheel and the ground [Merzouki 2006] Depending on the type of the wheel tire, a part of the energy is not preserved due to the damping effect in the tires. The aerodynamic loss is proportional to the square velocity [Hucho 1993], so when the vehicle velocity is high, it can constitute a significant fraction of energy consumption.

#### 2.3.1.2 Power consumption for the steering

Steering system [Hassan 2012] represents another source of multi-domain energy consumption for a URV. The energy chain configuration for the steering system is almost the same as the propulsion configuration (2.5). This consumption is hard to quantify as it depends on multiple factors such as ground (terrain) type, traverse path, steering modes, etc.

When the vehicle's turning velocity is slow, the Ackerman-based kinematic steering is considered [Harrer 2017]. Significant lateral acceleration is needed when the vehicle turns fast, and therefore the wheels operate at high angles of slip. The loads on the inner wheels will also be significantly lower than the outer wheels. Tire-based wheel performance curves show that less slip angle is needed to reach the peak of lateral force by increasing the wheel load. Under these conditions, a kinematic steering vehicle's inner front wheel would be at a higher slip angle than the maximum lateral force required. Consequently, a vehicle's inner wheel in a high-velocity turn must operate at a lower steering angle than kinematic steering. Reducing the internal wheel steering angle minimizes the difference between the inner and outer wheel steering angles. Parallel or reverse steering is standard for race vehicles. Parallel and reverse Ackerman's steering are illustrated in Fig. 2.6 in [Jazar 2017].

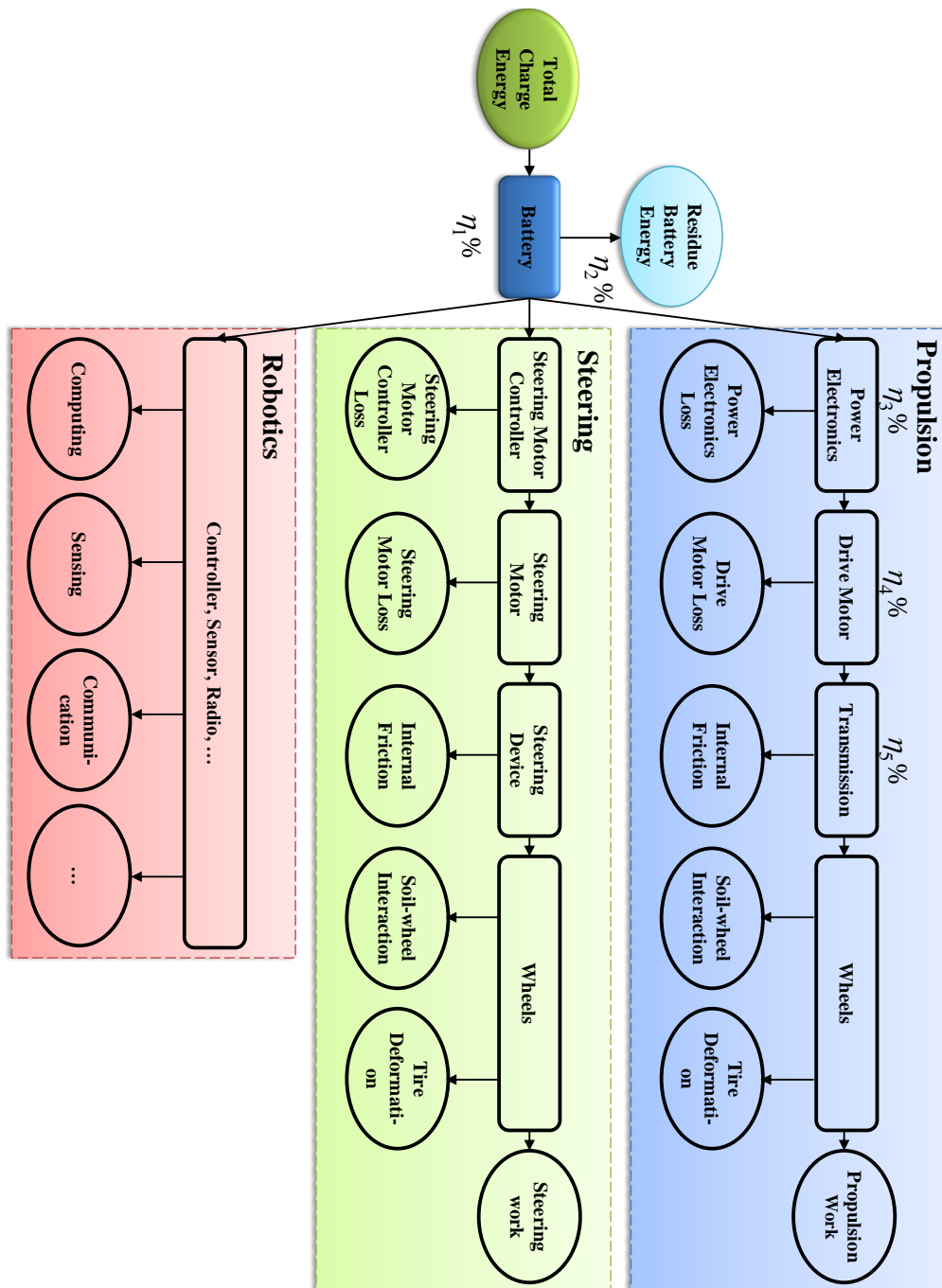


Figure 2.5: Energy Utilization for URVs [Xiao 2014]

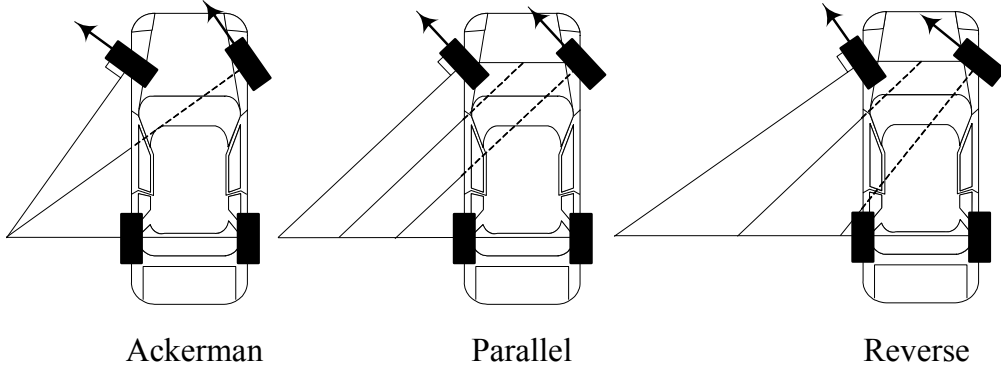


Figure 2.6: Steering type of Vehicle [Jazar 2017]

The correct steering angle depends on instantaneous characteristics: wheel load, road condition, wheel velocity, and wheel tire. In addition, under an Ackerman's steering condition, the vehicle must also be able to turn at low velocity. Therefore, there is no ideal steering mechanism unless the use of a smart system to independently control the steering angle of each steerable wheel.

### 2.3.1.3 Power consumption for vehicle-like robotics functions

Robotics functions consume a large percentage of all the energy extracted from the battery. Unlike most distance-dependent propulsion and steering energy, robotics consumption is calculated by mission time. URV must consume energy during traverse to perform the assigned tasks, such as sensing environment, data collection, photography, or rescuing survivors in unknown situations. Some URVs must communicate with the base. The onboard computer, GPS(Global Positioning System), Inertial Unit, etc..., is also continually consuming energy. The URV may have other robotic consumption, such as the lighting in caves, mines, and sewers, to operate. As they vary significantly from URV to URV, it is impossible to generalize all types of consumption in one model. There are three main groups of sensor systems which consume more power: camera, radar, and lidar-based systems, as shown in Fig. 2.7 and Fig. 2.8.

Here, several energy efficiency for the intermediate steps in the energy chain are defined [Xiao 2014]:

$$\text{Battery Efficiency : } \eta_1\% = 1 - \frac{\text{Residual Battery Energy}}{\text{Total Charged Energy}} \quad (2.9)$$

$$\text{Propulsion Branch Efficiency : } \eta_2\% = 1 - \frac{\text{Steering Consumption} + \text{Robotics Consumption}}{\text{Available Battery Energy}} \quad (2.10)$$

$$\text{Power Electronics Efficiency : } \eta_3\% = 1 - \frac{\text{Power Electronics Loss}}{\text{Propulsion Branch Energy}} \quad (2.11)$$

$$\text{Motor Efficiency : } \eta_4\% = 1 - \frac{\text{Motor Loss}}{\text{Power Electronics Energy}} \quad (2.12)$$

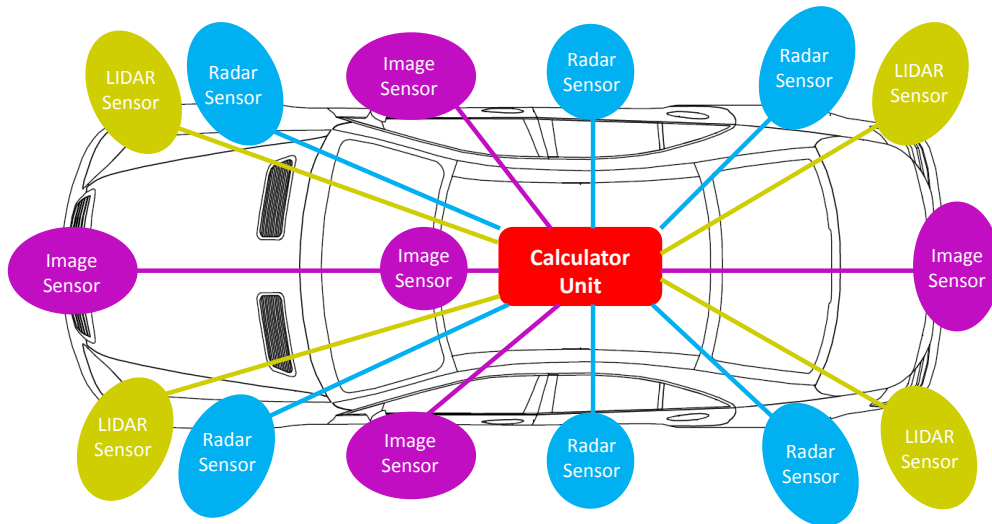


Figure 2.7: Power Vs Radius Bars



Figure 2.8: Sensors in URV [Takeda 2011]

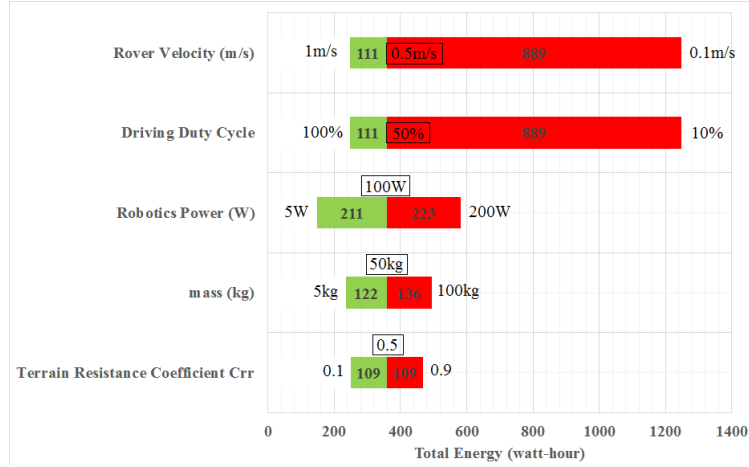


Figure 2.9: Influence of Different URV Parameters on Total Required Battery Energy to Accomplish a 2km Traverse [Hou 2019].

$$\text{Mechanical Efficiency : } \eta_5\% = 1 - \frac{\text{Internal Friction Loss}}{\text{Mechanical Energy}} \quad (2.13)$$

We are taking into account other factors such as URV power, URV mass, terrain resistance coefficient Fig. 2.9 in [Xiao 2014] shows that URV velocity and driving duty cycle, have the most significant impact on the energy required to finish a defined trajectory.

In Fig. 2.10 in [Hou 2019], the URV can use the energy model to calculate and predict the energy consumption, which provides a guide for facilitating energy-efficient strategy. The URV's energy consumption is first modelled by taking into account three main factors: the sensor system, the control system, and the motion system. The authors in this work developed a global formula for the three systems. The experimental results showed that energy consumption for the motion is the most important in the four omni-directional wheeled URV with 94.7%. The control consumption power and the sensor consumption power represent 4%, and 1.25% respectively.

In the literature, the power consumption is studied for different kinematic configurations. For instance, [Shamah 1999] presents an experimental power consumption comparison of skid steering and explicit steering for a URV Fig. 2.11.

The moon rover Fig. 2.11 is a URV, where each wheel is independently driven to apply any desired angular velocity. We can distinguish an explicit steering and skid steering Fig. 2.12. Furthermore, the steerable wheels of such vehicles can turn more than 90 deg to the left and right. Such a vehicle is highly maneuverable at a low velocity. Fig. 2.12 illustrates the advantages of such a steerable vehicle and its possible turnings. The arrows by the rear

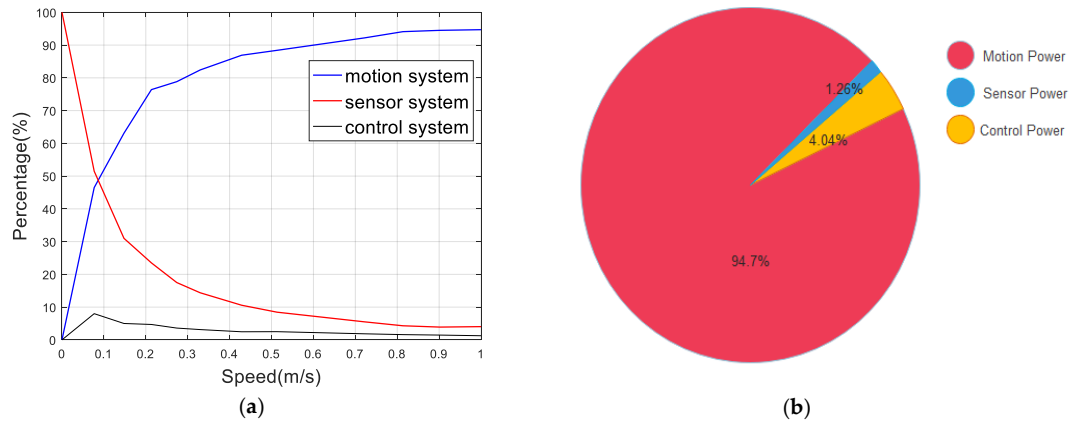


Figure 2.10: Percentage of Power Consumption for URVs [Hou 2019].



Figure 2.11: Nomad URV.

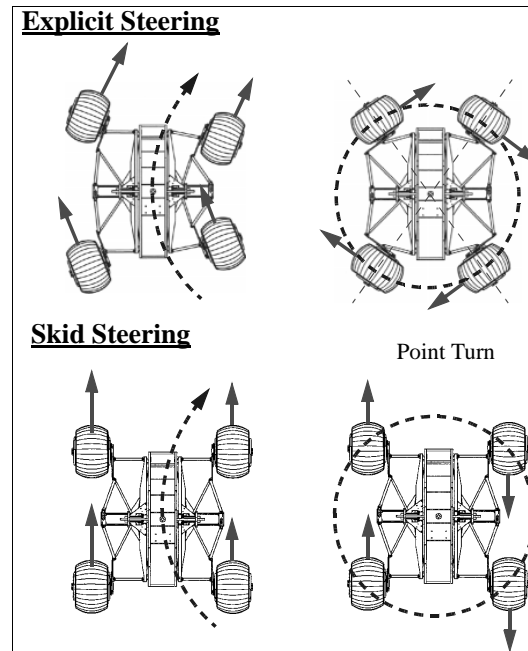


Figure 2.12: Nomad URV Configurations. [Shamah 1999]

wheels, illustrate the magnitude of the angular velocity of the wheel, and the arrows on the front wheels illustrate the direction of their motion.

For some special-purpose vehicles, such as moon rovers and other URVs, we may attach each actuated wheel to an independently controlled motor to apply any desired angular velocity. Furthermore, the steerable wheels of such vehicles are able to turn more than 90 deg to the left and the right. Such a vehicle is highly manoeuvrable at a low velocity. Having such a vehicle allows to have many driving configurations based on its steering. Front steering, Rear steering, dual steering, and point turning are the different driving modes. In any of the above scenarios, the steer angle of the front or rear wheels should be determined using a proper equation.

Refer to Fig. 2.13a and Fig. 2.13b, a comparison between the power consumption for explicit and skid steering for Nomad URV is given with respect to the radius of the trajectory ([Shamah 1999]). The experiments show that the power consumption of the Nomad URV decreases with the increase of the radius of the trajectory, while the skid steering consumes more than the explicit steering.

Most of the works given in the literature studied the case of modeling the power consumption of one single driving mode. For example, [Yu 2010] studied the case of a skid-steered wheeled vehicle as Fig. 2.16b. The authors elaborate a power consumption model for different types of contact surfaces for general 2-D motion and linear 3-D motion. However, the authors in



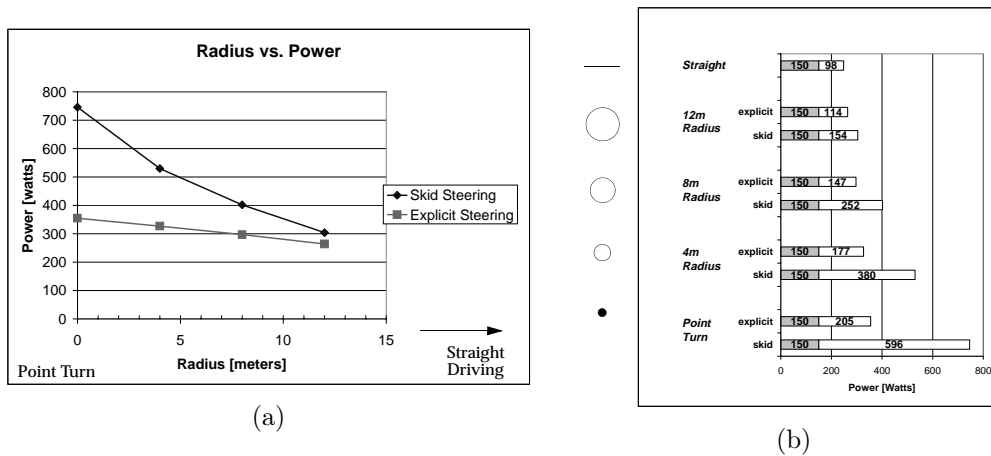


Figure 2.13: Power consumption for Nomad Vehicle [Shamah 1999]

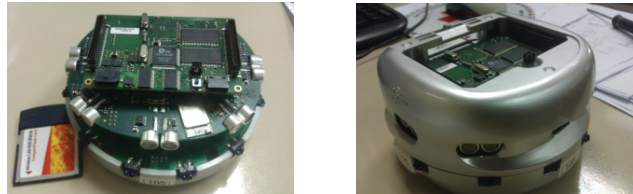


Figure 2.14: Khepera robot [Parasuraman 2014]

[Parasuraman 2014] developed a generic approach for on-line energy prediction modelling system for a miniature URV Fig. 2.14. The power consumption is divided into two components, static and motion power.

In addition, the authors in [Morales 2009], proposed a static power model for skid-steer tracked URVs, moving at walking velocity on hard plane terrains Fig. 2.15a.

In [Morales 2010], the authors proposed a simplified model of power consumption for skid-steered robotic vehicles on the hard horizontal ground at walking velocities based on a kinematic approach. This static model provides an estimation of the power consumption of the actuator as a function of the velocities of the left and right wheels Fig. 2.16a. Furthermore, [Tokekar 2011] presented a problem of computing a velocity profile for a vehicle-like robot, so as to minimize the energy consumed while traveling along a given path on a flat surface Fig. 2.16c. [Guo 2013] presented a simplified model to computer torque and power consumption of tracked URV, driving on soft terrain (i.e. sand) Fig. 2.15b. The authors in [Maclaurin 2008] analyzed the steering performance of an 18tons and 6×6 skid-steered URV and compare it with the performance of an equivalent Ackerman steered vehicle Fig. 2.17c. The Skid configuration of the vehicle presented in [Maclaurin 2008] is shown in Fig.



(a) Auguira URV [Morales 2009]



(b) PackBot robot [Guo 2013]

Figure 2.15: Tracked vehicles



(a) Quadriga robot [Morales 2010]



(b) Pioneer robot [Yu 2010]



(c) Vehicle Like robot [Tokekar 2011]

Figure 2.16: Wheeled mobile robots

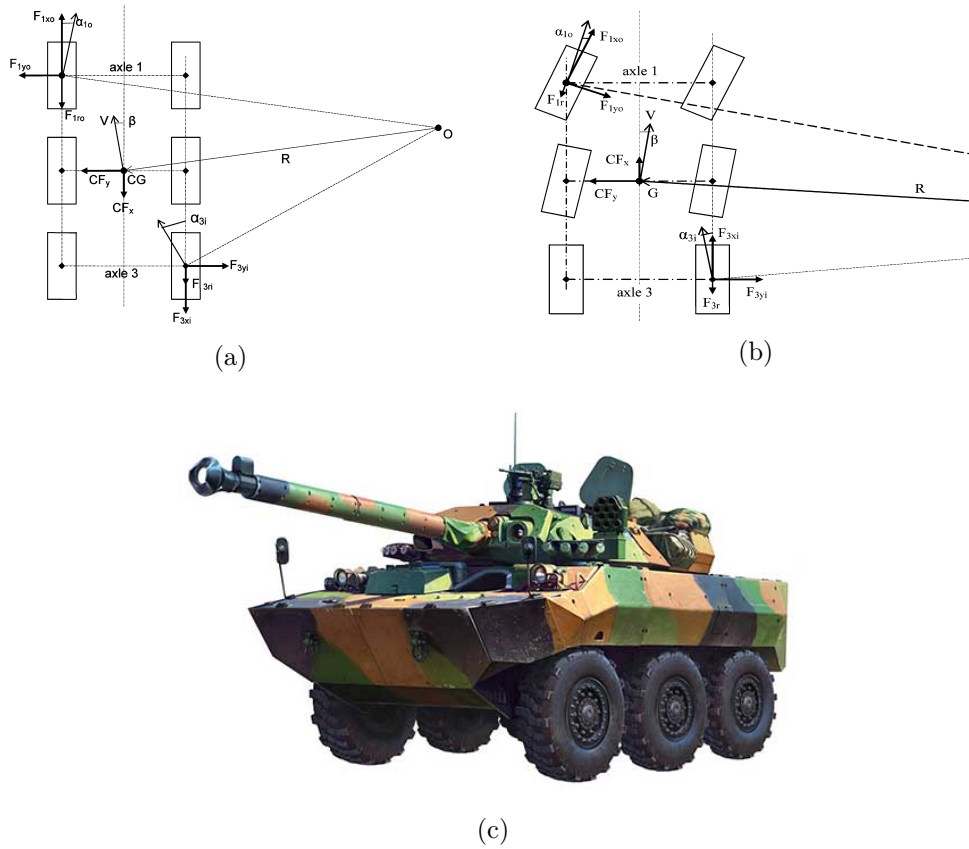


Figure 2.17: GIATAMX10RC URV with multiple configurations [Maclaurin 2008]

2.17a. The steering configuration of the URV is made by the four front wheels of the vehicle as shown in Fig. 2.17b.

In [Brembeck 2012], optimal control strategy for a highly manoeuvrable URV (ROboMObil) is applied, Fig. 2.18.

Most of power consumption models are developed for a single configuration mode, and in the literature, no generic model or formula is elaborated for power consumption estimation for different driving modes. Such, in chapter 3, a generic formula is proposed for power consumption modeling in the function of the degree of steerability, degree of actuation redundancy, and the kinematic and dynamic parameters of an over-actuated URV. Hereafter, we propose in the following chapters a new energy planning methodology for optimal autonomous driving, where the power consumption estimation plays an important role for planning the power distribution on the trajectory traversed by the URVs.



Figure 2.18: RomoRobot URV [Brembeck 2012]

## 2.4 Optimal autonomous driving of URVs

Many fields for autonomous driving of URVs are studied in the literature [Coutinho 2018], such as optimal path planning, optimal task assignment, trajectory optimization, and routing. In this thesis work, we proposed an offline energy planning that comes before the assignment of the previously mentioned techniques of autonomous navigation as shown in Fig. 2.19.

### 2.4.1 URV path planning problem

The Path Planning (PP) problem consists of finding a feasible pathway to a URV that visits the sequence of way-points (objectives) in 2D space, without taking into consideration the dynamics of the URV. PP is a geometrical problem, according to [Gasparetto 2015], where it is defined as a geometric path, irrespective of any specific time law. However, Trajectory Optimization (TO) consists of assigning a time law to a controlled geometric way. More sophisticated variants of the PP problem such as motion constraints require substantial simplifications and assumptions to be solved heuristically [Kunchev 2006], [Betts 1998] and [Betts 2010]. The field of TO has, however, not considered routing decisions, i.e. given a set of ordered way-points, it is possible to find a feasible trajectory for a generic URV  $\mathcal{D}$ : Let  $\mathcal{A}$  be an object (URV) moving in a workspace  $\mathcal{S}$  (e.g., in an euclidean space  $\mathcal{S} = \mathbb{R}^n$ ,  $n=2$  or  $3$ ). A set of obstacles  $\mathcal{B}_1, \dots, \mathcal{B}_m$  is assumed to be distributed over  $\mathcal{S}$ . The problem of PP consists in, given initial and final configurations (position and orientation) for  $\mathcal{A}$ , then finding a path in  $\mathcal{S}$  that avoids collisions with the objects  $\mathcal{B}_1, \dots, \mathcal{B}_m$  ([Latombe 2012]). It has been shown that the problem of PP is  $\mathcal{NP}$ -hard if the velocity of the object  $\mathcal{A}$  is unbounded and no rotation is considered [Reif 1994]. For [Gasparetto 2015], a PP problem consists of find-

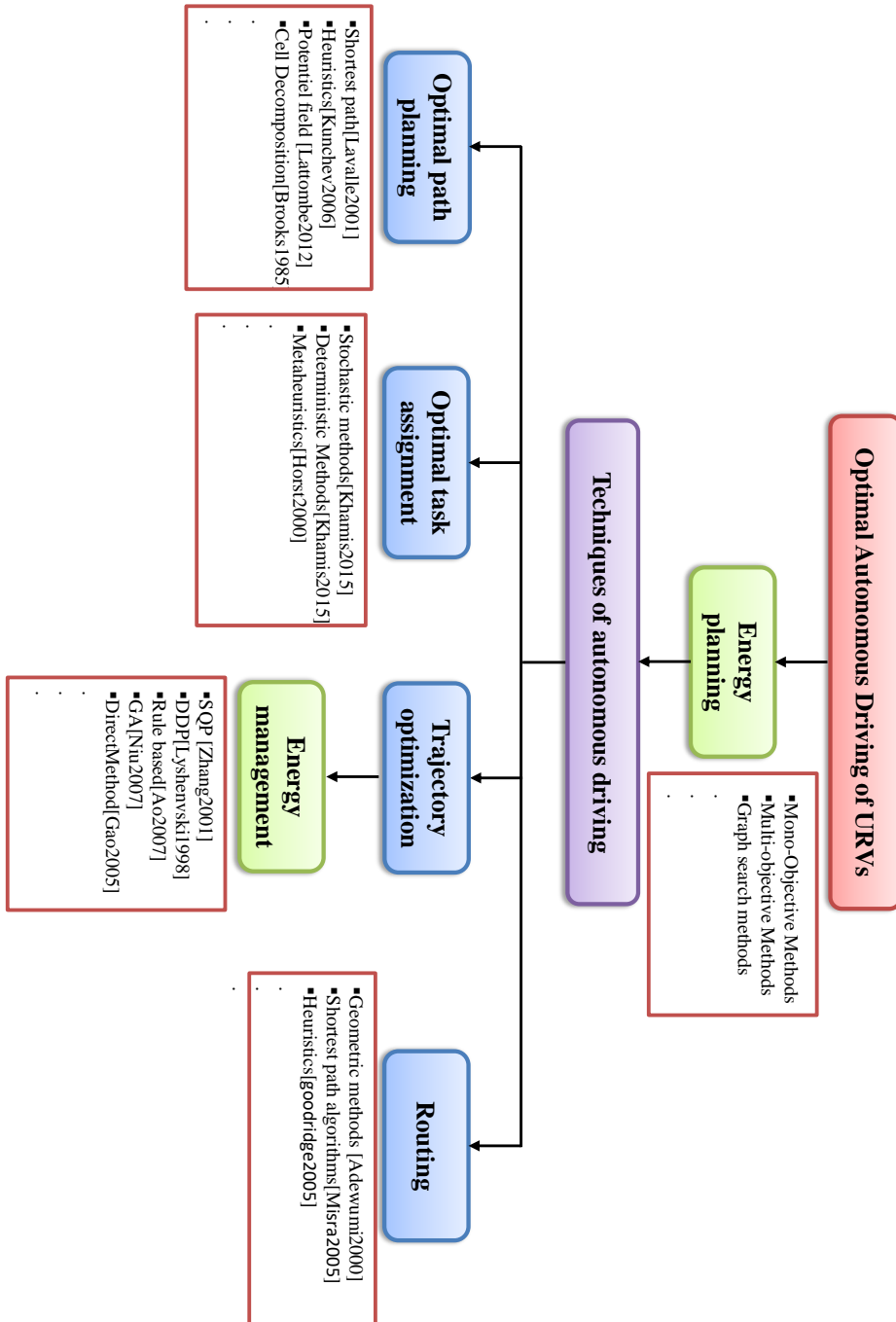


Figure 2.19: Optimal Autonomous Driving

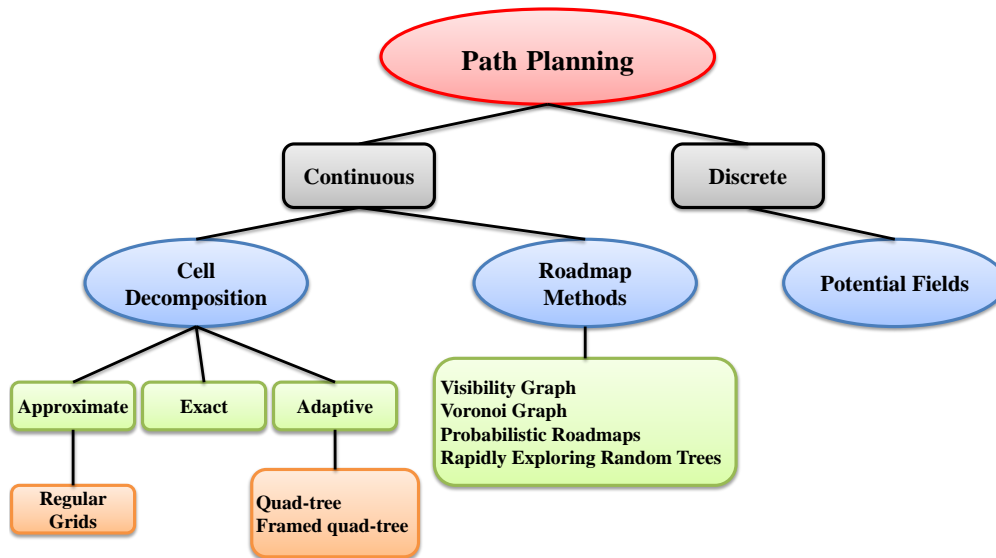


Figure 2.20: Family Tree of Path Planning Methods

ing a collision-free path among an environment from an initial point to a final goal. PP algorithms can be classified into discrete and continuous methods Fig. 2.20. In the former, workspace  $\mathcal{S}$  is transformed by discretization into a graph. Conventional heuristics or exact shortest path algorithms are then used to identify the path between a certain initial setting and a final setup. The output of discrete methods is often polygonal paths, i.e. paths with no limitation of curvature. Continuous methods represent  $\mathcal{S}$ , through the use of a continuous function using a potential field method [Barraquand 1992].

Most of PP methods use one of three types, called roadmap, cell decomposition and potential fields of space configuration. Roadmap model links particular targets in the graph, while cell decomposition methods decompose the workspace into grids, and possible areas model the workspace with mathematical fields. From the three most common ways, cell decomposition methods are the most used for PP. These methods can be either topological or metric. All methods listed below should be discrete with the exception of the Potential Field method, that can be continuously implemented in state space as well.

- **Cell decomposition methods** are methods for outdoor robotics and the most studied. The planning space is divided by these methods into discrete, non-overlapping regions that are subsets of the c-space and whose union exactly forms part of space  $\mathcal{S}$ . The result is a graph that is adjacent to each other cell. The connectivity graph is called the methods to go from one cell to adjacent cells. In cell decomposition, it can be distinguished approximate decomposition using regular grids [Brooks 1985]

and [Zhu 1990], exact decomposition [Sleumer 1999], [Schwartz 1983], [Avnaim 1988] and adaptive decomposition using quad-tree and framed quad-tree [Chen 1995], [Samet 1988], and [Noborio 1990].

- **Roadmap Methods** Roadmap Methods are the second most significant type of representation. Roadmaps are graphs that show how to go from one node to another node. Roadmap planning methods identify a set of one-dimensional curve connections between the URV's free space. Once the roadmap has been created, the planner will use it as a set of normalized paths to find the optimal solution. As examples, visibility graph [Nilsson 1984] and [Choset 1996], Probabilistic Roadmap (PRM) [Kavraki 1994]. and Exploring Random Trees RRT [Cheng 2001], [Frazzoli 2001], [Kuffner Jr 2000], and [LaValle 2001].

- **Potential Fields**

The third primary form of representation used in path planning is Potential Fields. The potential field methods are quite different from the planning methods and have been widely used in the past. A mathematical description is used in the whole area of robotic travel. This method treats the URV motion like an electron in an electrical field, as a point under the influence of fields generated by the world's objectives and obstacles. Obstacles create repulsive forces, and free-obstacles generate attractive forces [Khatib 1985] and [Latombe 2012].

Once a method of representing the environment has been established, it is then necessary to search for the best path through that representation. Graph search algorithms are used with the cell decomposition or roadmap methods of path planning, and also with the potential field methods. These search algorithms come from a wide variety of applications including general problem solving, artificial intelligence, computer networking, and mechanical manipulation. After an environment representative process is established, the best path through that representation must be searched. Graph search algorithms are used in path planning methods with cell decomposition methods, roadmaps methods, and also with potential field methods. Many graph search algorithms have been studied in the literature such as Dynamic Programming (DP), Dijkstra,  $A^*$ , ... etc.

## 2.4.2 Trajectory optimization problem of URVs

### 2.4.2.1 General formulation of optimal control problem

An optimal control problem is posed formally as follows. Determine the state (equivalently, the trajectory or path),  $\mathbf{x}(t) \in \mathbb{R}^n$ , the control  $\mathbf{u}(t) \in \mathbb{R}^m$ , the vector of static parameters  $\mathbf{p} \in \mathbb{R}^q$ , the initial time,  $t_0 \in \mathbb{R}$  and the terminal

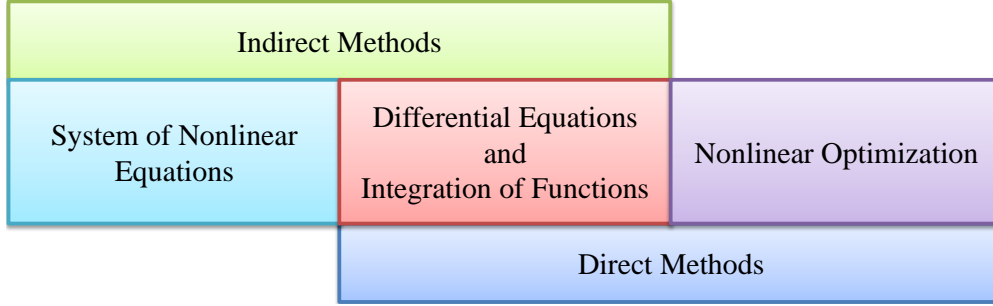


Figure 2.21: Components Of Optimal Control

time,  $t_f \in \mathbb{R}$  (where  $t \in [t_0, t_f]$  is the independent variable) that optimizes the performance index

$$J = \Phi [x(t_0), t_0, x(t_f), t_f; p] + \int_{t_0}^{t_f} \mathcal{L} [x(t), u(t), t; p] dt \quad (2.14)$$

subject to the dynamic constraints (i.e., differential equation constraints),

$$\dot{x}(t) = f [x(t), u(t), t; p] \quad (2.15)$$

the path constraints

$$C_{\min} \leq C [x(t), u(t), t; p] \leq C_{\max} \quad (2.16)$$

and the boundary conditions

$$\phi_{\min} \leq \phi [x(t_0), t_0, x(t_f), t_f; p] \leq \phi_{\max} \quad (2.17)$$

The state, control, and static parameter can each be written in component form as

$$x(t) = \begin{bmatrix} x_1(t) \\ \vdots \\ x_n(t) \end{bmatrix}; \quad u(t) = \begin{bmatrix} u_1(t) \\ \vdots \\ u_m(t) \end{bmatrix}; \quad p = \begin{bmatrix} p_1 \\ \vdots \\ p_q \end{bmatrix} \quad (2.18)$$

#### 2.4.2.2 Numerical methods used in optimal control

The following three fundamental components are at the heart of a reliable method to resolve optimal control problems: (1) ways to solve the differential equations and integrating functions; (2) a method to determine the system of nonlinear algebraic equal treatment; and (3) a process to resolve a nonlinear optimization problem. For all statistical purposes under optimal control, techniques for solving differential equations and integrating functions are re-choired. An indirect method is used to conjugate the numerical solution of



differential equations with the numerical solution of nonlinear equations, while a direct way combines the numerical solution of differential equations with nonlinear optimization. A scheme showing the components of the optimum control methods used for each class is presented in Fig. 2.21.

### 2.4.2.3 The trajectory optimization problem

A trajectory is usually associated with a set of Equations of Motions (EOMs), which describes the spatial-temporal change relationship of a system. The problem of TO is closely related to the issue of Optimal Control (OC) [Betts 2010]. Trajectory Optimization Problems (TOPs) include specific cases of Optimal Control (OC) problems, which determine a system trajectory (e.g., URVs) while minimizing performance and satisfying boundary conditions, path limitations and system dynamics.

Usually, system dynamics are modelled by a set of EOMs that can be non-linear and discontinuous. six degrees of freedom (6DOF) EOMs are composed by translational equations (containing forces, position, velocity, acceleration, etc.) and rotational equations (containing moments, angular velocities, angular acceleration, etc.). Under simplifying assumptions, 6DOF EOMs can be decoupled into three degrees of freedom (3DOF) EOMs.

For example, in the case of 3DOF, the state vector may represent the URV position, velocity, path angle, and yaw angle. Solving a Trajectory Optimization Problem (TOP) for a URV consists of generating the control vector inputs for the URV to deliver an optimal set of maneuvers. Dynamic and kinematic constraints are considered in TOP, and the optimal solution is produced as time-indexed states and controls such as positions, velocities, and accelerations. The TOP can be more complex and difficult if the considered boundary conditions depend on unknown variables or if the URV dynamics and kinematics vary over time.

In this case, TOPs can be divided into two or more phases so that changes of URV, operational or physical characteristics can be properly modelled. A phase in which the dynamic system remains unchanged can be defined as a segment of a trajectory. Phases can be described through their own constraints, differential equation of the system, operational constraints, and time.

For example, Euler methods are the most common single-step methods, while Adams-Bashforth and Adams-Moulton multi-step methods [Dahlquist 2003] are the most commonly used multi-step methods. The ability to resolve nonlinear optimization or nonlinear programming problems is a key ingredient in solving trajectory optimization problems, [Sherali 2006], [Bertsekas 2006] and [Boyd 2004] (NLPs). In addition, [Gear 1971] showed that the implicit methods are more stable than explicit methods. Runge-Kutta is used by [Butcher 2008] as an explicit method. The divided methods of collocation [Betts 2010] fall into three general categories: Gauss methods,

Radau methods, and Lobatto methods. TO problem can be solved by using two main methods class Direct methods and indirect methods [Rao 2014].

### 3.1. Direct and indirect methods for trajectory optimization problems

Two main classes of numerical methods, direct and indirect methods, became very common in solving TOPs. The direct methods depend on discretization into a problem of finite-dimensional optimization of an infinite-dimensional OC. This approach is frequently known as "discretize, then optimize", [Sherali 2006], [Bertsekas 2006], [Betts 2001], [Boyd 2004], and [Gill 1981]. For instance, the controls are discretized on a fixed grid using an arbitrary parametrization scheme in a direct single shooting method. The next phase of this technique is to solve the problem of non-linear programming to identify an optimal parameter vector. The indirect techniques are to determine the optimal criteria needed for an OC problem and then use a discretization method to solve the resulting equations. Indirect methods usually use "optimize, then discretize" strategy, [Athans 2013], [Bliss 1946], [Bryson 1975], [Fleming 2012], [Hildebrand 2012], [Hull 2013], [Leitmann 2013], [Vintner 2000]. For instance, the resulting optimality conditions in an indirect single shooting method consist of a boundary value problem that can be solved by a means of simple single shooting algorithm [Betts 2010]. In order to solve TOPs, several advanced algorithms were created.

### 2.4.3 URV routing problem

The Vehicle Routing Problem (VRP) in operational research and combinatorial optimization is a very well-known problem. In the VRP, it is necessary to assign routes to a set of vehicles that have to serve a set of customers to minimize the total cost of the operation. Its classic variant is called the Capacitated Vehicle Routing Problem (CVRP), in which each URV is allocated a load capability. The CVRP can be described generally as follows. A set of vertices  $V = \{0, \dots, \}$  and a set of arcs  $A$  are provided to connect these vertices. Each vertex reflects a client with cost  $d_i, i \in V \setminus \{0\}$ . A value of  $c_{ij}$  is allocated to each arc  $(i, j) \in A$ , which represents the travel cost between two customers. Let  $C = \{1, \dots, m\}$  be a collection of  $Q$  capacity homogeneous URVs. Here we specify the depot vertex  $I = 0$  (launching site). The CVRP consists of finding a minimum cost set of  $m$  routes starting and ending at the depot so that all customers are visited exactly once, the demands of all customers are met and the vehicles' capacity is respected. It is known that the CVRP is  $\mathcal{NP}$ -hard. More explanation and details about the VRP and its variants, such as [Cao 2017], [Caceres-Cruz 2015], [Kumar 2012], [Zirour 2008], [Ousingsawat 2004], and [Adewumi 2018].

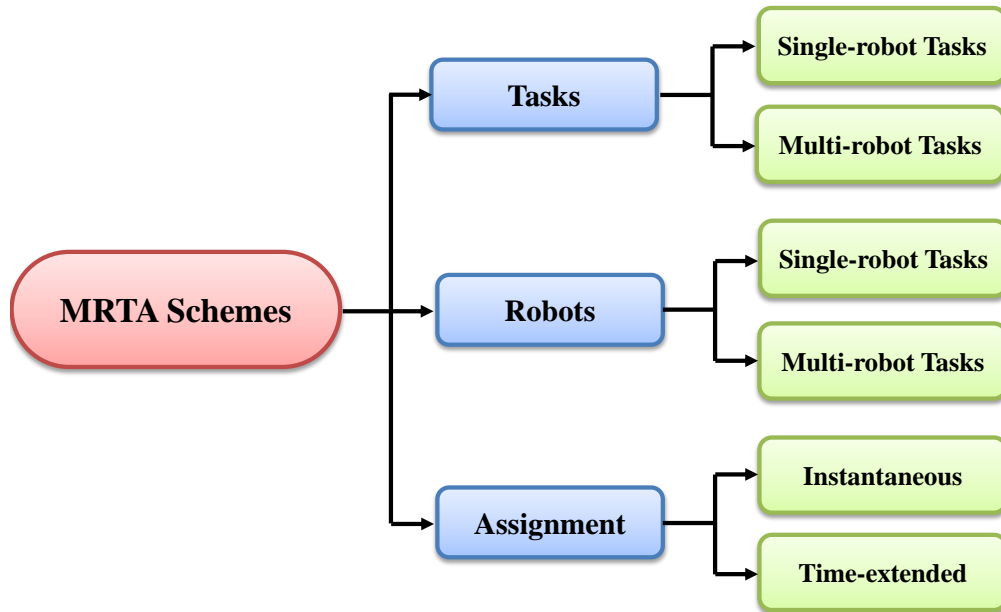


Figure 2.22: MRTA schemes

#### 2.4.4 URV task assignment problem

The problem of URV task assignment (URVTAP) is to find an optimal allocation of URVs to a set of tasks. The URVs frequently have distinguishable features and characteristics, and the jobs depend on the application's nature. This issue has been shown to be  $\mathcal{NP}$ -hard [Alidaee 2010]. Every day new complicated assignment issues arise due to the rapid growth of URV technology and many algorithms have been designed to defeat the unique challenges. One can notice that the science community has gained attention in this field of research. More literature review can be contained in [Khamis 2015] on algorithms for Multi-Robot Task Assignment (MRTA) issues.

As illustrated in Fig. 2.22, existing task allocation schemes can be categorized according to several dimensions [Dasgupta 2011]:

- Single task (ST) versus multi-task (MT), related to the parallel task performing capabilities of robots,
- Single robot (SR) versus multi-robot (MR), related to the number of robots required to perform a task, and
- Instantaneous assignment (IA) versus time extended assignment (TA), related to the planning performed by robots to allocate tasks.

Single task (ST) signifies that each robot can perform as most of one job at the moment, while MT implies that some robots can perform various functions at the same moment. Very similarly, SR indicates that to achieve

this, each task needs precisely one robot, while MR implies that numerous robots may be needed for specific tasks. In IA approaches, the accessible data about robots, jobs, and environment allows only instant distribution of tasks to robots (i.e. tasks independence is a strong assumption). Sometimes these methods are used to prevent the need for algorithms with high computational scheduling. In the other side, there are continuous task allocation or time extended assignment, where more information can be collected. TA is more challenging from a planning viewpoint because robots have to worry about the dependencies between tasks [Khamis 2011].

There are two popular approaches to the problem of task allocation from the planning viewpoint: decompose-then-allocate and allocate-then-decompose. In the first method, the complex task is decomposed into simplified sub-tasks and then these sub-tasks are distributed to the team members based on their ability and accessibility to finish the sub-tasks as needed, [Aylett 1998] and [Botelho 1999]. The cost of the final plan cannot be fully regarded in this sort of methods, because the task is decomposed without identifying to whom tasks need to be assigned. Another disadvantage of this form is that modifications in the constructed strategy are inflexible. So, even if it is found expensive, the plan designed by the central agent cannot be rectified. On the other hand, the complicated tasks are assigned to mobile sensors in the allocate-then-decompose strategy [Botelho 1999], and then each mobile sensor decomposes the assigned tasks locally. The major disadvantage of this strategy is that all functions are allocated to only one mobile sensor and therefore the preferred task decomposition is solely dependent on that mobile sensor's plan, which improves the chance of achieving a sub-optimal solution. Allocating tasks to more than one mobile sensor to consider distinct methods for the desired job may be more useful. While the techniques of decomposing-then-allocating and allocating-then-decomposing may be able to find possible plans, then both approaches have disadvantages.

Optimization-Based Approaches are the branch of applied mathematics that focuses on solving a particular problem to find the optimum solution to this issue from a set of available solutions. This set of possible solutions are limited by a set of constraints, and the optimum solution is selected. This criteria defines the objective function of the problem describing the system goal quantitatively [Horst 2000]. There are a large variety of available optimization approaches, and the use of these approaches depends on the nature and complexity of the problem to be optimized. Besides, optimization-based approach algorithms have more exceptional ability to explore new search domains in the search space because the randomness of the algorithm variables also allows for increased efficiency when dealing with noisy input information [Spall 2012], [Diwekar 2008], and [Lenagh 2013]. Fig. 2.23 presents a general classification of optimization methods, [Khamis 2015].

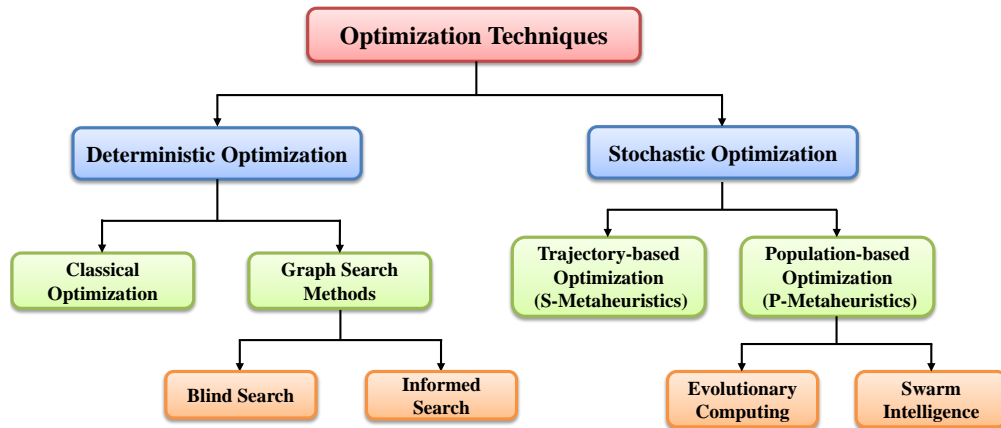


Figure 2.23: Optimization Techniques

Deterministic methods follow a strict procedure. The path and the values of variables of the functions are repeatable. The methods used are numerical and classical methods, such as quadratic programming, graphical methods, penalty methods, gradient and hessian based methods, derivative-free approaches, q sequential quadratic programming, etc. In these methods, the same path will be followed every time. They also involve graphics techniques like blind/uninformed searches and informed search procedures.

Stochastic techniques always have some randomness. These techniques can be classified into trajectory-based and population-based algorithms. A trajectory-based metaheuristic algorithm such as simulated annealing uses a single agent or solution which moves through the design space or search space in a piecewise style. A better move or solution is always accepted, while a not-so-good step can be taken with a certain probability. The steps or moves trace a trajectory in the search space, with a non-zero probability so that this trajectory can reach the global optimum. On the other hand, population-based algorithms such as genetic algorithms, ant colony optimization, and particle swarm optimization use multiple agents to search for an optimal or near-optimal solution.

Stochastic methods are always random. These methods can be categorized into algorithms based on trajectory and population. A metaheuristic trajectory algorithm such as simulated annealing utilizes one agent or solution that moves in a piece-wise manner through the design area or searches space. It is always acceptable to move better, while a less good move with a certain probability can be chosen. The steps or motions trace a search space trajectory, with a non-zero probability to make this trajectory achieve the global optimum. Population-based algorithms, for instance, such as genetic algorithms, optimization of the ant colony and optimization of particle swarm use multiple agents to find an optimal or nearly optimal solution.

#### 2.4.4.1 URV energy management

Energy Management (EM) for URVs is a special case in optimal control. The energy management approach uses different techniques. Dynamic programming, for example, is often used to reach the world's best. As described in Fig.2.24, a clustering review of co-words is also done in particular energy management approaches to further explore distinct types of energy management approaches such Genetic Algorithms (GA), Pontryagin's Minimum Principle (PMP), Model Predictive Control, NN and Edge Cloud Management Controller (ECMS). The two most commonly utilized energy management strategies are DP and Fuzzy Logic Control. The other energy management strategies include rule-based control, Particle Swarm Optimization (PSO), robust control, stochastic optimal control, Evolutionary Algorithm (EA), Support Vector Machine(SVM), convex optimization, Bees Algorithm(BA), direct method, machine learning, simulated annealing (SA), Quadratic Programming(QP), simplex method, shooting method, extremum seeking(ES), Game Theory (GT), Parallel Chaos Optimization Algorithm(PCOA), Dividing RECT angles algorithm(DIRECT), varying-domain optimization and soon.

Two major classes can be classified for the energy management strategy [Zhang 2015]. Rule-based energy management strategy, and optimization-based energy management strategy. Rule-based energy management strategy can be considered as a deterministic rule-based and a fuzzy rules-based energy management strategy, while optimization energy management strategies can be classified into a global energy management optimization strategy and real-time energy management optimization strategy based on operating driving conditions.

There are three primary solution techniques in consideration of the optimization problem of HEVs. The first approach optimizes the strategy parameters of a rules-based energy management strategy and therefore, the energy management problem becomes the parameter optimization problem, also known as the static optimization problem. The second approach formulates energy management as dynamic, nonlinear, and constrained optimization problem, Dynamic optimization algorithms can solve this problem. The third one simplifies the URVs optimal control problems with model approximations such as a mathematical programming, like sequential quadratic programming problem [Zhang 2001], quadratic programming problem [Kessels 2007], mixed integer linear programming problem [Salman 2005], [Wu 2014a], and convex programming problem [Elbert 2014]. Since Lyshevski et al. [Lyshevski 1998] first apply Deterministic Dynamic Programming (DDP) to optimal energy management of series HEVs in 1998, DDP has been widely used to optimization control for various types of HEVs, covering parallel HEV [Lin 2003], power-split HEV [Chen 2009], and PHEV [Gong 2007]. DDP is generally aimed to obtain, or evaluate the high performance of HEVs, easy, imple-

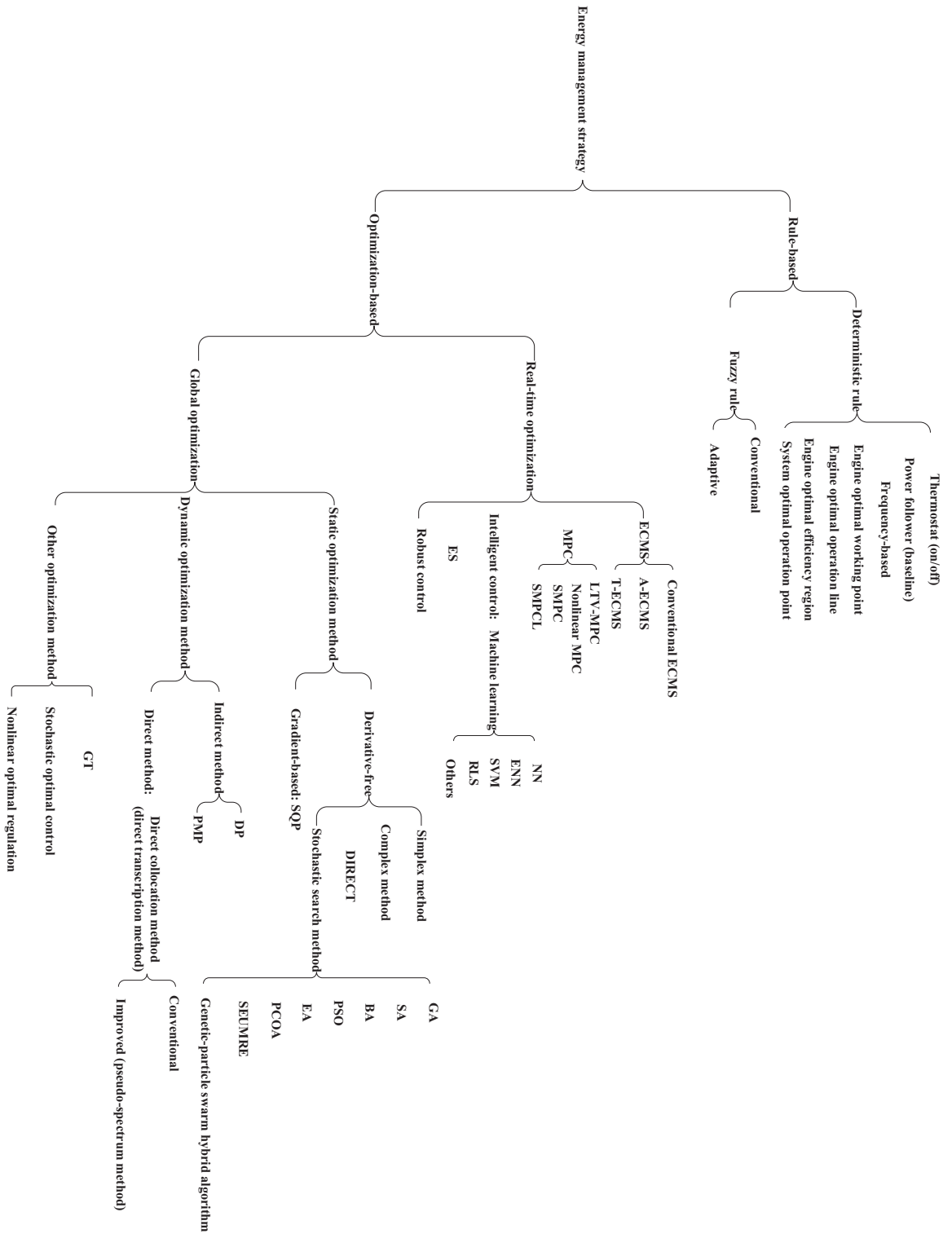


Figure 2.24: All EMS [Zhang 2015]

mentable, and best-performing rules in a rule-based energy management strategy [Ao 2007]. Although some feasible rule extraction methods have been proposed [Bianchi 2010], [Yu 2009], the rule extraction process is generally time-consuming; moreover, extracted rules are only suitable for a specific driving cycle. To overcome the above drawbacks of DDP, [Lin 2004] first propose SDP energy management strategy.

SP-SDP can benefit from an SDP-based energy management strategy with better SOC control and fewer parameters to adjust without a discount factor. After that, [Opila 2011], [Opila 2013], developed an energy management strategy based on SP-SDP, with a series-parallel HEV that takes account of fuel saving and drivability; while Moura et al. designed a battery health-conscious energy management strategy by applying SP-SDP. Various extended algorithms based on DP are implemented to decrease computational load and dependence on future driving cycles of DP. Fast Dynamic Programming (FDP) [Bin 2009], Neuro-Dynamic Programming (NDP) [Boyalı 2010], Iterative Dynamic Programming (IDP) [Wang 2012], boundary-line DP [Sundström 2010], two-scale DP [Gong 2007], multi-rate DP [Johri 2013], and hybrid optimal energy management strategy combining DP and classical control theory [Ngo 2010] are proposed to improve computational efficiency.

Also, an online learning energy management strategy composed of SDP and Temporal Difference (TD) method is used to improve the robustness to varying driving cycles and lower computational cost simultaneously [Li 2012].

To overcome the above disadvantages, the second approach is based on the future driving condition from the driving cycle [Kim 2011], [Boehme 2013] or driving cycle recognition [Jeong 2011]. For driving cycle prediction, the driving information is collected from a global position system (GPS). The optimal value of initial costate is approximated on the basis of effective SOC drop rate and effective mean required power in [Kim 2011] while it is estimated based on cruise time and available regenerative energy in [Razavian 2012]. Different from the methods proposed by [Kim 2011] and [Razavian 2012], Boehme et al. [Boehme 2013] and Kim et al. [Kim 2011] determine initial costate by solving an obvious optimal control problem with an indirect variation of extremals such as dampened Newton-method and a shooting method with multiple initial conditions based on Newton-Raphson method. Except for the estimation of initial costate, the discrepancy between the computation load of PMP and computational power of the vehicle controller also limits the application of PMP on a real-time control system. Generally, the look-up table is an excellent solution to the limits of storage capacity and computational power for the vehicle controller, which has been used to implement PMP online [Boehme 2013]. However, the size of the table will grow exponentially with the number of dimensions. Therefore, approximate PMP (A-PMP) is introduced by Hou et al. [Hou 2014]. Due to difficulty in dealing with inequality constraints, control



variable parameterization methods are not suitable for solving optimal control problems of HEVs. So, only direct collocation methods are employed to solve optimal control problems of HEVs [Pérez 2010]. Other optimization methods that were used in energy management optimization control for HEVs include GT [Dextreit 2013], stochastic optimal control [Kolmanovsky 2008] and non-linear optimal regulation feedback control [Sampathnarayanan 2014].

For example, the Sequential Quadratic Programming (SQP) algorithm has been applied in the optimization of energy management strategy parameters for a parallel HEV [Oh 2007].

Derivative-free methods that applied to energy management methodology optimization of HEVs mainly include simplex method [Tseng 2008], modified simplex method [Zhang 2001], complex method [Shuaiyu 2007], DIRECT [Gao 2005] and stochastic search methods (also called meta-heuristic search methods) [[Montazeri-Gh 2006]-[Wu 2014b]]. Due to global optimality and robustness, stochastic search methods are more suitable for optimal control problems of HEVs and thus attract more attention. These stochastic search methods include GA [Montazeri-Gh 2006], SA [Wang 2007], PSO [Wu 2008], EA [Zhang 2009], BA [Long 2012], and PCOA [Wu 2014a]. Each algorithm has its advantages and disadvantages, Adaptive SA(ASA) [Wang 2014], Adaptive Differential Evolution Algorithm (ADEA) [Wu 2011], genetic-algorithm swarm hybrid algorithm [Niu 2013], Real-valued GA (RGA) [Xiong 2009], space exploration and unimodal region elimination (SEUMRE) [Younis 2011] also have been proposed to improve convergence velocity and robustness.

In order to overcome the above limits, a varying-domain the method is presented to give a flexible priority among multi-objectives [Zhang 2014], improved non-dominated sorting genetic algorithm (NSGA-II) is utilized to solve multi-objective problems directly [Fang 2011]. However, like dynamic optimization methods, all above static optimization methods are sensitive to the driving cycle. Hence, driving cycle recognition is also necessary for improving the adaptability of this kind of method [Liang 2009].

#### 2.4.5 URV energy planning

Most of the URVs used for robotics and civil applications present a low autonomy. Therefore, it is essential for URV routing algorithms to accurately model battery life. According to [Abousleiman 2016] and [Thibault 2018], this can be achieved by integrating the URVs dynamics with routing. As mentioned by the authors, for powered URVs, a proper modelling of the actual fuel consumption must include, for instance, the current weight, the distance, the velocity and climb/descent rate. URV energy planning can be defined as the operation to execute before the realization of the everyday tasks in autonomous driving, as trajectory planning, path planning, routing, and task allocation. In our work, we proposed two main methodologies for energy planning, Discrete

methodology, and continuous methods. The Discrete methodology is based on the application of graph search methods on a digraph where the energy represents the cost of travelling from one node to another. The nodes in the digraph represent the segments of the path obtained after geometrical filtering. Graph search methods like dynamic programming [Bensekrane 2018], Dijkstra, and  $A^*$  are applied to obtain the optimal energy consumption of the vehicle. The continuous methodology is another approach of energy planning. This methodology consists of the use of mono-objective algorithms which can be solved with fmincon solver, Interior Point OPTimizer (IPOPT) solver or YALMIP solver, etc ..., or with multi-objective algorithms which can be solved with Genetic Algorithms (GA).

## 2.5 Conclusion

This chapter presents the global positioning of our work in terms of power consumption estimation and energy planning strategies. The rest of the thesis manuscript is organized as follows. In Chapter 3 a power estimation consumption is studied for different configuration driving modes with a quantitative and qualitative approach. Chapter 4 present a discrete methodology of energy planning. Whereas in Chapter 5 a continuous energy planning methodology is developed. Finally, in Chapter 6 a continuous energy planning methodology is developed.

# Power Consumption Modeling for Over-actuated URVs

---

## Contents

---

<b>3.1</b>	<b>Introduction</b> . . . . .	<b>45</b>
<b>3.2</b>	<b>Quantitative approach of power consumption modeling estimation</b> . . . . .	<b>46</b>
<b>3.3</b>	<b>Qualitative approach of power consumption modeling estimation</b> . . . . .	<b>51</b>
	3.3.1 ANFIS architecture . . . . .	51
	3.3.2 Estimation of Power Consumption . . . . .	53
<b>3.4</b>	<b>Road profile</b> . . . . .	<b>54</b>
<b>3.5</b>	<b>Experimental results and Model validation</b> . . . . .	<b>54</b>
<b>3.6</b>	<b>Conclusion</b> . . . . .	<b>64</b>

---

## 3.1 Introduction

URVs consume a substantial amount of energy while executing their tasks and missions. As the primary source of energy for autonomous electric URVs, the energy efficiency of these robots should be taken into consideration. The energy consumption model is the solution to investigate and develop the energy efficiency of URVs. In chapter 2, a comprehensive literature review of power consumption modelling is studied for URVs. Generally, most of the robots used have a differentiated driving configuration of velocity or skid driving. Power consumption has been considered for conventional vehicles, but no generic modelling has been highlighted to model the case of an over-actuated URV. This chapter focuses on the energy consumption modeling of URVs with two main methods. An analytic model with a global formulation of the power consumption taking into account the different parameters of kinematic properties. The second method consists of the use of Artificial Intelligence (AI) based on Neuro-Fuzzy Logic. A comparison of the power consumption of the autonomous URV RobuCAR for its different driving configurations is studied.

### 3.2 Quantitative approach of power consumption modeling estimation

In the present work, we propose a model of power consumption calculation expressed in function of the degree of steerability, the degree of redundancy and the path curvature. The aim is to formulate the power consumption according to geometric (path curvature) and kinematic (degree of steerability and degree of redundancy) parameters of the URV and its surrounding environment (forces and torques) in expressions of ground interaction. In this work, we examine only wheeled unmanned road vehicle.

The schematic top view of the considered URV is shown in Fig. 3.1, where all the dimensions and the forces operating on the system are described. The body-fixed frame is attached to the CoG of the URV, where  $X$  and  $Y$  axes represent longitudinal and lateral directions, respectively. The yaw motion of the URV is about an axis perpendicular to the  $X - Y$  plane.

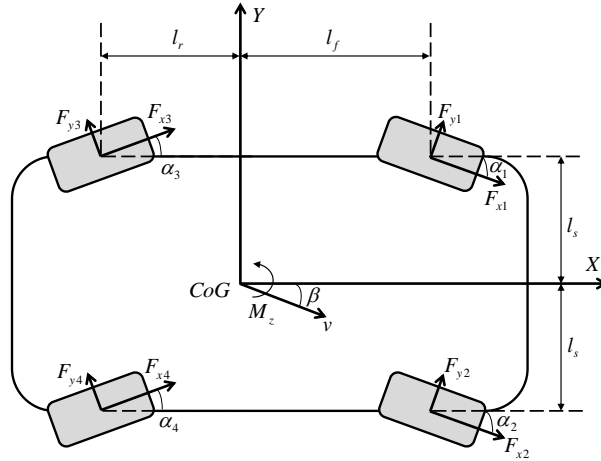


Figure 3.1: URV schematic diagram in Dual configuration

Referring to Fig. 3.1,  $F_{x_i}$  and  $F_{y_i}$  represent the traction and cornering forces acting on the  $i^{th}$  wheel, respectively, where the subscript  $i$  represents the wheel number ( $i=1, 2, 3,$  and  $4$ , for the front left, front right, rear left, and rear right wheel, respectively). The steering angle of the  $i^{th}$  wheel is denoted by  $\alpha_i$ , and the dimensions of the chassis are represented by  $l_s$ ,  $l_r$ , and  $l_f$ . The yaw angle of the vehicle is denoted by  $\beta$ . The forces acting on CoG are represented by  $F_x$  and  $F_y$  in the longitudinal and lateral directions, respectively. The yaw moment of CoG is represented by  $M_z$ . The effects of the suspensions are neglected on the overall dynamics because the URV is moving with low velocity and on a plane area.

The overall power consumption can be decomposed into three elements of power estimation including inertia power  $\hat{P}_i$ , rolling resistance power  $\hat{P}_r$ , and

### 3.2. Quantitative approach of power consumption modeling estimation 47

gravitational power  $\hat{P}_g$ . For general formulation of power consumption, we add the static power  $\hat{P}_s$  caused by various electrical components.

$$\hat{P} = \hat{P}_i + \hat{P}_r + \hat{P}_g + \hat{P}_s \quad (3.1)$$

where,

$$\hat{P}_i = \dot{q}^T M(q) \ddot{q} \quad (3.2)$$

$$\hat{P}_r = \dot{q}^T H(\dot{q}, q) \quad (3.3)$$

$$\hat{P}_g = \dot{q}^T G(q) \quad (3.4)$$

The power caused by the rolling resistance has a relation with the curvature of the trajectory  $C$ , the degree of steerability  $\delta s$ , and the degree of redundancy  $\delta_R$ .

$$\begin{aligned} \hat{P}_r &= \dot{q}^T H(\dot{q}, q) = [v \quad \dot{\beta}] [F_t \quad M_Z]^T \\ &= (F_t + \frac{M_Z \dot{\beta}}{v}) v \end{aligned} \quad (3.5)$$

$$C = \frac{\dot{\beta}}{v} \quad (3.6)$$

The linear and angular velocities of the URV are denoted by  $v$  and  $\dot{\beta}$ , respectively. From equations (3.5) and (3.6):

$$\hat{P}_r = (F_t + M_Z C) v \quad (3.7)$$

where,  $F_t$  is total traction force, which is given by:

$$F_t = \sqrt{(F_x^2 + F_y^2)} \quad (3.8)$$

The Ackerman steering angles [Jazar 2017] are given by:

$$\tan \alpha_1 = \frac{l_f}{\frac{1}{C} - \frac{l_s}{2}} \quad (3.9) \quad \tan \alpha_2 = \frac{l_f}{\frac{1}{C} + \frac{l_s}{2}} \quad (3.10)$$

$$\tan \alpha_3 = \frac{l_r}{\frac{1}{C} - \frac{l_s}{2}} \quad (3.11) \quad \tan \alpha_4 = \frac{l_r}{\frac{1}{C} + \frac{l_s}{2}} \quad (3.12)$$

$$\cot \alpha_f = \frac{\cot \alpha_1 + \cot \alpha_2}{2} \quad (3.13)$$

$$\cot \alpha_r = \frac{\cot \alpha_3 + \cot \alpha_4}{2} \quad (3.14)$$

where,  $\alpha_f$  and  $\alpha_r$  denote the equivalent angles for front and rear steering respectively. Power consumption for a URV can be estimated in terms of longitudinal  $F_x$  and lateral  $F_y$  forces, and yaw moment  $M_z$  about the axis perpendicular to the plane of motion.  $F_x$ ,  $F_y$ , and  $M_z$  can be given by [Wang 2009]:

$$F_x = \sum_{i=1}^4 F_{x_i} \cos \alpha_i - \sum_{i=1}^4 F_{y_i} \sin \alpha_i \quad (3.15)$$

$$F_y = \sum_{i=1}^4 F_{x_i} \sin \alpha_i + \sum_{i=1}^4 F_{y_i} \cos \alpha_i \quad (3.16)$$

$$M_z = \sum_{i=1}^4 (-1)^i l_s (F_{x_i} \cos \alpha_i - F_{y_i} \sin \alpha_i) + \sum_{i=1}^2 l_f (F_{x_i} \sin \alpha_i + F_{y_i} \cos \alpha_i) - \sum_{i=3}^4 l_r (F_{x_i} \sin \alpha_i + F_{y_i} \cos \alpha_i) \quad (3.17)$$

In the above equations (3.15) to (3.17),  $F_x$ ,  $F_y$ , and  $M_z$  are calculated for a single configuration only, while  $\delta_S$  and  $\delta_R$  are not included in the model. Therefore, we propose a model for calculating  $F_x$ ,  $F_y$ , and  $M_z$  in terms of  $\delta_S$  and  $\delta_R$ , so that these forces can be calculated for different configurations. The forces and moment can be given by [Bensekrane 2017]:

$$F_x = \sum_{i=1}^{\delta_R - \delta_S + 3} F_{x_i} \cos \alpha_i - \sum_{i=1}^{\delta_R - \delta_S + 1} \left( \frac{\delta_S}{2} (3 - \delta_S) \right) F_{y_i} \sin \alpha_i - \sum_{i=\delta_R - \delta_S + 2}^{\delta_R - \delta_S + 3} \left( \frac{\delta_S}{2} (\delta_S - 1) \right) F_{y_i} \sin \alpha_i \quad (3.18)$$

$$F_y = \sum_{i=1}^{\delta_R - \delta_S + 3} F_{y_i} \cos \alpha_i + \sum_{i=1}^{\delta_R - \delta_S + 1} \left( \frac{\delta_S}{2} (3 - \delta_S) \right) F_{x_i} \sin \alpha_i + \sum_{i=\delta_R - \delta_S + 2}^{\delta_R - \delta_S + 3} \left( \frac{\delta_S}{2} (\delta_S - 1) \right) F_{x_i} \sin \alpha_i \quad (3.19)$$

### 3.2. Quantitative approach of power consumption modeling estimation 49

$$\begin{aligned}
M_z = & \sum_{i=1}^{\delta_R - \delta_S + 3} (-1)^i l_s F_{x_i} \cos \alpha_i + \\
& \left[ \sum_{i=1}^{\delta_R - \delta_S + 1} l_f F_{y_i} \cos \alpha_i - \sum_{i=\delta_R - \delta_S + 2}^{\delta_R - \delta_S + 3} l_r F_{y_i} \cos \alpha_i \right] + \\
& \left[ \sum_{i=1}^{\delta_R - \delta_S + 1} (-1)^{i+1} l_s \left( \frac{\delta_S}{2} (3 - \delta_S) \right) F_{y_i} \sin \alpha_i + \right. \\
& \left. \sum_{i=\delta_R - \delta_S + 2}^{\delta_R - \delta_S + 3} (-1)^{i+1} l_s \left( \frac{\delta_S}{2} (\delta_S - 1) \right) F_{y_i} \sin \alpha_i \right] + \\
& \left[ \sum_{i=1}^{\delta_R - \delta_S + 1} l_f \left( \frac{\delta_S}{2} (3 - \delta_S) \right) F_{x_i} \sin \alpha_i \right] - \\
& \left[ \sum_{i=\delta_R - \delta_S + 2}^{\delta_R - \delta_S + 3} l_r \left( \frac{\delta_S}{2} (\delta_S - 1) \right) F_{x_i} \sin \alpha_i \right] \quad (3.20)
\end{aligned}$$

Refer to equations (3.5) to (3.17) and (3.18) to (3.20), the power consumption estimation for the URV is developed, which includes  $\delta_R$ ,  $\delta_S$ , and  $C$ . Therefore, the power consumption for a URV can be estimated for the different configurations (single, dual, and skid) and for the different degree of actuation redundancy for a given trajectory of varying curvature. The wheel and ground contact forces  $F_{x_i}$  and  $F_{y_i}$  can be estimated using the magic formula given by Pacejka [Pacejka 2005]. Hence, the proposed model for the power consumption estimation can be exploited for power planning of a URV for a specific task with different configurations.

The formulation given in [Bensekrane 2017] for the analytic model is considered for fully actuated URV. How this new formulation compared to the one given in [Bensekrane 2017], and how it is derived for  $F_x$ ,  $F_y$ , and  $M_z$  which can also handle the case of not-actuated wheels.

$$\begin{aligned}
F_x = & \sum_{i=1}^{\delta_R - \delta_S + 1} F_{x_i} \cos \alpha_i + \sum_{i=\delta_R - \delta_S + 2}^{\delta_R - \delta_S + 3} \frac{1}{2} (1 - \delta_S + \delta_R) F_{x_i} \cos \alpha_i - \\
& \sum_{i=1}^{\delta_R - \delta_S + 1} \left( \frac{\delta_S}{2} (3 - \delta_S) \right) F_{y_i} \sin \alpha_i - \\
& \sum_{i=\delta_R - \delta_S + 2}^{\delta_R - \delta_S + 3} \left( \frac{\delta_S}{4} (\delta_S - 1) (1 - \delta_S + \delta_R) \right) F_{y_i} \sin \alpha_i \quad (3.21)
\end{aligned}$$

$$\begin{aligned}
 F_y = & \sum_{i=1}^{\delta_R - \delta_S + 3} F_{y_i} \cos \alpha_i + \sum_{i=\delta_R - \delta_S + 2}^{\delta_R - \delta_S + 3} \frac{1}{2} (1 - \delta_S + \delta_R) F_{y_i} \cos \alpha_i + \\
 & \sum_{i=1}^{\delta_R - \delta_S + 1} \left( \frac{\delta_S}{2} (3 - \delta_S) \right) F_{x_i} \sin \alpha_i + \\
 & \sum_{i=\delta_R - \delta_S + 2}^{\delta_R - \delta_S + 3} \left( \frac{\delta_S}{4} (\delta_S - 1) (1 - \delta_S + \delta_R) \right) F_{y_i} \sin \alpha_i \quad (3.22)
 \end{aligned}$$

$$\begin{aligned}
 M_z = & \sum_{i=1}^{\delta_R - \delta_S + 1} (-1)^i l_s F_{x_i} \cos \alpha_i + \\
 & \sum_{i=\delta_R - \delta_S + 2}^{\delta_R - \delta_S + 3} \frac{1}{2} (1 - \delta_S + \delta_R) (-1)^i l_s F_{x_i} \cos \alpha_i + \\
 & \left[ \sum_{i=1}^{\delta_R - \delta_S + 1} l_f F_{y_i} \cos \alpha_i - \sum_{i=\delta_R - \delta_S + 2}^{\delta_R - \delta_S + 3} \frac{1}{2} (1 - \delta_S + \delta_R) l_r F_{y_i} \cos \alpha_i \right] + \\
 & \left[ \sum_{i=1}^{\delta_R - \delta_S + 1} (-1)^{i+1} l_s \left( \frac{\delta_S}{4} (\delta_S - 1) (1 - \delta_S + \delta_R) \right) F_{y_i} \sin \alpha_i + \right. \\
 & \left. \sum_{i=\delta_R - \delta_S + 2}^{\delta_R - \delta_S + 3} (-1)^{i+1} l_s \left( \frac{\delta_S}{2} (\delta_S - 1) \right) F_{y_i} \sin \alpha_i \right] + \\
 & \left[ \sum_{i=1}^{\delta_R - \delta_S + 1} l_f \left( \frac{\delta_S}{2} (3 - \delta_S) \right) F_{x_i} \sin \alpha_i \right] - \\
 & \left[ \sum_{i=\delta_R - \delta_S + 2}^{\delta_R - \delta_S + 3} l_r \left( \frac{\delta_S}{4} (\delta_S - 1) (1 - \delta_S + \delta_R) \right) F_{x_i} \sin \alpha_i \right] \quad (3.23)
 \end{aligned}$$

Due to the presence of unknown dynamic parameters of the URV and uncertainties about its interaction with the environment, it is difficult to estimate with accuracy the efforts due to the interaction wheel-ground. Thus, an artificial intelligence technique based on a data-learning qualitative method for power consumption estimation is proposed, namely: Adaptive Neuro-Fuzzy Inference System (ANFIS).



### 3.3 Qualitative approach of power consumption modeling estimation

In this section, we present a qualitative data-learning approach, based on Adaptive Neuro Fuzzy Inference System (ANFIS) for power consumption estimation, where both of the velocity profile and the driving modes are considered. The estimation is compared with the experimental measurements taken from a real URV, i.e. RobuCAR. This choice is motivated mainly by the topology of the sampled input-output data pairs. However, the power consumed by the URV abruptly can change from one range of the input parameter values to another. This is due to the conditions of driving the URV and uncertainties on vehicle dynamics and interfered environment. Thus, the aim of this work is to classify the sampled input-output data pairs in clusters and proceed in local regression, thereafter. The fuzzy logic layers perform clustering while the neural network layers handle local regressions. The principle is to build an ANFIS model which emulates the different URV's driving modes. However, if we consider the six driving modes described above, the URV's dynamic behavior can change from one mode to another. To improve the regression performance, six separate ANFIS models are considered, one for each driving mode. In the following subsections, the ANFIS architecture and the data-learning algorithm are presented.

#### 3.3.1 ANFIS architecture

The considered ANFIS is structured as in Fig. 3.2, where the model inputs are the curvature of the road  $C$ , the velocity  $V$  and the acceleration  $A$  of the URV, while the power  $P$  which is consumed by the URV is considered as an output of the ANFIS model. For that, the Takagi and Sugeno's type rules are considered [Jang 1993] as follows:

Rule1: If  $C$  is  $C_1$  and  $V$  is  $V_1$  and  $A$  is  $A_1$ , then  $P$  is  $p_1C + q_1V + r_1A + s_1$ . Where,  $p_1$ ,  $q_1$ ,  $r_1$ , and  $s_1$  are constants, while,  $V_1$ ,  $A_1$ , and  $C_1$ , are the fuzzy sets in the antecedents parts of the rule, and  $P = f(C, V, A)$  is a crisp function in the consequent part.

The output of each ANFIS layer is evaluated as follows:

**Layer 1:** Each  $i^{th}$  node in this layer is given by:

$$O_i^1 = \mu_{A_i}(x) \tag{3.24}$$

where,  $x$  is the input to  $i^{th}$  node,  $A_i$  is the linguistic variable associated with this node function, and  $\mu_{A_i}$  is the membership function of  $A_i$ . The generalized

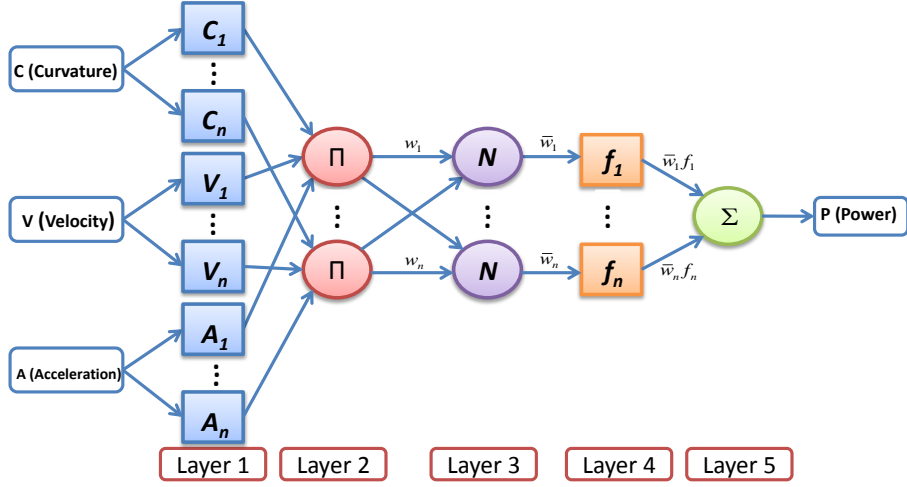


Figure 3.2: ANFIS architecture.

bell-shaped membership function is chosen for  $\mu_{A_i}(x)$ :

$$\mu_{A_i}(x) = \frac{1}{1 + [(x - c_i/a_i)^2]^{b_i}} \quad (3.25)$$

where,  $\{a_i, b_i, c_i\}$  is the premise parameter set.

**Layer 2:** Each node in this layer calculates the firing strength  $w_i$  of a rule. The output of each node is the product of all the incoming signals to it:

$$O_i^2 = w_i = \mu_{C_i}(C) \times \mu_{V_i}(V) \times \mu_{A_i}(A), \quad i = 1, 2, \dots, n. \quad (3.26)$$

**Layer 3:** The output of each node represents the normalized firing strength, which is given by:

$$O_i^3 = \bar{w}_i = \frac{w_i}{w_1 + w_2 + \dots + w_n} \quad (3.27)$$

**Layer 4:** Every  $i^{\text{th}}$  node in this layer is an adaptive node, associated to a function given by:

$$O_i^4 = \bar{w}_i f_i = \bar{w}_i (p_i C + q_i V + r_i A + s_i) \quad (3.28)$$

where,  $\bar{w}_i$  is the output of Layer 3 and  $\{p_i, q_i, r_i, s_i\}$  is the consequent parameter set.

**Layer 5:** This layer comprises one node, and computes the overall output as the summation of all incoming signals, i.e.,

$$O_i^5 = \sum_i \bar{w}_i f_i = \frac{\sum_i w_i f_i}{\sum_i w_i} \quad (3.29)$$

### 3.3. Qualitative approach of power consumption modeling estimation 53

#### 3.3.1.1 Data-Learning algorithm

By observing the ANFIS structure, it can be observed that the values of the premise parameters and the output of the system can be expressed as a linear combination of the consequent parameters  $(p_1, q_1, r_1, s_1, \dots, p_n, q_n, r_n, s_n)$  as follows:

$$\begin{aligned} P &= \frac{w_1}{w_1 + w_2 + \dots + w_n} f_1 + \frac{w_2}{w_1 + w_2 + \dots + w_n} f_2 + \dots \\ &\quad + \frac{w_n}{w_1 + w_2 + \dots + w_n} f_n \\ &= \bar{w}_1 f_1 + \bar{w}_2 f_2 + \dots + \bar{w}_n f_n \\ &= (\bar{w}_1 C) p_1 + (\bar{w}_1 V) q_1 + (\bar{w}_1 A) r_1 + (\bar{w}_1) s_1 + (\bar{w}_2 C) p_2 \\ &\quad + (\bar{w}_2 V) q_2 + (\bar{w}_2 A) r_2 + (\bar{w}_2) s_1 + \dots + (\bar{w}_n C) p_n \\ &\quad + (\bar{w}_n V) q_n + (\bar{w}_n A) r_n + (\bar{w}_n) s_n \end{aligned} \tag{3.30}$$

In the learning process, the following parameters are recognized by using the least squares calculated in the forward pass. In the backward pass, the premise parameters are updated by the mean of the gradient descent algorithm using the error signals [Jang 1993].

#### 3.3.2 Estimation of Power Consumption

The database for ANFIS model learning is built by SCANer<sup>TM</sup> studio. Different training paths containing data of the curvature points in the vehicle's trajectory are considered. In SCANer<sup>TM</sup> studio environment, the velocity profile is varied in the range [1, 16] km/h with a step size of 1 km/h for each driving mode; then, velocity profile, acceleration, path curvature, and the consumed power are recorded. We obtained the databases described in Table 3.1. Each database is divided into three subsets: training, validation and test sets. The training set is used during the learning phase, and the test set is only used to evaluate the performance of ANFIS models. For a good generalization and to avoid the over-fitting situation, the validation set is used during the training phase and the early-stopping method is applied for training. The early-stopping method requires that after a period of training (an epoch) using the training set, the weight matrices of ANFIS are fixed, and the ANFIS operates in the forward mode utilizing the validation set. The process is reiterated until the mean square error from learning (ML) on the validation set reaches its minimum value. Fig. 3.3 describes the flowchart for the estimation of power consumption. For a given trajectory, the inputs of the training model are driving modes, road profile (curvature of the trajectory), velocity and acceleration profiles.

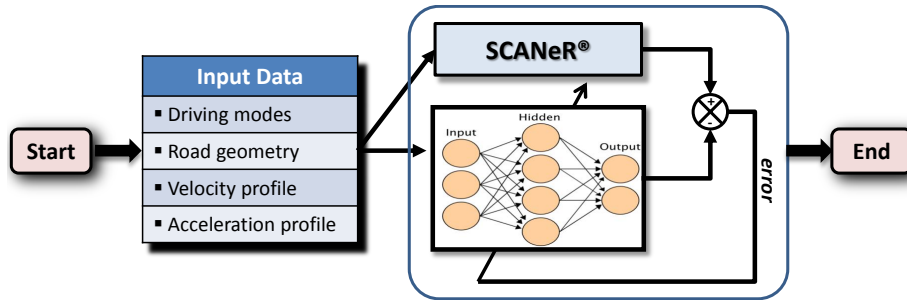


Figure 3.3: Flowchart for the estimation of the power consumption.

### 3.4 Road profile

For the road geometry, we used a Geographical Information System (GIS) to represent the road by polylines [Jakkula 2007], describing the central axis of its surface. Each point of this polyline is defined by the 3D geographic coordinates (longitude, latitude, and altitude). This discrete representation is not always appropriate for realistic simulation or path planning. A continuous representation, often parametric, is necessary to estimate all the parameters required for the calculation (contact angle of yaw, radius, etc.) in each point of the curve. To simplify this representation, the road path is decomposed into horizontal and vertical curves representing respectively the roads mapped onto the plane (Fig. 3.4). In this work, the cubic spline interpolation approach for polylines is used to describe the real trajectory [Ahlberg 1967].

The GIS data for real road is often affected by errors of acquisition systems, which explains the fluctuations presented in the estimated curvature of the 2D trajectory for the University of Lille campus as shown in Fig. 3.5.

For ANFIS parameters initialization, three membership functions are considered for each linguistic variable, and the grid partitioning method is used to initialize the fuzzy rules, the premise, and the consequent parameters. The ANFIS models converge approximately after 2000 epochs. In Table 3.1, different ML are obtained on the corresponding test sets.

### 3.5 Experimental results and Model validation

To estimate the URV's power consumption with all possible driving modes and velocity profile along a defined trajectory, it is useful to use a professional real-time simulation software of vehicle dynamics [Okt] called SCANer<sup>TM</sup> studio, that can emulate the numerous experimental scenarios that we should realize with the real URV Fig. 3.6. With SCANer<sup>TM</sup> studio, it is possible to simulate both: the vehicle dynamics, the terrain, and the environment. For that, we need first to validate the vehicle dynamics of the URV from the simulator. To



Figure 3.4: Trajectory from the Campus of University of Lille

reach this objective, we equipped the RobuCAR URV with a GPS (Septentrio Asterx4) to measure the position of the CoG, and an inertial unit (x-IMU) to measure the longitudinal and lateral accelerations. For battery measurement, current and voltage are measured directly from the battery.

Fig. 3.7 indicates the executed 2D path and its associated curvature by the real RobuCAR with their validated model from SCANeR™.

A comparison between experimental and simulated angular velocities for each wheel, the longitudinal acceleration of CoG, steering angles for each wheel, the lateral acceleration of CoG, of the RobuCAR URV are given respectively in Fig. 3.8, Fig. 3.9, Fig. 3.10 and Fig. 3.11 respectively.

Fig. 3.12 compares between experimental and simulated (a) battery voltage, (b) battery current, and (c) power consumption of the RobuCAR URV. The difference in the battery voltage and power consumption amplitudes between the real measures and simulated data can be explained in part by the presence of uncertainties related to the driving wheel-road efforts, where they are difficult to reproduce accurately as in the experiments. Therefore, the estimated power consumption using the simulator SCANeR™ studio conforms macroscopically to the profile of the power of the real RobuCAR. Due to the use of a numerical filter, the amplitude of the power consumption differs from

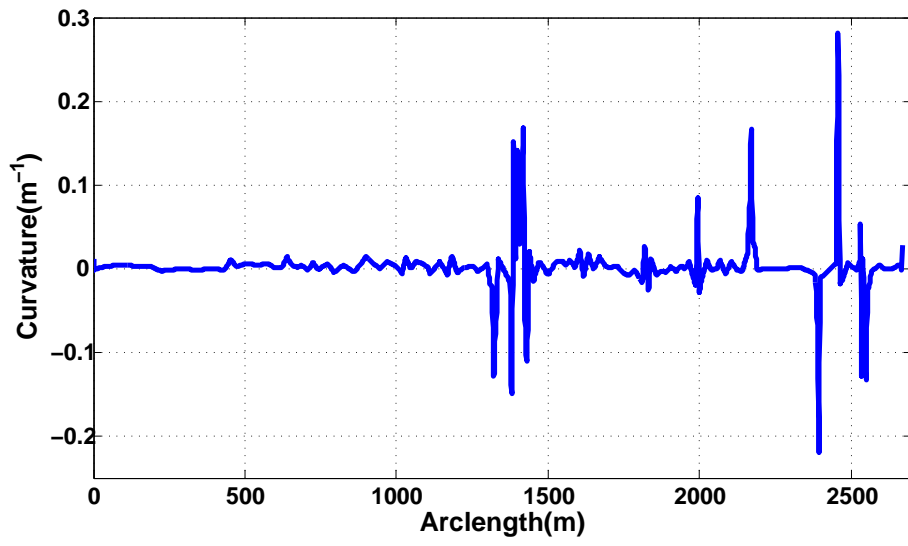


Figure 3.5: Curvature of the trajectory



Figure 3.6: RobuCAR

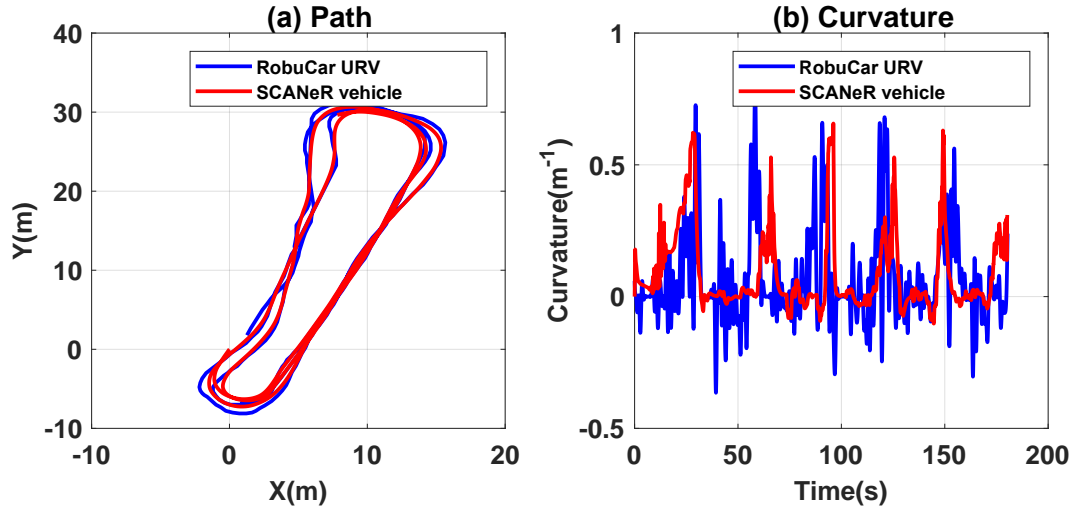


Figure 3.7: Comparison between SCANeR model and Experimental path with curvature profile for Dual4 driving mode.

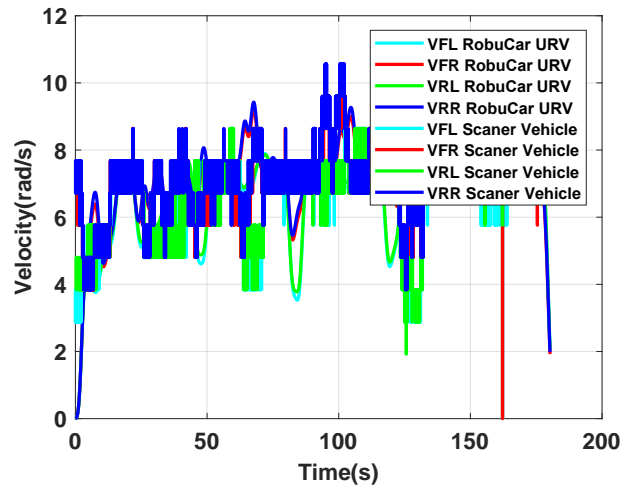


Figure 3.8: Comparison between experimental and simulated angular velocities for each wheel.

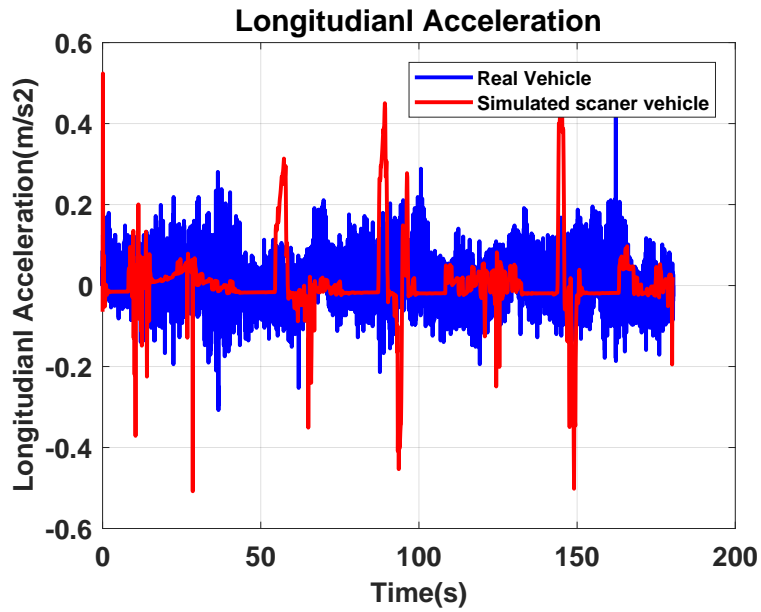


Figure 3.9: Comparison between experimental and simulated longitudinal acceleration for each wheel.

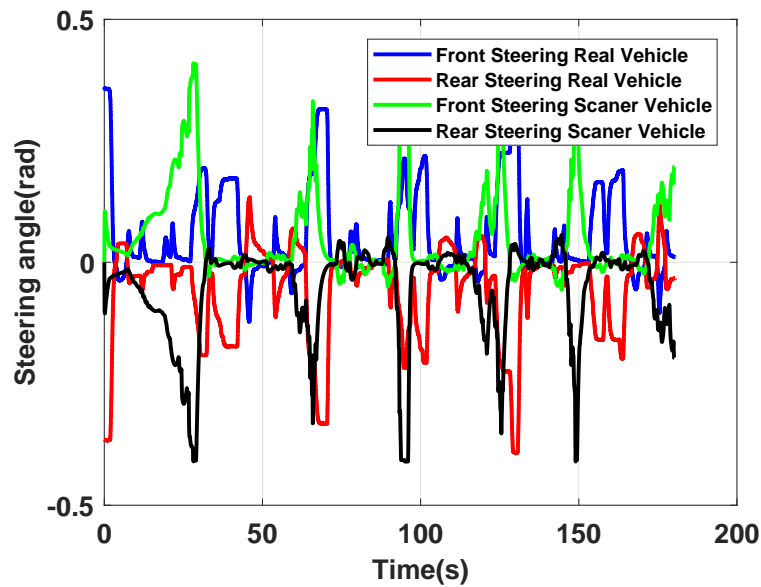


Figure 3.10: Comparison between experimental and simulated steering angles for each wheel.



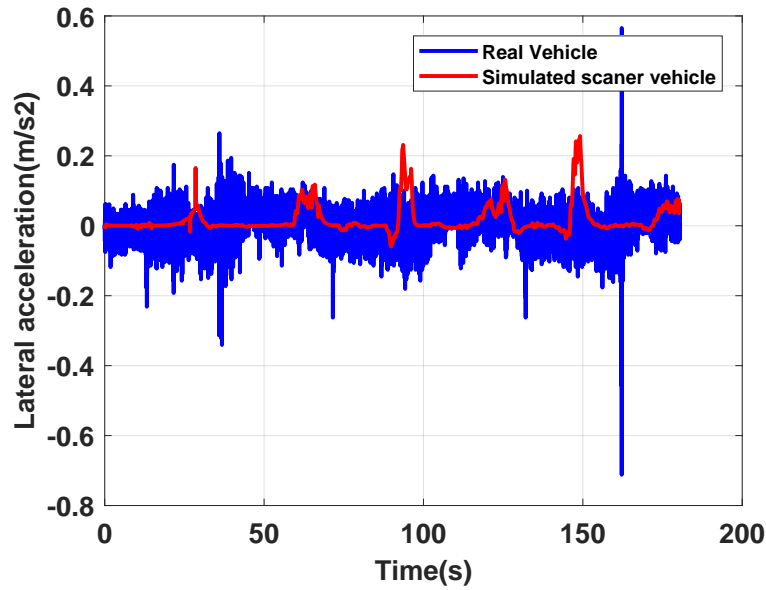


Figure 3.11: Comparison between experimental and simulated lateral acceleration for each wheel.

the simulated and the real power consumption.

In Fig. 3.13(a) and (b), a superposition between the power-time consumption, calculated from ANFIS, from Analytic model, and the experiments are shown for the Skid4 and Skid2 cases, while in Fig. 3.14(a) and (b), show the comparison between the power consumption, calculated from ANFIS, from Analytic model, and the experiments in case of Single4 and Single2. Finally, in Fig. 3.15(a) and (b), comparison between the power consumption from ANFIS, from Analytic model, and the experiments in case Dual4 and Dual2 steering configurations is shown. From the results of power consumption estimation, it can be observed that ANFIS and analytic models follow the experimental power consumption, and it can be seen that the Skid2/4 consume more power than other modes, but the power consumption can be less with Single2, Single4, Dual2, or Dual4 mode at different points of trajectory as shown in Fig. 3.14-Fig.3.15. It can be noticed also that the ANFIS model show better accuracy than the analytic models. The values of mean errors for each mode are given in Table 3.1.

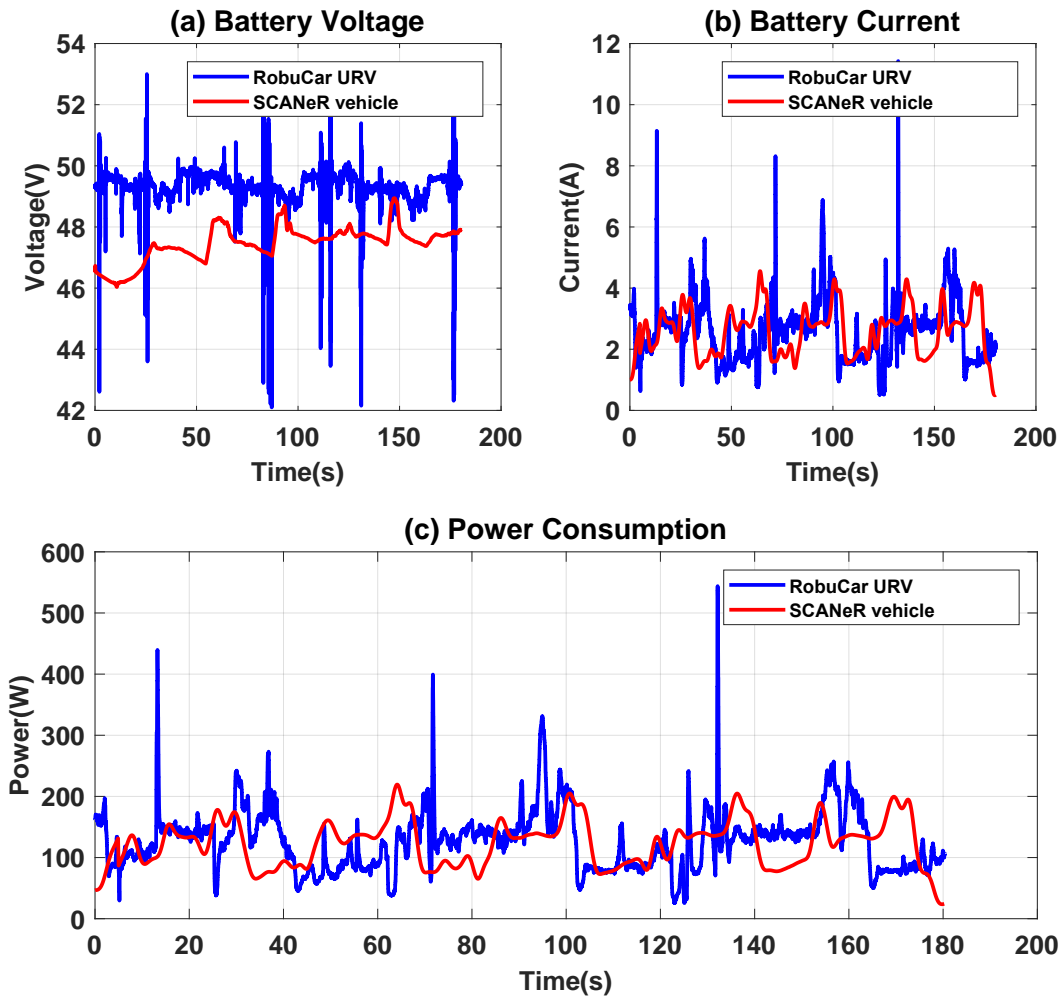


Figure 3.12: Comparison between (a) battery voltage, (b) battery current, and (c) Power consumption of Real Vehicle and simulated model in SCANeR<sup>TM</sup>

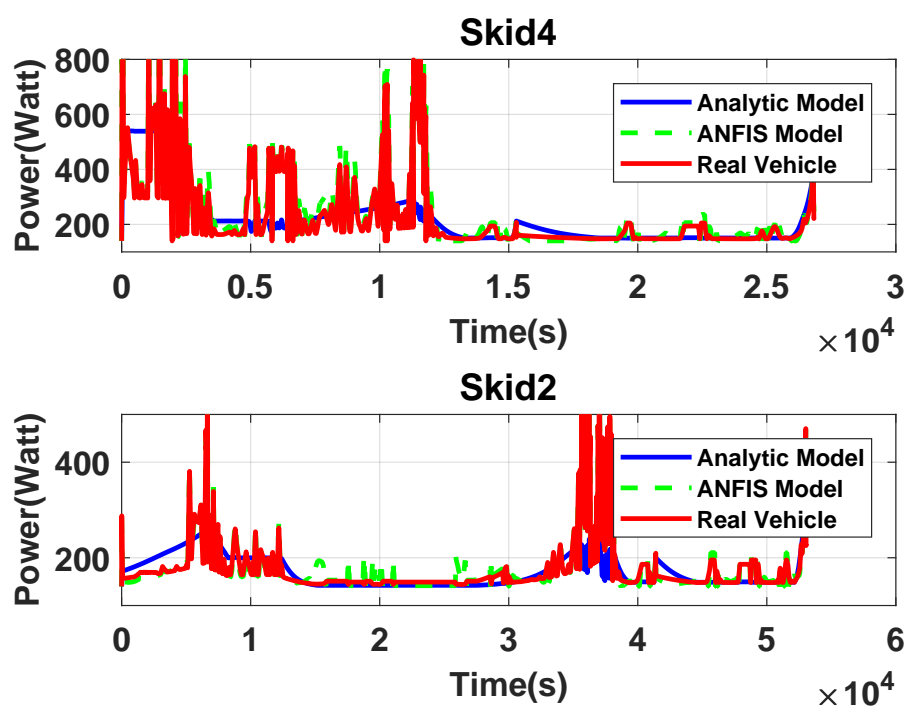


Figure 3.13: Comparison of the power consumption of URV using ANFIS and experiment with (a) Skid4 and (b) Skid2 configurations.

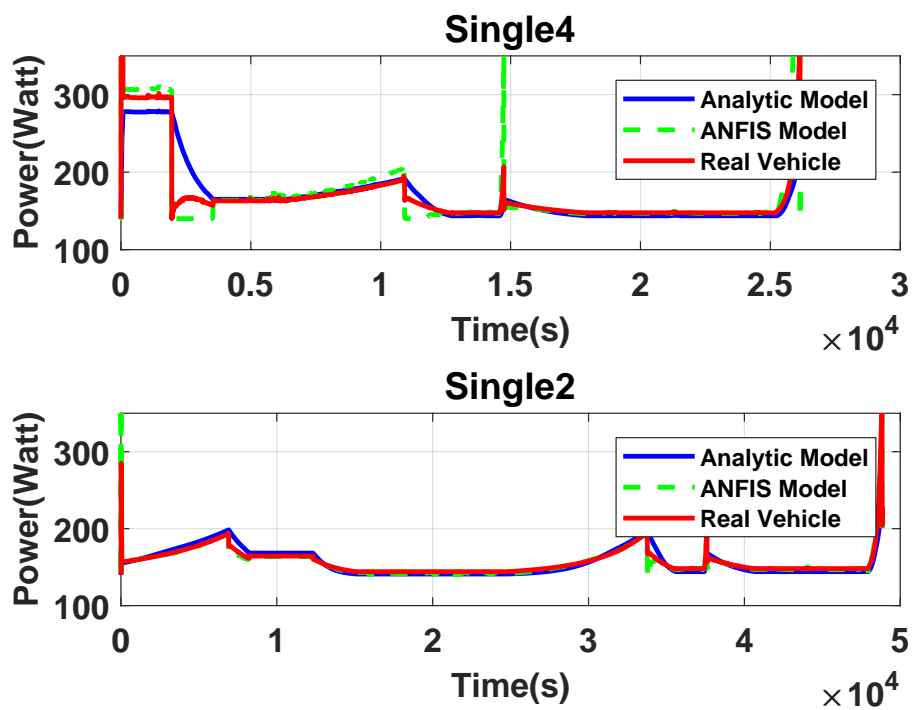


Figure 3.14: Comparison of the power consumption of URV using ANFIS and experiment with (a) Single4 and (b) Single2 configurations.

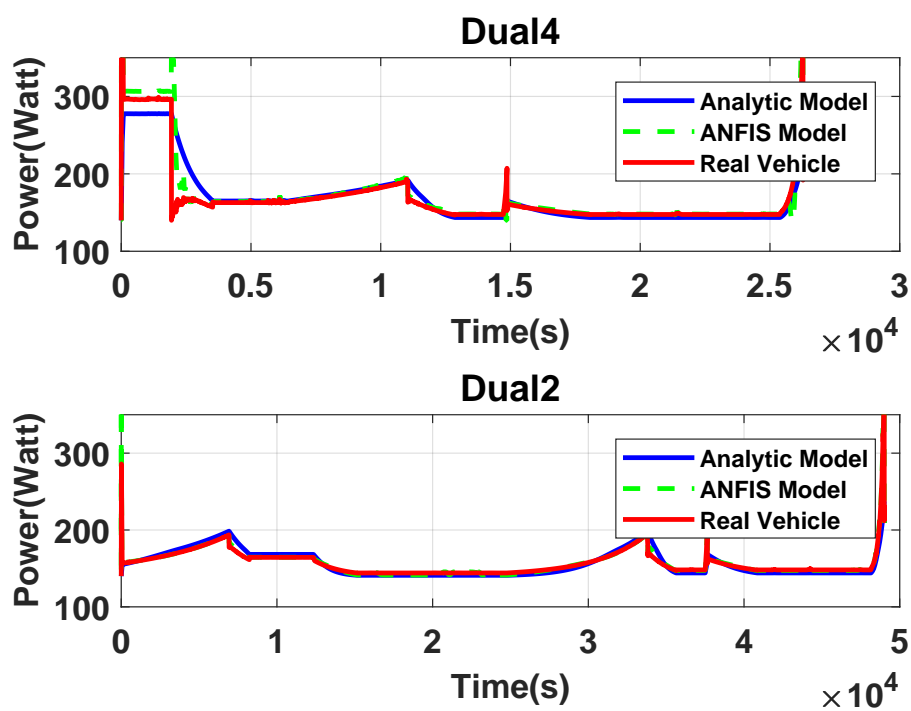


Figure 3.15: Comparison of the power consumption of URV using ANFIS and experiment with (a) Dual4 and (b) Dual2 configurations.

Table 3.1: Mean errors in power estimation

	Skid4	Single4	Dual4	Skid2	Single2	Dual2
DS	400965	264634	262079	541280	264119	263802
ML	$3.03e^{-2}$	$2.27e^{-3}$	$2.56e^{-3}$	$2.01e^{-2}$	$8.21e^{-4}$	$1.06e^{-3}$
MS	8.8919	2.0727	2.0524	1.5669	1.1424	0.1241

DS- Database sample; ML(Watt) - Mean square error from learning;  
MS(Watt) - Mean square error from simulation

In Table 3.1, MS is mean square error from simulation, where the unit of ML and MS is Watt. DS is a set of data samples for the learning process in ANFIS, the duration time for a skid2 sample with 1 km/h is 7.82e3 seconds and the traveling length is 2177.1 m. Similarly, the time duration for other driving modes depends on the given velocity.

### 3.6 Conclusion

The estimation of power consumption for an over-actuated URV is important for power planning, due to its different configurations and significant power consumption in the curvature of the trajectory. In this chapter, two approaches are proposed to estimate the power consumption estimation for different configurations of a URV in terms of the degree of steerability, the degree of actuator redundancy, and the curvature of the trajectory. The proposed models are validated through experiments of a URV called RobuCAR. Therefore, the proposed models can be used for power planning of a URV to perform a specific task for its different configurations. For future work, it is interesting to extend the proposed work for power estimation in the presence of faults in actuators.

# Discrete Approach of Energy Planning Methodology

---

## Contents

---

<b>4.1 Introduction</b> . . . . .	<b>65</b>
4.1.1 Main contributions . . . . .	66
4.1.2 Problem formulation . . . . .	66
<b>4.2 Discrete Energy Planning for Autonomous Navigation of the URV</b> . . . . .	<b>67</b>
4.2.1 Pre-Processing Phase: Power Consumption Estimation . . . . .	67
4.2.2 Optimization Phase: Energy planning . . . . .	68
<b>4.3 Results and discussion</b> . . . . .	<b>73</b>
<b>4.4 Conclusion</b> . . . . .	<b>79</b>

---

## 4.1 Introduction

In the last decade, autonomous vehicles have been increasingly used in many sectors such as industry and planetary exploration. These vehicles contribute to reducing  $CO_2$  emission inside big cities and enable to perform autonomous operations in unknown and confined spaces [Kumar 2014]. The performances of these systems to achieve successful missions depend strongly on the deployment of efficient algorithms for path planning [Chen 2018], velocity planning [Goto 2010], autonomous control [Barthelmes 2017], energy management [Chen 2014]. Despite the numerous advantages of using Unmanned Road Vehicles, their autonomous navigation is substantially dependent on the performances of the batteries. Thus, the management of the battery's power is a recent research topic, dealing with the issue of sustainable URV. The estimation of the power consumption needs an accurate behavioral model to evaluate the overall energy, necessary to drive the vehicle autonomously. In this chapter, a discrete energy planning for over-actuated unmanned road vehicles (URVs) with redundant steering configuration is proposed. After that, an optimization algorithm is applied on the digraph to get a global optimal solution combining driving mode, power consumption and velocity

profile of the URV. Results are compared with those given by the dynamic programming method for global offline optimization. Finally, the obtained simulations and experimental results, applied to RobuCar URV, highlight the effectiveness of the proposed energy planning.

#### 4.1.1 Main contributions

the main contributions of this work can be summarized as follows:

- Energy digraph is developed with all feasible configurations taking into account kinematic and dynamic constraints based on a 3D grid map, in the function of velocity, arc-length and driving mode.
- Discrete Energy planning for over-actuated URVs is developed with a variable step in time or in the distance. It calculates the optimal velocity profile and the corresponding driving mode for each segment of the trajectory, taking into account the road curvature and the kinematic parameters of the URV.
- Simulations and Experimental results have been applied on a real over-actuated URV called Robucar, in presence of six decentralized driving modes.

#### 4.1.2 Problem formulation

The problem of energy planning can be stated as an optimization problem as follows:

$$\min_{V_{i,k}, M_{i,m}} J = \sum_{i=1}^n \hat{P}_{i,k}(t_i, V_{i,k}, A_{i,k}, C_i, M_{i,m}) \times (\Delta t_i) \quad (4.1)$$

*subject – to*

$$\begin{aligned} t_i &< t_{max} \\ V_{min} &\leq V_{i,k} \leq V_{max} \\ A_{min} &\leq A_{i,k} \leq A_{max} \end{aligned} \quad (4.1a)$$

Where,  $V_{i,k}$ ,  $A_{i,k}$  represent respectively the  $k^{th}$  velocity and the acceleration profiles, defined for the  $i^{th}$  road segment.  $M_{i,m}$  is the  $m^{th}$  driving modes for the  $i^{th}$  road segment and  $\hat{P}_{i,k}$  is the  $k^{th}$  consumed power by the URV for the  $i^{th}$  road segment. The parameters  $t_i$  and  $C_i$  represent respectively the traveling time and the curvature of the  $i^{th}$  road segment respectively.  $m$  depends on the number of the independent steering system and actuated wheels.  $t_{max}$  is the maximum time imposed to finish the travel, while lower and upper limits of



## 4.2. Discrete Energy Planning for Autonomous Navigation of the URV

$V_{i,k}$  and  $A_{i,k}$  are  $A_{\min}$  to  $A_{\max}$  and  $V_{\min}$  to  $V_{\max}$ , respectively. The longitudinal velocity is bounded by the lateral acceleration  $A_y$  for the stability of URV, which can be given as follows.

$$A_y = V_{i,k}^2 C_i \quad (4.2)$$

The condition for the non-rollover of URV:

$$mA_y h < mg \frac{d}{2} \quad (4.3)$$

where,  $m$ ,  $g$ ,  $d$ , and  $h$  are mass, acceleration due to gravity, wheel base, and height of CG from ground, respectively. Hence,  $V_{i,k}$  is given by:

$$V_{i,k} < \sqrt{\frac{mgd}{2C_i h}} \quad (4.4)$$

This optimal control problem will be solved by an optimal search on a power digraph as explained in the following section.

## 4.2 Discrete Energy Planning for Autonomous Navigation of the URV

The proposed methodology for energy planning is briefly described in Fig.4.1. The approach is categorised into two main phases. In the first phase of pre-processing, power consumption estimation is developed based on data of the terrain, the vehicle, and the assigned task. The second phase concerns the optimization process of the power concerning the velocity profile and the driving modes.

**Modeling assumptions:** i) RobuCAR URV moves in a known situation and the dynamic limitations including other road users are not taken into consideration, ii) the URV moves on a planar surface and the road elevations are not considered i.e, the roll and pitch effects are neglected, iii) frequent switching of driving modes from one mode to another mode is possible, and iv) the URV moves with a low velocity under 16 km/h which is the most extreme speed of RobuCAR; thus, effects of aerodynamics are ignored. These assumptions can be justified because of the known condition and low speed of URV, which decrease unnecessary complexity in the model and computational expense.

### 4.2.1 Pre-Processing Phase: Power Consumption Estimation

In this subsection, we present a qualitative data-learning approach, based on Adaptive Neuro Fuzzy Inference System (ANFIS) for power consumption estimation, where both of the velocity profile and the driving modes are

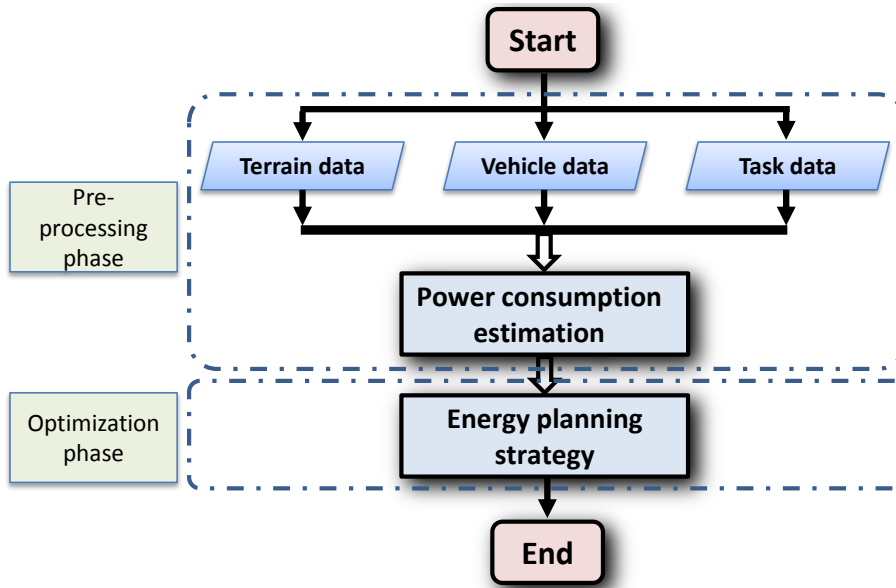


Figure 4.1: methodology for URV energy planning.

considered. The estimation is compared with the experimental measurements taken from a real URV, i.e. RobuCAR. This choice is motivated mainly by the topology of the sampled input-output data pairs. However, the power consumed by the URV abruptly may vary from one range of the input parameter values to another. This is because of the conditions of driving the URV and difficulties on vehicle dynamics and interfered environment. Thus, this work aims to categorize the sampled input-output data pairs in clusters and proceed in local regression, after that. The fuzzy logic layers perform clustering while the neural network layers handle local regressions. The principle is to build an ANFIS model which emulates the different URV's driving modes. However, if we consider the six driving modes described above, the URV's dynamic behaviour can change from one mode to another. Therefore, six separate ANFIS models are considered, one for each driving mode, to improve the regression performance. In the following subsections, the ANFIS architecture and the data-learning algorithm are presented.

#### 4.2.2 Optimization Phase: Energy planning

The proposed energy planning methodology is elaborately shown in Fig.4.2. Graph theory is used to evaluate the optimal path for satisfying the driving mode and the energy minimization concerning the velocity profile and road-path curvature. A graph is a discrete form of the intricate problem described by the relation (4.1).

## 4.2. Discrete Energy Planning for Autonomous Navigation of the URV

First, a directed graph is created to promote the optimization process (Fig. 4.5). The assigned mission path is divided into a finite set segments based on the curvature information by taking into consideration three types of road segments, namely: *line*, *clothoid* and *arc*.

The digraph is a weighted directed graph, where the edges have directions associated with them [West 2001]. A directed graph is an ordered pair  $G = (Ve, Ed)$ , where  $Ve$  is a set of vertices representing endpoints of each segment, and  $Ed$  is a set of edges representing the connection between vertices as a function of velocity, driving mode, and arc-length. The weight on each edge represents the energy consumed by the URV to travel on the corresponding segment for each driving mode.

Each vertex is denoted with a specific number say,  $jkl$ ; where  $j$ ,  $k$ , and  $l$  represent  $j^{th}$  row of the velocity vector,  $k^{th}$  row of the driving mode vector, and  $l^{th}$  row of the segment vector. In addition, a starting and an ending vertex are added on the top and the bottom of the digraph. The starting vertex is connected to the first set of vertices with zero weights on edges. Similarly, the ending vertex is connected to the last set of vertices with zero weights on edges.

In fact, for the  $i^{th}$  segment, the curvature of the trajectory can take three forms [Olver 2010]:

$$C_i = \begin{cases} 0 & \text{Straight line} \\ constant & \text{Arc} \\ as + b & \text{Clothoid} \end{cases} \quad (4.5)$$

where,  $s$  represents the arc-length; while  $a$  and  $b$  are constant parameters of the Clothoid in  $C - s$  plan.

For the subsequent development, a road profile of the "cit  scientifique" campus of the University of Lille is taken into consideration. The calculated and filtered curvatures of this road geometry are represented in Fig. 4.3 ( $C - s$  plane). In Fig. 4.4, the estimated and filtered trajectories of this 2D-road are discretized into 138 segments. The difference between real and filtered curvature is due to the change of interpolation of the real curvature from cubic spline to linear interpolation in filtered curvature. Due to this interpolation change, the corresponding actual and filtered trajectory are represented in Fig. 4.4.

Further, a 3D grid is developed according to three axes: *velocity*, *segment arc-length*, and *driving mode* (Fig.4.5). In this grid, all feasible points for each driving mode are identified based on kinematic constraints of the URV. Indeed, in each segment, a unique drive pattern is applied, as shown in Fig. 4.6. Besides, it is considered that each section (line, clothoid, arc) has the constraint of driving mode, which is detailed in Table 4.1. After that, the required energy to travel each segment of the road is calculated. This allows us to set up the weights on the edges of the digraph.

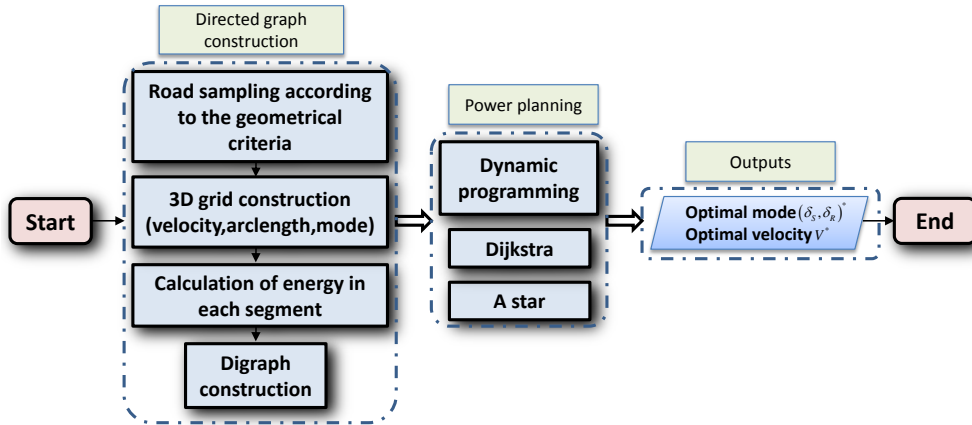


Figure 4.2: Energy planning schema.

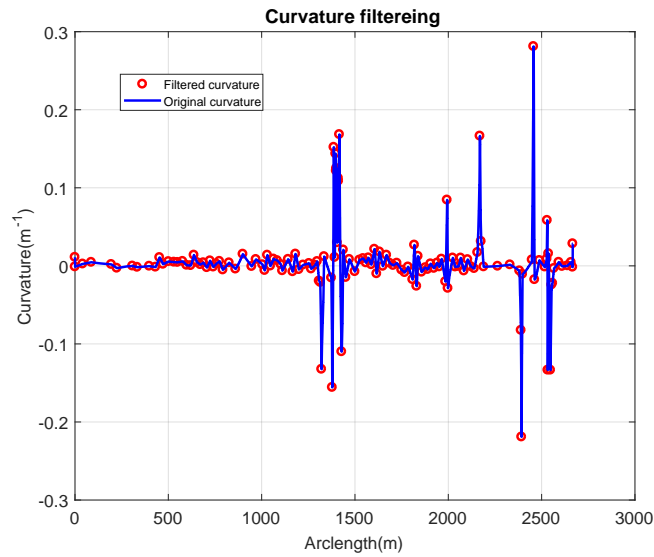


Figure 4.3: Real and filtered curvature.

Table 4.1: Constraints of driving mode for each type of road segment.

Driving mode	Line $c = 0$	Clothoid $c = var$	Arc $c = cst$
Skid4 ( $\delta_s = 0, \delta_R = 1$ )	X	X	X
Single4 ( $\delta_s = 1, \delta_R = 2$ )		X	X
Dual4 ( $\delta_s = 2, \delta_R = 3$ )		X	X
Skid2 ( $\delta_s = 0, \delta_R = -1$ )	X	X	X
Single2 ( $\delta_s = 1, \delta_R = 0$ )		X	X
Dual2 ( $\delta_s = 2, \delta_R = 1$ )		X	X

## 4.2. Discrete Energy Planning for Autonomous Navigation of the URM

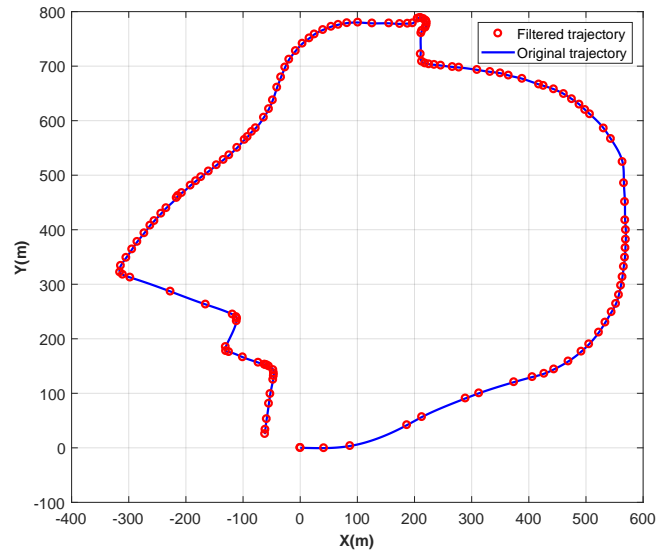


Figure 4.4: Real and filtered trajectory.

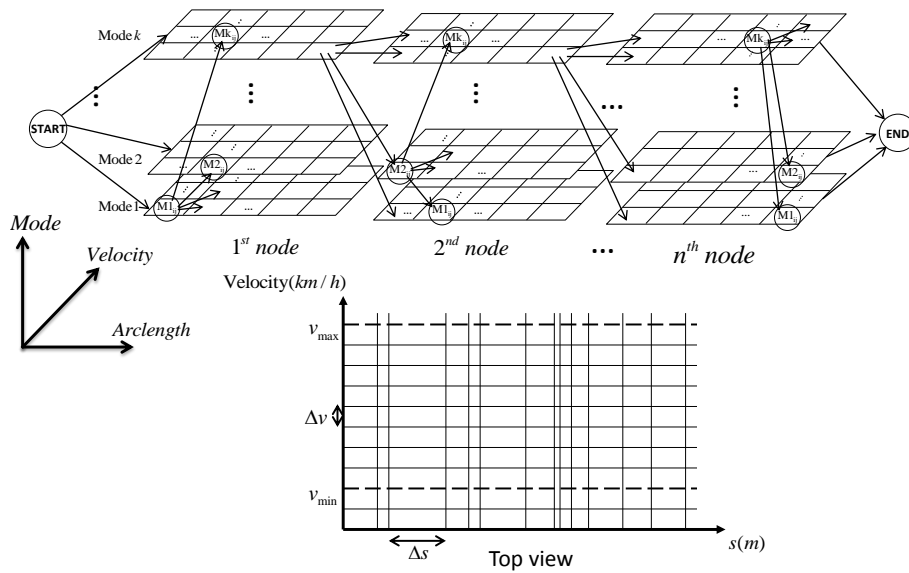


Figure 4.5: Energy digraph in 3D grid.

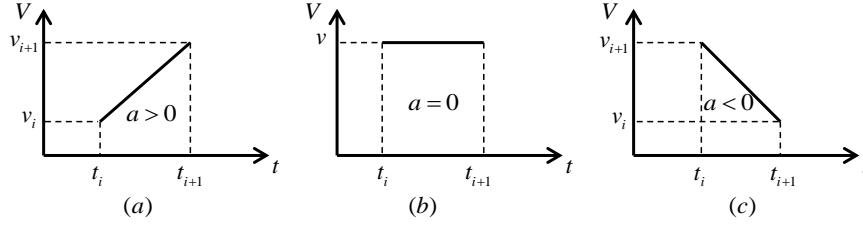


Figure 4.6: Driving pattern during sampling intervals.

Energy planning is calculated from the constructed digraph by starting at one vertex and exploring adjacent vertices until the destination vertex is reached to find the optimal path. The research is conducted employing two methods, namely Dijkstra and  $A^*$  algorithms and associated with the dynamic programming (DP) method as a reference. The output of the complete process is the optimal driving mode and the optimal velocity profile for each segment of the trajectory. Based on the built graph, the energy optimization problem (4.1) is formulated in a discrete form as follows:

$$E_k(t_i, V_i, C_i, M_{i,k}) = \sum_{t_k}^{t_{k+1}} P_k \Delta t_i \quad (4.6)$$

Where,  $P_k$  represents instantaneous power consumption calculated from the ANFIS model for the  $k^{th}$  configuration of the URV, and  $\Delta t_i$  is the travel time for  $i^{th}$  segment. In the following, we resume the principle of the global offline optimization methods used for energy planning.

#### 4.2.2.1 Dynamic Programming

To resolve the nonlinear problem of energy planning, an algorithm, often used to get a globally optimal, based on dynamic programming [Bertsekas 1995] is taken into consideration. Here dynamic programming is applied on the weighted digraph. Then a 3D constructed grid consists of 3 axes: i) arc-length which is represented with a set of samples of distance  $d = \{d_0, d_1, d_2, \dots, d_n\}$ , ii) velocity  $v = \{v_{min} : \Delta v : v_{max}\}$ , and iii) driving mode  $m = \{Skid4, Single4, Dual4, Skid2, Single2, Dual2\}$ . Each point in the grid is obtained with respect to all constraints described in equation (4.1a); as shown in Fig. 4.5. In this approach, arc-length is segmented according to the geometrical criteria, which is usually a non-uniform segmentation. The sampling step of the velocity  $\Delta V$  is about 0.5 km/h.

#### 4.2.2.2 Dijkstra and $A^*$ algorithms

Unlike the dynamic programming, Dijkstra algorithm finds the optimal global solution without covering all possible edges in the graph [LaValle 2006].  $A^*$  algorithm is a modified Dijkstra algorithm with a heuristic function, which minimizes the following function:  $f(n) = g(n) + h(n)$ , where  $n$  is the last vertex on the path,  $g(n)$  is the cost of the path from the starting vertex to the  $n^{\text{th}}$  one, and  $h(n)$  is a heuristic that estimates the cost of the cheapest path from vertex  $n$  to the goal. The choice of a good heuristic is very important to reduce the time calculation. In this work, a heuristic function  $h(n)$  is proposed, based on the curvature of the trajectory. The heuristic function  $h(n)$ , is defined as the cost of energy from any point of the trajectory to the end with a curvature equal to zero in  $C - s$  plane, corresponding to a straight line in the  $x - y$  plane.

### 4.3 Results and discussion

The following assumptions are taken into consideration for the proposed algorithm: i) only 2D road geometry is considered, ii) the URV has a constant acceleration in each segment, and iii) the switching between any two driving modes is possible. The developed algorithm is applied for the real trajectory of the University of Lille campus, as shown in Fig. 3.4.

In Fig. 4.7 and 4.8, the optimal velocity profile and the optimal driving mode for minimum energy consumption are presented for each segment of the filtered trajectory in  $s - v$  and  $X - Y$  planes, respectively. The constraint of traveling time is set to less than 40 min. The fluctuations in velocity and mode distribution are due to the noise in data acquisition and trajectory filtering. The algorithm shows that Single2 and Single4 modes are the best for the given optimal velocity profile as shown in Fig. 4.9. Moreover, the algorithm suggests a combination of Single2, Single4, Dual2, and Dual4 in sharp turns with a variation of velocity (Fig. 4.8). However, the transition from one mode to another mode is not appropriate at the sharp turns for the vehicle in real autonomous navigation. Hence, we make some correction in mode selection at sharp turns, and it is suggested to use only one steering mode as shown in Fig. 4.11 and Fig. 4.10.

In the same purpose, in Fig. 4.12, Fig. 4.13, Fig. 4.14, and Fig. 4.15 the optimal velocity profile and the optimal driving mode for minimum energy consumption are presented for each segment of the filtered trajectory with time constraints of 30 min and 20 min, respectively. These results show that time constraint affects the optimal driving mode and the optimal velocity profile, but are almost the same on the sharp turns.

A comparison of energy consumption for different driving modes is given

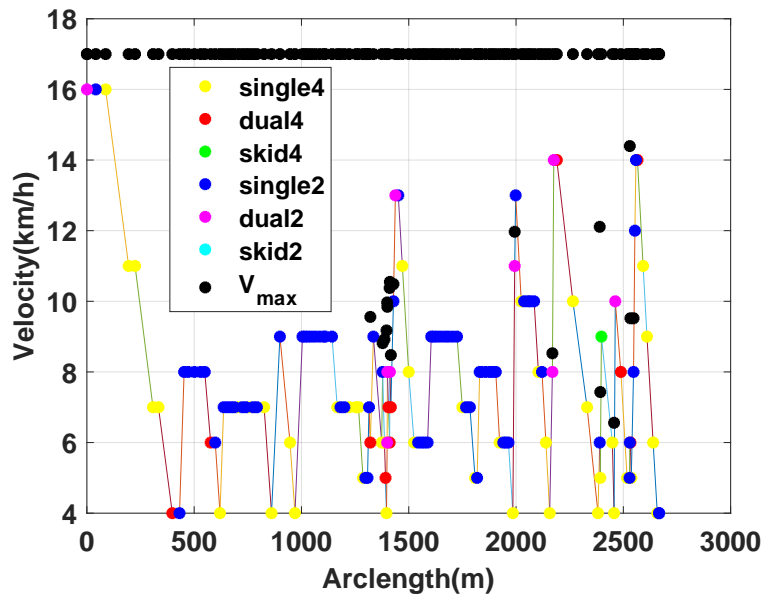


Figure 4.7: Optimal velocity profile for the campus trajectory ( $t < 40min$ ).

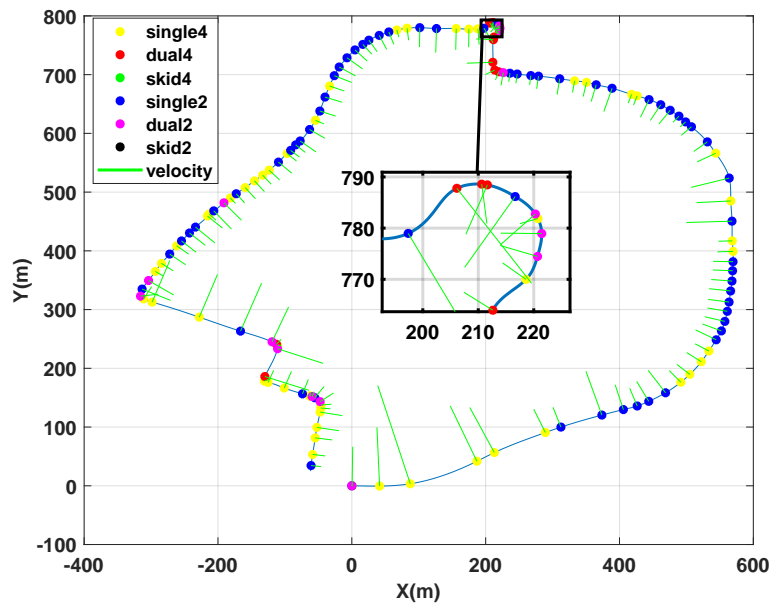


Figure 4.8: Optimal mode distribution for the campus trajectory ( $t < 40min$ ) (zoom in at sharp turn).



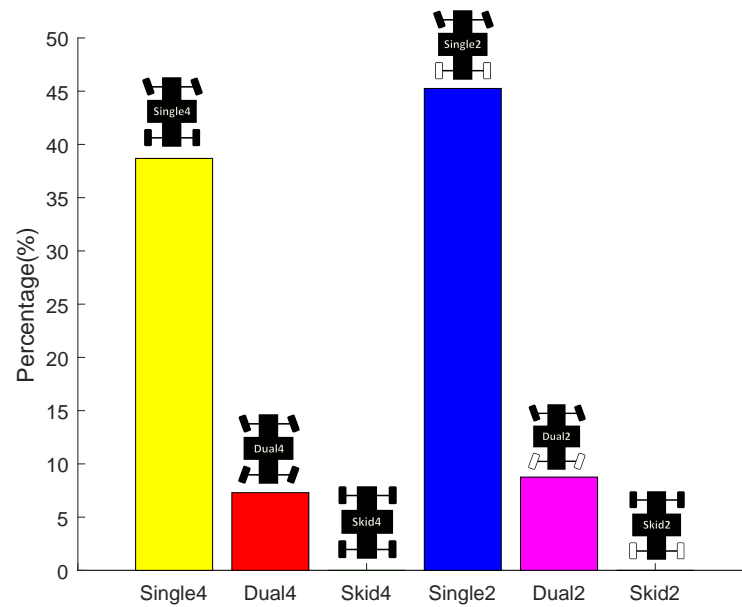


Figure 4.9: Percentage of modes use before correction in campus trajectory with traveling time ( $t < 40min$ ).

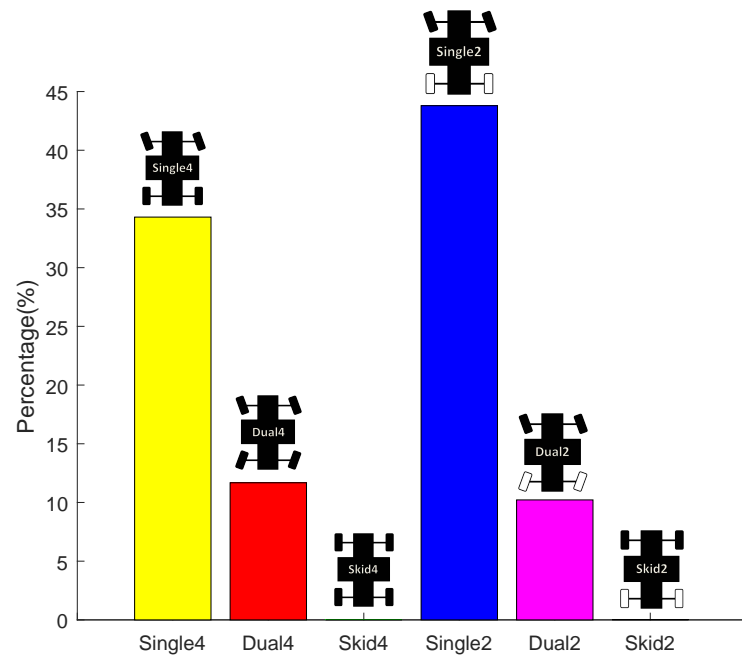


Figure 4.10: Percentage of modes use after correction in campus trajectory with traveling time ( $t < 40min$ ).

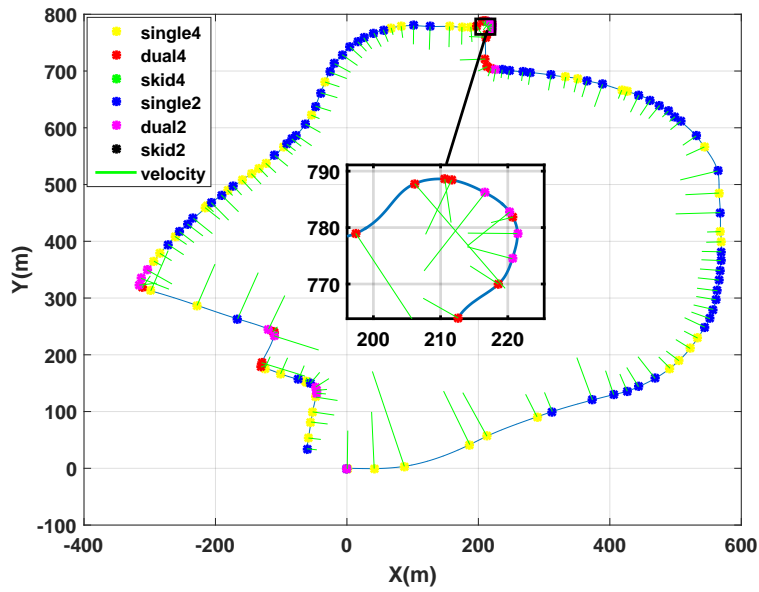


Figure 4.11: Post-processing with correction in mode distribution at sharp turn.

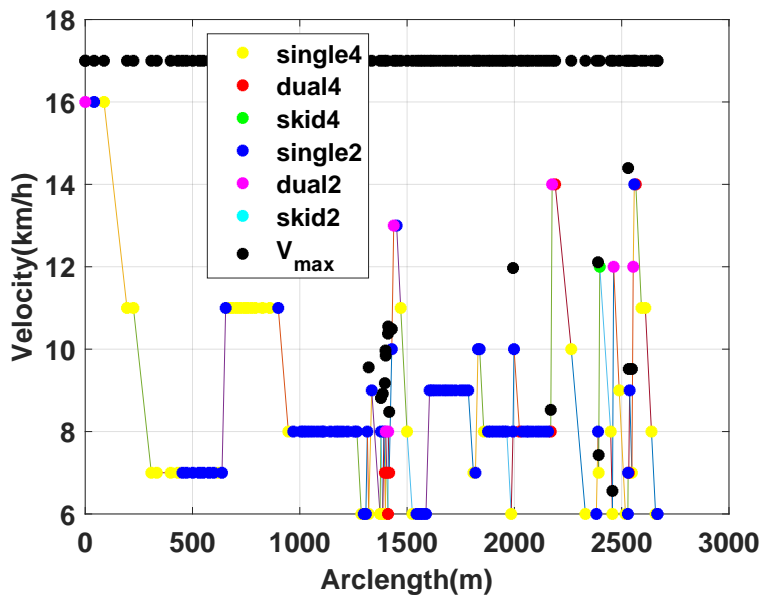


Figure 4.12: Optimal velocity profile for campus trajectory with traveling time ( $t < 30min$ ).

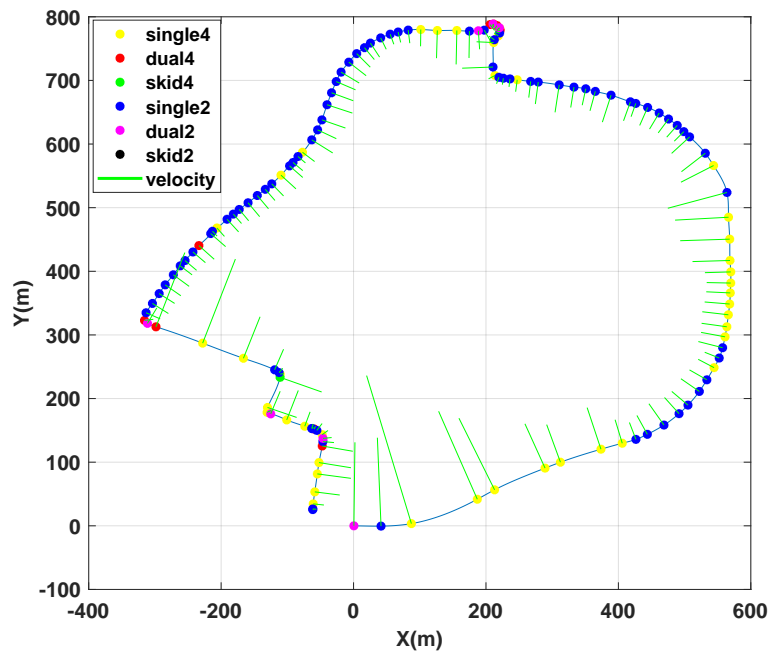


Figure 4.13: Optimal driving modes for campus trajectory with traveling time ( $t < 30min$ ).

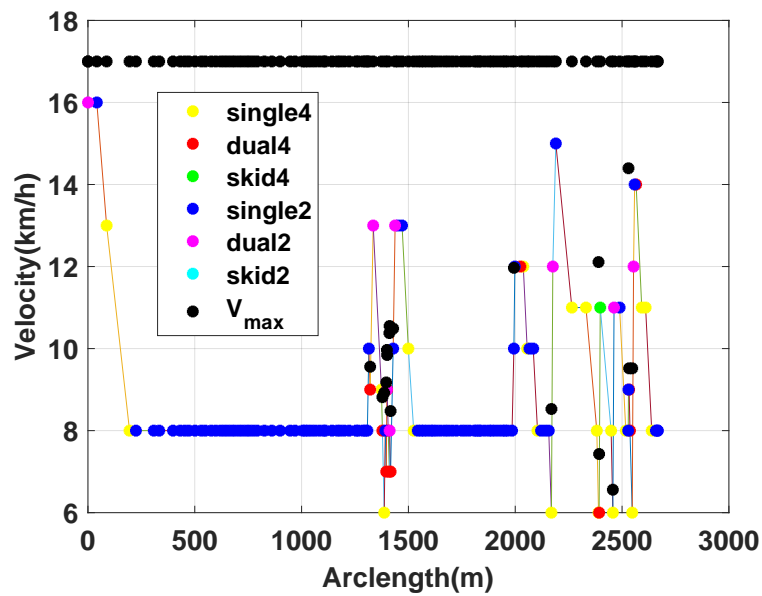


Figure 4.14: Optimal velocity profile and for campus trajectory with traveling time ( $t < 20min$ ).

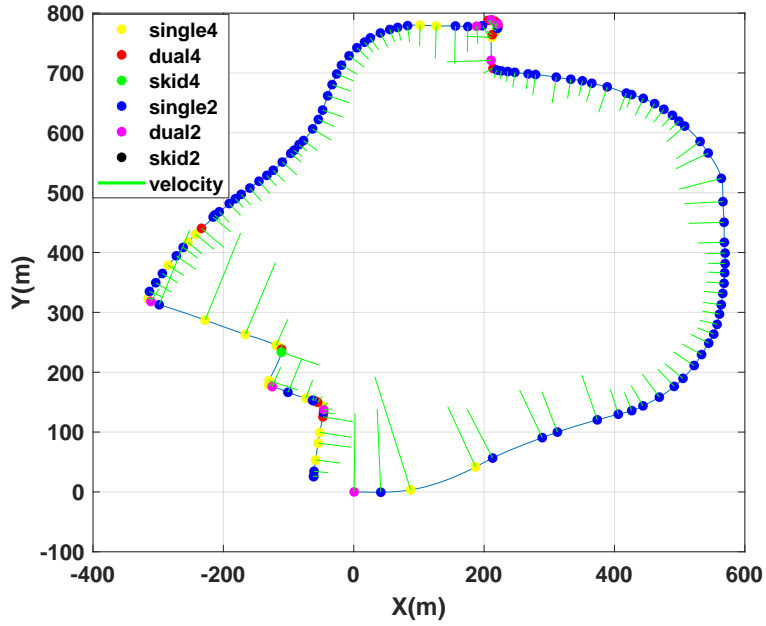


Figure 4.15: Optimal driving modes for campus trajectory with traveling time ( $t < 20min$ ).

in Table 4.2. It can be observed that with the same optimal velocity profile, the energy consumption is reduced by using the optimal driving mode during the autonomous navigation of the URV. Moreover, it is corrected with the proposed post-processing at the sharp turn which leads to an increased value of energy consumption.

In Table 4.3, the time cost of the global optimization algorithms in different steps is summarized. The time taken for the construction of the 3D grid is big, which is around 99 percent of the total time. It can be noticed that  $A^*$  takes very less time than Dijkstra and dynamic programming.

Table 4.2: Comparison of energy consumption with traveling time ( $t < 40min$ )

	Energy (J)	loss (%)
Skid4 for optimal velocity	3.1573e+06	186.69
Single4 for optimal velocity	3.0279e+05	17.90
Dual4 for optimal velocity	4.5242e+05	26.75
Skid2 for optimal velocity	6.8776e+06	406.66
Single2 for optimal velocity	3.9955e+05	23.62
Dual2 for optimal velocity	4.1341e+05	24.44
Optimal modes and optimal velocity	<b>1.6912e+04</b>	
Corrected modes and optimal velocity	<b>1.9329e+04</b>	

Table 4.3: Time consumed for the different steps in the algorithm ( $t < 40min$ )

	Computing time (s)
3D grid construction	12642.504
Digraph construction	5.32224
Dynamic programming	30.924936
Dijkstra	13.503235
A star	0.038087

#### 4.4 Conclusion

This chapter presents a methodology for the energy planning of an over-actuated URV. Data-learning qualitative method (ANFIS) is utilized for power consumption estimation. The latter is calculated for different driving modes of the redundant steering system of the URV. Three optimization algorithms are tested and compared to obtain the global optimization of the velocity and the driving mode of the URV for each segment of the trajectory with the time constraint. The results show that dynamic programming, Dijkstra and  $A^*$  give the global optimum, but  $A^*$  is faster when a useful heuristic function is selected. For future work, the energy planning methodology is to be extended to manage URV's faults. Besides, some dynamic constraints can be added to the model to consider other road users in a dynamic environment. Discrete energy planning methodology depends on the number of segments of the path, according to its geometry, and the length of the considered path. If the path is very long, the computation time of the optimization algorithm will increase accordingly. For this case, continuous planning of the energy can be very useful to solve this optimization problem with short computation time.

# Continuous Approach of Energy Planning Methodology

---

## Contents

---

<b>5.1 Introduction</b> . . . . .	<b>81</b>
5.1.1 Related Work . . . . .	82
5.1.2 Main contributions . . . . .	83
<b>5.2 Path Smoothing</b> . . . . .	<b>85</b>
5.2.1 Road Profile . . . . .	85
5.2.2 Method 1: . . . . .	86
5.2.3 Method 2: . . . . .	86
<b>5.3 Energy Planning</b> . . . . .	<b>88</b>
5.3.1 Vector of Objectives and constraints . . . . .	88
5.3.2 Energy optimization methodology . . . . .	89
<b>5.4 Experimental data-based results with virtual point control for an indoor TOMR</b> . . . . .	<b>92</b>
<b>5.5 Robot Modeling</b> . . . . .	<b>92</b>
<b>5.6 Velocity planning using kinetic energy planning</b> . . . . .	<b>94</b>
<b>5.7 Virtual Point Following Methodology</b> . . . . .	<b>95</b>
5.7.1 Energy Model of Robotino . . . . .	97
<b>5.8 Experimental Results And discussion</b> . . . . .	<b>97</b>
5.8.1 Description of holonomic robot Robotino . . . . .	97
5.8.2 Constant kinetic energy approach . . . . .	97
5.8.3 Multi-criteria optimization . . . . .	98
<b>5.9 Experimental data-based results for an outdoor over- actuated URV</b> . . . . .	<b>100</b>
<b>5.10 Conclusion</b> . . . . .	<b>110</b>

---

## 5.1 Introduction

Autonomous URVs occupy a principal place in academic research activities and industrial applications. This encourages scientists to contribute more,

particularly on the topics of design, control and planning among the fundamental issues addressed in this framework, power consumption evaluation, and management during tasks execution. In fact, despite the numerous advantages of autonomous vehicles, their limited source energy constitutes an essential constraint that should be handled carefully for rational exploitation. The need to plan and manage the available batteries power has prompted the researchers to open new research axes. The effective estimation of vehicle power consumption is the main issue. It is addressed to establish an accurate model that permits to avoid the situation of battery discharge during the autonomous navigation.

### 5.1.1 Related Work

#### 5.1.1.1 Energy Planning of a URV

In addition to power consumption estimation modeling, it is essential to have a good methodology for energy planning. Indeed, the main objective of energy planning is to optimize energy consumption and the travel time of the URV for a given trip. Many researchers developed discrete methods for energy optimization strategies. Dynamic programming has been used to obtain the optimal energy consumption of vehicles [Ozatay 2014], [Zhang 2010]. Moreover, authors developed energy optimization methods using model predictive control (MPC) and compared with dynamic programming based methods [Chen 2014], [Quaglia 2016]. Furthermore, the power management has been studied by using control allocation for an over-actuated URV, based on parametric torque distribution [Dizqah 2016]. But this approach considered only vehicle dynamics and not the road profile.

Chen et al. [Chen 2014] estimated the optimal velocity profile and torque using the dynamic programming method for a URV considering its front steering. In [Zhang 2017], neural network and MPC based method are developed for energy optimization and compared with dynamic programming algorithm. In [Liu 2017], quadratic programming is used to develop energy optimization for a URV. In a previous work of the authors [Bensekrane 2018], a discrete energy planning methodology has been developed for over-actuated URVs with the geometrical segmentation. The discrete methodology can be very greedy in time calculation according to the number of segments of the considered path. Extending to that work, and to improve the time calculation, this work presents a continuous energy planning methodology. **For most of the existing algorithms, continuous energy planning is not considered, and the influence of the curvature smoothing is not discussed.**

### 5.1.2 Main contributions

Based on the above literature review, the main contributions of this work can be summarized as follows:

- A continuous energy planning methodology based on a multi-objective optimization technique is applied to each driving mode of the URV, while the considered road path is smoothed using two different methods to evaluate the effect of the path smoothness (curvature) on the energy planning methodology. The road path is modeled by using two smooth geometrical combinations: the first one is "lines, clothoids, and arcs", and the second one is "lines and Pythagorean Hodograph (PH) curves"
- A composite velocity profile is constructed based on specific points selected from the generated Pareto fronts corresponding to the different driving modes. Each selected point represents the optimum of compromise between energy consumption and the travel time. Furthermore, a Directed weighted Graph is built to achieve the optimal velocity profile and the corresponding driving mode distributions.

The main advantage of the proposed approach is its ability to generate, for the considered URV on an assigned road path, an optimum smooth velocity profile defining the adequate transitions between the driving modes.

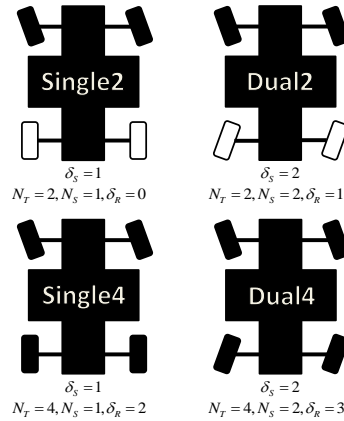


Figure 5.1: Different driving modes of RobuCAR

The proposed methodology for energy planning is briefly described in Fig.5.2. The energy planning methodology is divided into three main phases. In the first phase of pre-processing, a power consumption model is developed using a set of input data related to the terrain, vehicle, and the assigned task. The second phase concerns the path smoothing, where the generated path is obtained from filtered GIS data, according to geometrical criteria. These data are then modelled by using two smooth geometrical combinations: the first



Table 5.1: Parameters describing driving modes of RobuCAR

	Tractive actuators	Steering actuators
Single4 ( $\delta_s = 1, \delta_R = 2$ )	4	1(front)
Dual4 ( $\delta_s = 2, \delta_R = 3$ )	4	2
Single2 ( $\delta_s = 1, \delta_R = 0$ )	2	1(front)
Dual2 ( $\delta_s = 2, \delta_R = 1$ )	2	2

one is lines, clothoids, and arcs, and the second one is lines and Pythagorean Hodograph (PH) curves. Finally, the optimization phase gives an optimal composite velocity profile and the corresponding driving modes. hereafter, the vector of cost functions includes URV’s energy and travel time. Additionally, the problem is treated under a set of constraints inherent to the vehicle’s kinematic and dynamic performances and the path characteristics.

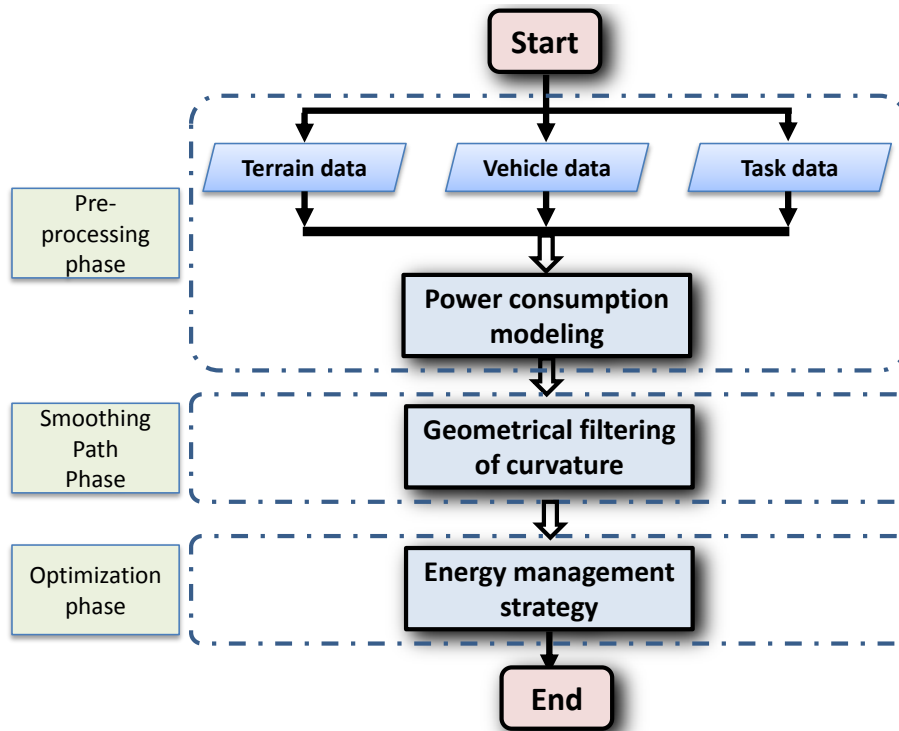


Figure 5.2: The proposed methodology for power consumption estimation and energy planning.

## 5.2 Path Smoothing

### 5.2.1 Road Profile

In a Geographical Information System (GIS), a road is represented by polylines [Jakkula 2007], describing the central axis of its surface. Each point of this polyline is defined by the 3D geographic coordinates (longitude, latitude, and altitude).



Figure 5.3: Campus trajectory of the University of Lille

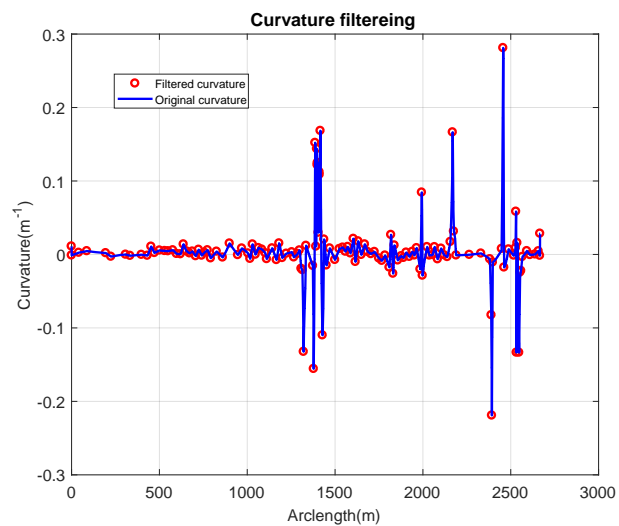


Figure 5.4: The filtered and real curvature

This discrete representation is not always appropriate for realistic simu-

lation or path planning. A continuous representation, often parametric, is necessary to estimate all the parameters required for the calculation (contact angle of yaw, the radius of curvature, etc.) in each point of the curve. To simplify this representation, the road path is decomposed into horizontal and vertical curves representing respectively the roads mapped onto the plane (Fig. 5.3). In this work, we use the cubic spline interpolation approach for polylines describing the considered trajectory [Ahlberg 1967].

The GIS data for real road is often tainted by errors of acquisition systems, which explains the fluctuations presented in the estimated curvature of the 2D trajectory. In this work, the following two methods are used to make a smooth path.

### 5.2.2 Method 1:

A discrete filter is developed to construct the road with its main components, namely, lines, arcs, and clothoids. The discrete filter takes one point among  $n_s$  samples if the curvature is bounded between 0 and a predefined threshold  $e_g$  of the curvature. If the curvature is higher than the threshold value, then only one point is selected from  $n_t$  samples.

$$\begin{cases} 1/n_t & 0 \leq C < e_g \\ 1/n_s & C \geq e_g \end{cases} \quad (5.1)$$

The curvature of the trajectory can take three forms:

$$C_i = \begin{cases} 0 & \text{Straight line} \\ \text{Constant} & \text{Arc} \\ as + b & \text{Clothoide} \end{cases} \quad (5.2)$$

where,  $s$  represents the arc length; while  $a$  and  $b$  are constant parameters of clothoid in  $C - s$  plane. The estimated and filtered curvature for the campus of the University of Lille is shown in Fig. 5.4 ( $C - s$  plane), where  $e_g = 0.05m^{-1}$ ,  $e_d = 20m$ ,  $n_s = 5$ ,  $n_t = 2$ , and total of 138 segments.

### 5.2.3 Method 2:

The road path is smoothed using lines and Pythagorean Hodograph (PH) curves. PH curves are synthetic parametric curves. These curves were introduced by Farouki and Sakkalis [Farouki 1990] in 1990 to overcome the drawbacks of the previously used curves, e.g., Bezier, B-splines, NURBS, etc. The most notable properties of these curves are, their arc-length has closed form solution, and they possess rational offset curves. Since then, PH curves have been used in many fields such as 3D path planning and obstacle avoidance of Unmanned Aerial Vehicles (UAVs) [Shanmugavel 2007], [Shah 2010].

In [Bruyninckx 1997], PH curves are used for path planning of mobile robots. In this work, we exploit PH curves to generate a smooth path. In this case, the curvature of the trajectory can take two forms:

$$C_i = \begin{cases} 0 & \text{Straight line} \\ \text{Variable} & \text{PH curve} \end{cases} \quad (5.3)$$

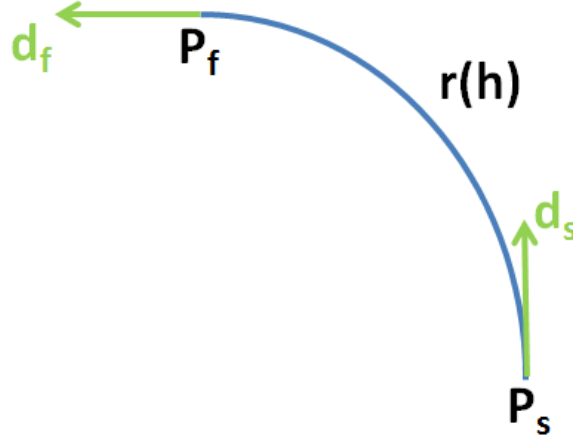


Figure 5.5: Basic conditions to generate a PH curve

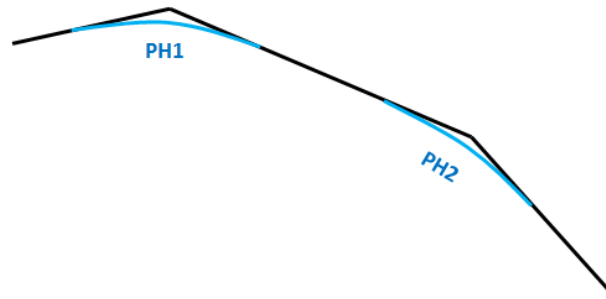


Figure 5.6: The filtered and real curvature

A PH curve  $r(h)$  can be constructed using the four known variables  $P_s$  (position vector at the start point),  $d_s$  (direction vector at the start point  $P_s$ ),  $P_f$  (position vector at the end point) and  $d_f$  (direction vector at the end point  $P_f$ ) as shown in Fig. 5.5.

$$P_s(x_s, y_s), d_s(d_{xs}, d_{ys}) \xrightarrow{r(h)} P_f(x_f, y_f), d_f(d_{xf}, d_{yf}) \quad (5.4)$$

where,  $h$  represents the curvilinear coordinate along the curve. Fig. 5.6 shows the real curvature and the smoothed curvature using PH curves for the real road path.

## 5.3 Energy Planning

### 5.3.1 Vector of Objectives and constraints

The objective functions to be minimized for the trajectory  $X(t)$  between initial and final states are generally expressions containing significant physical parameters related to the URV's behavior and to the efficiency of the system. Hereafter, we particularly consider the following functions :

$$F_1 = T, F_2 = E_k \quad (5.5)$$

where,  $T$  is the task duration,  $E_k$  represents the consumed energy which is linked to power consumption  $P_k$ , for a driving mode  $M_k$ , as follows:

$$E_k = \int_0^T P_k dt \quad (5.6)$$

The set of feasible motions is restricted by numerous constraints reflecting the physical limitations on URV's performances.

#### 5.3.1.1 Physical limitation

The velocity profile evaluated at the center of gravity is limited with upper and lower limits as follows:

$$V_{\min} \leq V \leq V_{\max} \quad (5.7)$$

The acceleration is also limited, In case of four wheels drive the limits are given by  $A_{1\min}$ ,  $A_{1\max}$ , while the limits for the two wheels drive are given by  $A_{2\min}$  and  $A_{2\max}$ .

$$\begin{aligned} A_{1\min} &\leq A_1 \leq A_{1\max} \\ A_{2\min} &\leq A_2 \leq A_{2\max} \end{aligned} \quad (5.8)$$

The different driving modes  $M_k$  considered for this work are:

$$M_k = \begin{cases} \delta_s = 1, \delta_R = 0 & \mathbf{Single2} \text{ (Over-actuated)} \\ \delta_s = 2, \delta_R = 1 & \mathbf{Dual2} \text{ (Over-actuated)} \\ \delta_s = 1, \delta_R = 2 & \mathbf{Single4} \text{ (Over-actuated)} \\ \delta_s = 2, \delta_R = 3 & \mathbf{Dual4} \text{ (Over-actuated)} \end{cases} \quad (5.9)$$

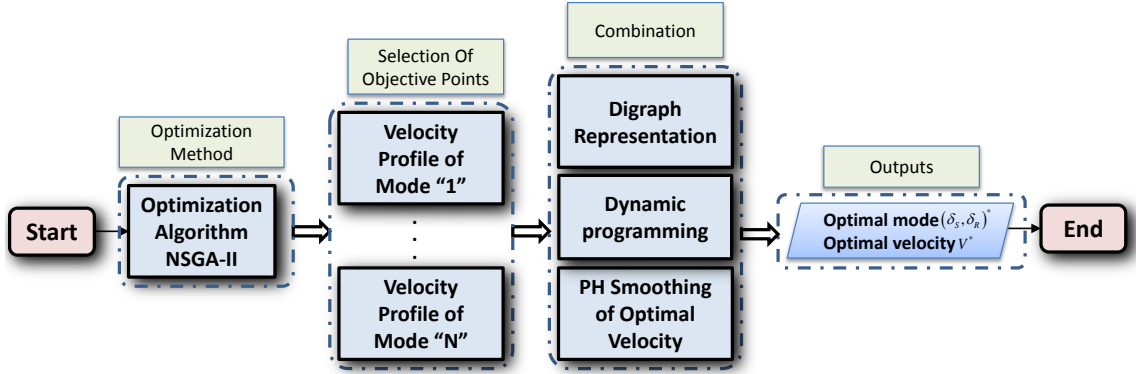


Figure 5.7: Energy optimization methodology.

### 5.3.2 Energy optimization methodology

In Fig. 5.7, the proposed methodology for the continuous energy planning of an over-actuated URV is presented. The methodology is divided into three steps.

The first step includes the calculation of a set of optimum velocity profiles for different driving modes on smoothed paths, obtained using two path smoothing methods described in the previous section. This is achieved using the NSGA-II algorithm [Deb 2001], which is one of the popularly used evolutionary algorithms which attempt to find multiple Pareto-optimal solutions in a multi-objective optimization problem. From each generated Pareto front, corresponding to individual driving modes, a set of solutions (objective points) are selected to generate a set of velocity profiles. Finally, the different driving modes are combined to obtain a composite velocity profile by using a digraph representation. Dynamic programming is used to obtain the optimal solution from the constructed digraph. A PH based interpolation is used to smooth the resulting velocity profile in the different nodes of the digraph.

#### 5.3.2.1 Pareto front generation

The procedure for generating optimal Pareto fronts regrouping the compromise URV velocity profiles is described in Fig. 5.8. As discussed earlier, we already have a smoothed path using two different methods. The algorithm aims to find, for each driving mode, solutions ensuring the compromise between the final time  $T_f$  and the consumed energy  $E$ . This phase is based on a parametrization of the velocity profile using a cubic spline interpolating a set of intermediate control points uniformly distributed along the time scale  $[0, T_f]$ , as shown in Fig.5.9. The positions of these control points are investigated within the limits imposed by kinematic constraints in equations 5.7 and 5.8. The ANFIS model calculates then the power consumption for each

solution candidate. Note that, a Pareto front is generated for each driving mode, thus the algorithm of Fig.5.8 is repeated for each mode.

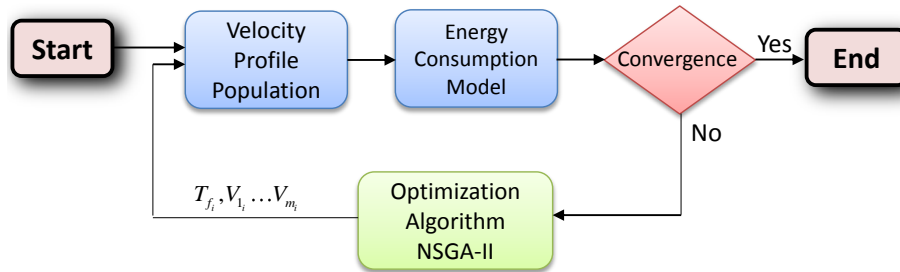


Figure 5.8: Generation of Pareto Fronts of velocity profiles

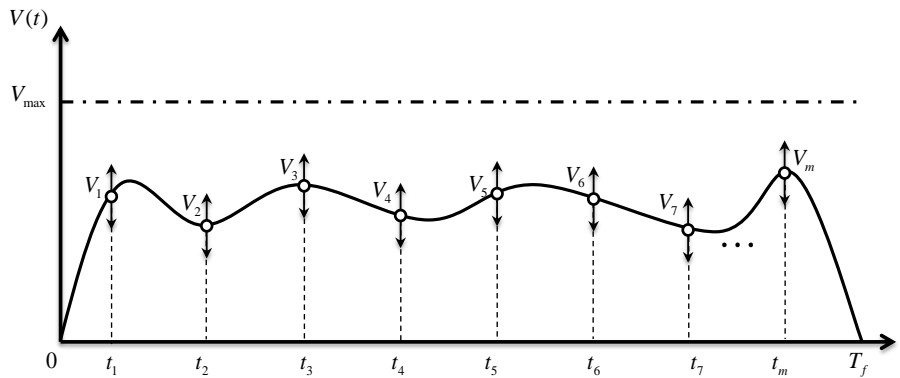


Figure 5.9: Generation of motion profile candidate

### 5.3.2.2 Compromise point selection

The optimization process provides different Pareto front according to the number of introduced driving modes. Furthermore, a compromise point is selected from each Pareto front in regards to the ideal point whose coordinates are minimum energy consumption and minimum travel time  $[\min(T_f), \min(E)]$ . The selected objective point corresponds to the nearest point to the ideal point as shown in Fig.5.10.

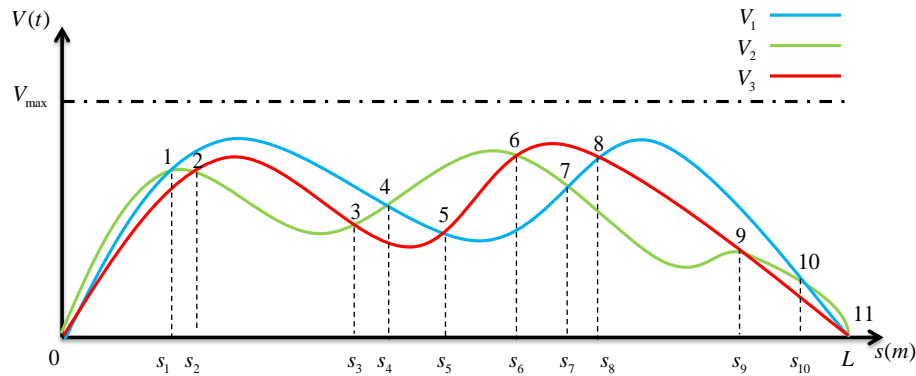


Figure 5.11: Example for superposition of velocity profiles

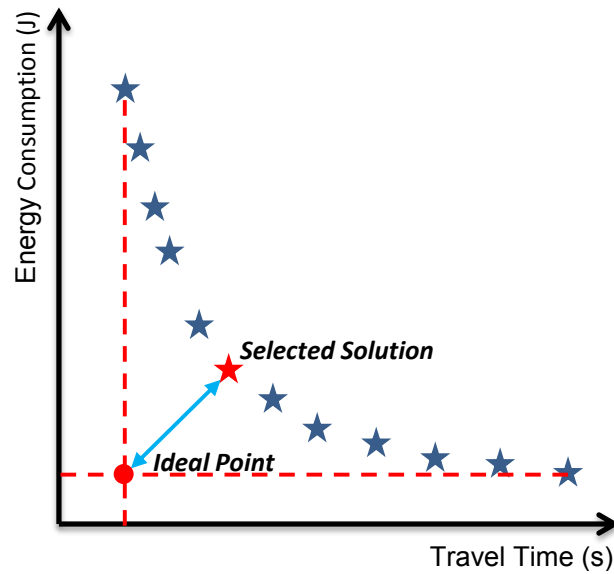


Figure 5.10: Selection of objective point from Pareto front

### 5.3.2.3 Composite Velocity profile construction

In order to combine the different velocity profiles obtained from the selected objective points, we superimpose the different velocity profiles for various driving modes as shown in the example of Fig. 5.11. The different velocity profiles are plotted according to their arc-length to have the same reference.

A directed graph is then generated to support this process (Fig. 5.12). The digraph is a weighted directed graph, where the edges have directions assigned to them [West 2001]. The directed graph is an ordered pair  $G = (Ve, Ed)$ , where  $Ve$  is a set of vertices representing the different intersection points in the different velocity profiles, and  $Ed$  is a set of edges representing the connection



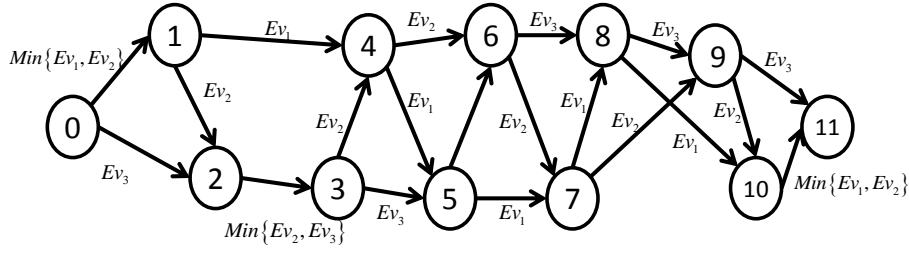


Figure 5.12: Example of digraph

between the different intersection points. The weight on each edge represents the minimum energy consumed by the URV to travel on the corresponding segment for each driving mode.

The developed digraph is used to find the minimum energy between the starting and ending points by applying dynamic programming. A PH curve interpolation is finally applied to the constructed composite velocity profile at the intersection points.

## 5.4 Experimental data-based results with virtual point control for an indoor TOMR

## 5.5 Robot Modeling

In this work, we consider Three-wheeled Omnidirectional Mobile Robot (TOMR) structure on a flat XY-surface. Thus, we concentrate on longitudinal and yaw dynamics, but the approach is general and allows taking into account motions such as lateral skid, pitch, and roll.

Fig. 5.13 represents the three-wheeled omnidirectional mobile robot structure, that is driven by three identical DC motors.  $q = [x \ y \ \theta]^T$  represents the robot coordinates, where  $x$  and  $y$  denote the linear coordinates relative to the global frame and  $\theta$  its orientation with respect to  $X$  axis. The kinematics equations of Robotino can be expressed as follows:

$$\begin{bmatrix} V_1 \\ V_2 \\ V_3 \end{bmatrix} = \begin{bmatrix} -\sin \theta & \cos \theta & b \\ -\sin(\frac{\pi}{3} - \theta) & -\cos(\frac{\pi}{3} - \theta) & b \\ \sin(\frac{\pi}{3} + \theta) & -\cos(\frac{\pi}{3} + \theta) & b \end{bmatrix} \begin{bmatrix} \dot{x} \\ \dot{y} \\ \dot{\theta} \end{bmatrix} \quad (5.10)$$

Where  $[V_1 \ V_2 \ V_3]^T$  is the vector of the linear velocities of wheels. The linear and angular velocities of the robot can be obtained from Fig. 5.13 as:

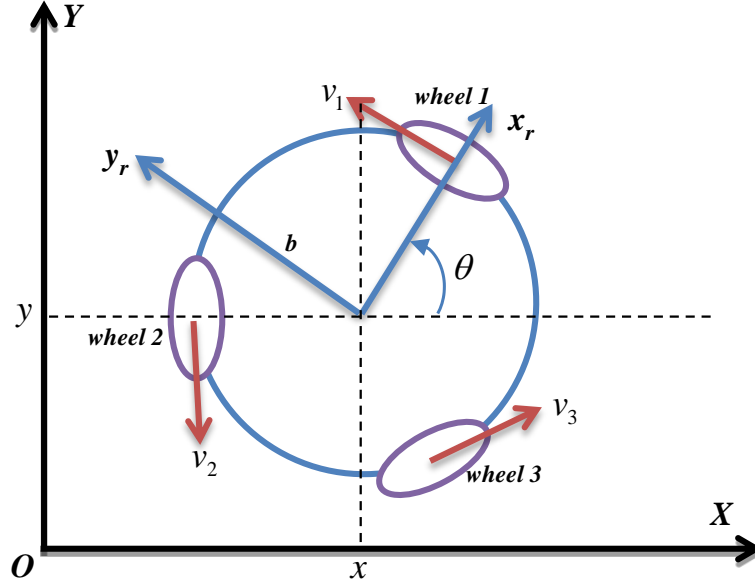


Figure 5.13: Three-wheeled omnidirectional mobile robot structure

$$\begin{bmatrix} v \\ \omega \end{bmatrix} = \begin{bmatrix} \cos(\theta) & \sin(\theta) & 0 \\ 0 & 0 & 1 \end{bmatrix} \begin{bmatrix} \dot{x} \\ \dot{y} \\ \dot{\theta} \end{bmatrix} \quad (5.11)$$

By combining equations (5.10) and (5.11) the equation establishing the relationship between the velocities of the wheels and those of the robot is derived.

$$\begin{bmatrix} V_1 \\ V_2 \\ V_3 \end{bmatrix} = \begin{bmatrix} 0 & b \\ -\sin(\pi/3) & b \\ \sin(\pi/3) & b \end{bmatrix} \begin{bmatrix} v \\ \omega \end{bmatrix} \quad (5.12)$$

The forces acting on CoG are represented by  $F_x$  and  $F_y$  in the longitudinal and lateral directions, respectively. The yaw moment of CoG is represented by  $M_z$ . The effects of the suspensions are neglected on the overall dynamics because the TOMR is moving with low velocity and on a plane area.

Let  $[x(t), y(t), z(t), \alpha(t)]$  represent respectively XYZ-positions of the center of mass and orientation (yaw angle) of the TOMR in an inertial coordinate system at time  $t$ . We assume that at all time  $z(t) = 0$ . Correspondingly  $v_x = \dot{x}$ ,  $v_y = \dot{y}$ ,  $v_z = 0$  are the coordinates of the heading vector  $\vec{v} = [v_x, v_y, v_z]$  and  $\vec{\omega}$  is a yaw rate vector which is perpendicular to XY-plane,  $\omega = \|\vec{\omega}\| = \dot{\alpha}$ .

Namely, let  $\vec{r}_c(t)$  be a radius vector from instant center of rotation of the TOMR on XY-plane to its center of mass. Then velocity vector for the center of mass is  $\vec{v} = \vec{\omega} \times \vec{r}_c(t)$ .

The angular velocity vector  $\vec{\omega}$  and velocity vector  $\vec{v}$  of the center of the TOMR are related as the vector

$$\vec{\omega} = \frac{\vec{r}_c \times \vec{v}}{R_c^2}, \quad (5.13)$$

where  $R_c = \|\vec{r}_c\|$ .

The center of instant rotation location can be expressed via XY-position of the TOMR center, normal unit vector  $\vec{n}$  to the velocity  $\vec{v}$  ( $\vec{n} \perp \vec{v}$ ) and radius of rotation  $R_c$  as

$$\vec{r}_c = -\vec{n}R_c = -\vec{n}\frac{1}{k}, \quad (5.14)$$

where  $k = R_c^{-1}$  is the trajectory curvature.

The TOMR can move on trajectory curvature  $k$ , with velocity vector  $\vec{v} = [v_x, v_y, 0]^T$  direction angle  $\theta = \text{atan}(\frac{v_y}{v_x})$  and the yaw angle  $\alpha$ .

The kinematic equations of the TOMR are

$$\begin{aligned} \dot{x} &= v \cos(\theta) \\ \dot{y} &= v \sin(\theta), \end{aligned} \quad (5.15)$$

where  $v = \|\vec{v}\| = \sqrt{v_x^2 + v_y^2}$ .  $v$  and  $\omega$  are related  $v = R_c\omega$ .

The equations of translational and yaw dynamics are

$$\begin{aligned} m\dot{v} &= F \\ I_{zz}\dot{\omega} &= \tau, \end{aligned} \quad (5.16)$$

where  $m$  is the TOMR mass,  $I_{zz}$  is inertia moment with respect to Z-axis,  $F$  is the force along  $\vec{v}$  vector, and  $\tau$  is the yaw torque.

The force  $F$  and the torque  $\tau$  can be expressed via torques applied to respective wheel  $\tau_1, \tau_2, \tau_3$  and resistance forces.

## 5.6 Velocity planning using kinetic energy planning

Let us consider a smooth path on XY-plane defined parametrically as

$$\begin{aligned} x &= X(s) \\ y &= Y(s), \end{aligned} \quad (5.17)$$

where  $0 \leq s \leq L$  is a distance along the path. So,

$$[X'(s)]^2 + [Y'(s)]^2 = 1. \quad (5.18)$$

We also assume that the curvature  $k(s) = X''(s)Y'(s) - Y''(s)X'(s)$  is a continuous function of  $s$ .

The velocity plan  $V(s)$  along the path is based on the following assumption: the TOMR constrained on the path should be moving in such a way that

$\alpha = \theta = \tan^{-1} \left[ \frac{Y(s)}{X(s)} \right]$ , i.e. its center line is collinear with the heading vector as well as tangent vector to the path at all times. Let  $\Omega(s)$  is the angular velocity at  $s$  then  $\Omega(s) = V(s)k(s)$ .

We assume that the time to reach the destination is fixed  $T$ .

$$T = \int_0^L \frac{ds}{V(s)}. \quad (5.19)$$

On the other hand, the kinetic energy of the TOMR moving on such path is

$$E_{kin}(s) = \frac{mV^2}{2} + \frac{I_{zz}\Omega^2}{2} = \frac{1}{2}[m + I_{zz}k^2(s)]V^2(s). \quad (5.20)$$

So,

$$V(s) = \sqrt{\frac{2E_{kin}(s)}{m + I_{zz}k^2(s)}}. \quad (5.21)$$

In our development, we will consider an electric TOMR without energy recuperation, so any braking results in energy loss.

Let us assume for a minute that there is no resistance for the TOMR moving along this path. Then neglecting the time to reach certain energy level and braking (this is a valid assumption for longer paths) it is easy to see that the optimal power saving methodology is to reach energy level  $E_0$  such that

$$E_0 = \frac{1}{2} \left[ \frac{1}{T} \int_0^L \sqrt{m + I_{zz}k^2(s)} ds \right]^2 \quad (5.22)$$

and then this kinetic energy should remain constant until the end of the path since slowing down results in unrecoverable energy loss.

Using this quasi optimal methodology the velocity plan along the path is

$$V(s) = \frac{\int_0^L \sqrt{m + I_{zz}k^2(\xi)} d\xi}{T \sqrt{m + I_{zz}k^2(s)}}. \quad (5.23)$$

As can be seen, increase in curvature of the path results in decrease of velocity and vice versa that is "natural" behavior of the TOMR.

In reality, the TOMR following this path will encounter resistance that includes friction, aerodynamic drag, etc., but following such preplanned velocity profile will ensure that the TOMR energy is spent only on overcoming resistance.

## 5.7 Virtual Point Following Methodology

Our approach to control the TOMR so that it follows robustly the planned velocity profile derived in the previous section is based on the idea of sliding mode control and virtual point following.

Let us consider a virtual point on the path with coordinates  $X(s^*), Y(s^*)$  following the path according to the following differential equation:

$$\dot{s}^*(t) = V(s^*(t)). \quad (5.24)$$

The equation 5.24 guarantees that the velocity of the virtual point at every  $s$  is equal to the plan  $V(s)$ .

Now we will derive a control for the TOMR that follows the virtual point.

If  $x(t), y(t)$  is current position of the TOMR (that is not necessarily on the path) then the coordinates of the deviation error from the virtual point are  $e_x(t) = x(t) - X(s^*(t)), e_y(t) = y(t) - Y(s^*(t))$ . Differentiating and using 5.15 we have

$$\begin{aligned} \dot{e}_x &= v \cos(\alpha) - X'(s^*)\dot{s}^* = v \cos(\alpha) - X'(s^*)V(s^*) \\ \dot{e}_y &= v \sin(\alpha) - Y'(s^*)\dot{s}^* = v \sin(\alpha) - Y'(s^*)V(s^*). \end{aligned} \quad (5.25)$$

Let us consider the following relations that will be considered as desired manifold in the system state space:

$$\begin{aligned} v \cos(\alpha) - X'(s^*)V(s^*) + \lambda e_x &= 0 \\ v \sin(\alpha) - Y'(s^*)V(s^*) + \lambda e_y &= 0, \end{aligned} \quad (5.26)$$

or  $\vec{v} = \vec{v}_{des}$ , where

$$\vec{v}_{des} = [X'(s^*)V(s^*) - \lambda e_x, Y'(s^*)V(s^*) - \lambda e_y, 0]^T. \quad (5.27)$$

This can be separated into two relations one of them concerns steering:

$$\alpha = \tan^{-1} \left[ \frac{X'(s^*)V(s^*) - \lambda(x - X(s^*))}{Y'(s^*)V(s^*) - \lambda(y - Y(s^*))} \right]. \quad (5.28)$$

and other concerning velocity

$$v = \sqrt{[X'(s^*)V(s^*) - \lambda(x - X(s^*))]^2 + [Y'(s^*)V(s^*) - \lambda(y - Y(s^*))]^2}. \quad (5.29)$$

If these equations are valid then

$$\begin{aligned} \dot{e}_x &= -\lambda e_x \\ \dot{e}_y &= -\lambda e_y. \end{aligned} \quad (5.30)$$

where  $\lambda > 0$ . It implies that  $e_x \rightarrow 0, e_y \rightarrow 0$  when  $t \rightarrow \infty$ .

The relations 5.23, 5.24, 5.28, 5.29 represent the control algorithm. Practical implementation may include additional features taking into account steering actuator dynamics as well as TOMR and engine dynamics, but the main idea remains the same: maintaining relations 5.26, or equivalently 5.27.

### 5.7.1 Energy Model of Robotino

The energy estimation model of Robotino can be expressed as follow [Liu 2013]:

$$E_{\text{Total}} = E_{\text{Motor}} + E_{\text{Other}}$$

$$= \int_t \left( m \max\{V(t)A(t), 0\} + I_{zz} \max\{\Omega(t)\Gamma(t), 0\} + 2\mu mg \max\{|V(t)|, |b\Omega(t)|\} \right) dt + P_s t \quad (5.31)$$

where  $E_{\text{Total}}$ ,  $E_{\text{Motor}}$ , and  $E_{\text{Other}}$  denote the total energy of the robot, motor energy and static energy respectively.  $\mu$ ,  $b$ , and  $\Gamma$  represent the friction coefficient, the distance between the wheel and CoG, and the angular acceleration respectively, while  $P_s$  represents the static power consumption of the embedded PC and different sensors.

## 5.8 Experimental Results And discussion

### 5.8.1 Description of holonomic robot Robotino

The Robotino robot is supplied with two 12V batteries which permit a running time of up to two hours. The robot's dimensions are 450 mm in diameter and 290 mm in height with an overall weight of approximately 21kg. The platform embeds numerous application programming interface layers. While the Linux layer provides standard user space, the platform can also be controlled by external PC via the wireless communication, by using the real time Linux layer. Experimental tests were performed by using a set of external Motion Capture Systems called OptiTrack. A total of 8 OptiTrack cameras (4 Prime-13 + 4 Prime-13W), are used to give the position and orientation of the robot with an error of 0.13mm. The path is generated inside an area of 4m x 6m as shown in Fig. 5.15.

### 5.8.2 Constant kinetic energy approach

The experiments are done for Robotino with constant kinetic energy  $E_{kin} = 0.117J$ . The results of the path following are given in Fig. 5.16, Fig. 5.17 and Fig. 5.18.

Refer to Fig. 5.16 and Fig. 5.18. we notice that the virtual control point algorithm shows a very good accuracy in path tracking and following the given velocity profile from constant kinetic energy. Fig. 5.17 represents a comparison Comparison of power consumption of Robotino with estimated model. The estimated model has some errors in estimation. These errors can be due to the non-uniform nature of the ground.



Figure 5.14: Robotino3 mobile robot



Figure 5.15: Experimental environment

### 5.8.3 Multi-criteria optimization

The results for optimal velocity profile obtained from NSGA-II are presented in Fig. 5.19, Fig. 5.20 and Fig. 5.21

Fig. 5.19 and Fig. 5.21 represents a comparison of path tracking and velocity following with virtual control point for the optimal velocity profile obtained from the NSGA-II. The obtained results show the robustness of the proposed controller. Fig. 5.21 represents a comparison Comparison of power consumption of Robotino with the estimated model. We notice that the errors are reduced. The remaining errors are due to the non-uniform surface of the ground.

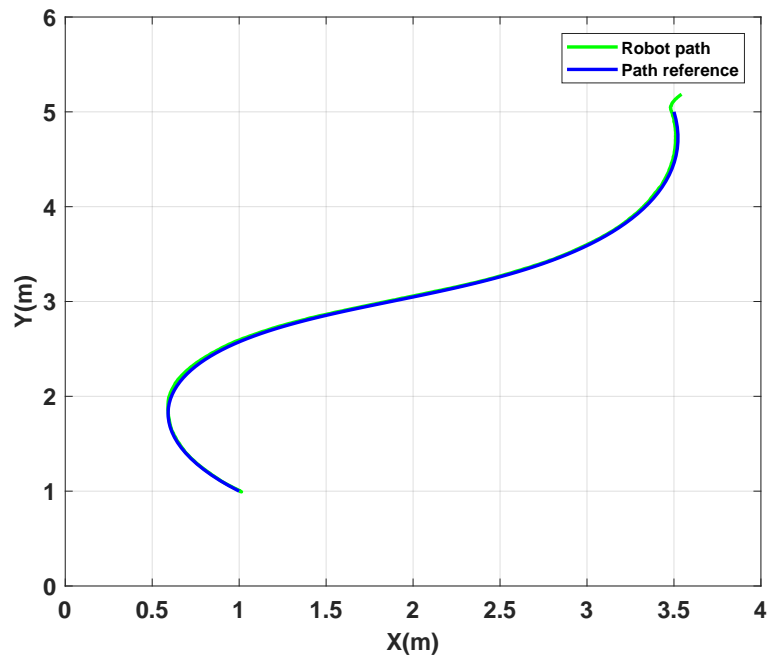


Figure 5.16: Comparison of Robotino path with reference path

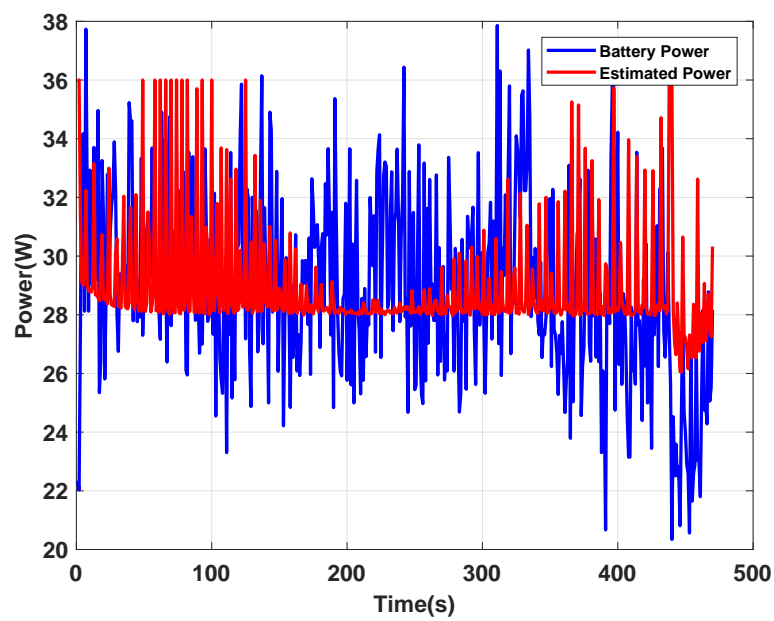


Figure 5.17: Comparison of power consumption of Robotino with estimated model



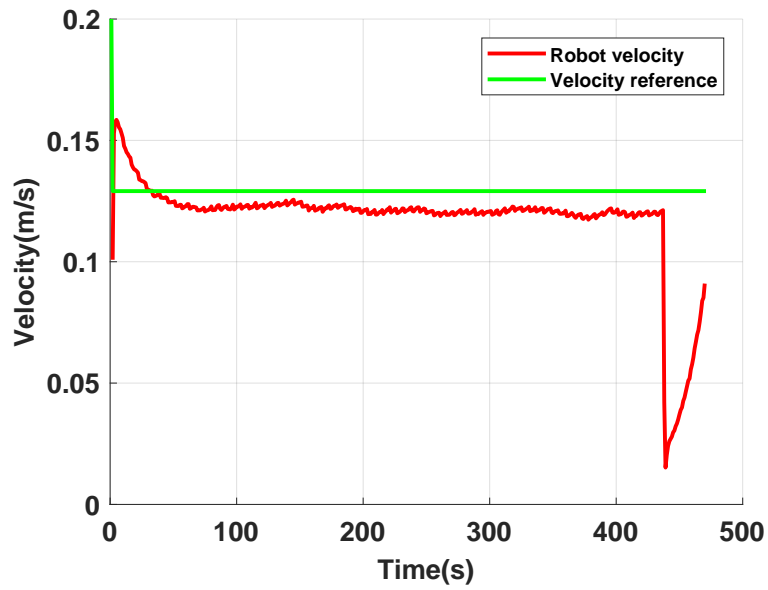


Figure 5.18: Comparison of Robotino velocity with reference velocity

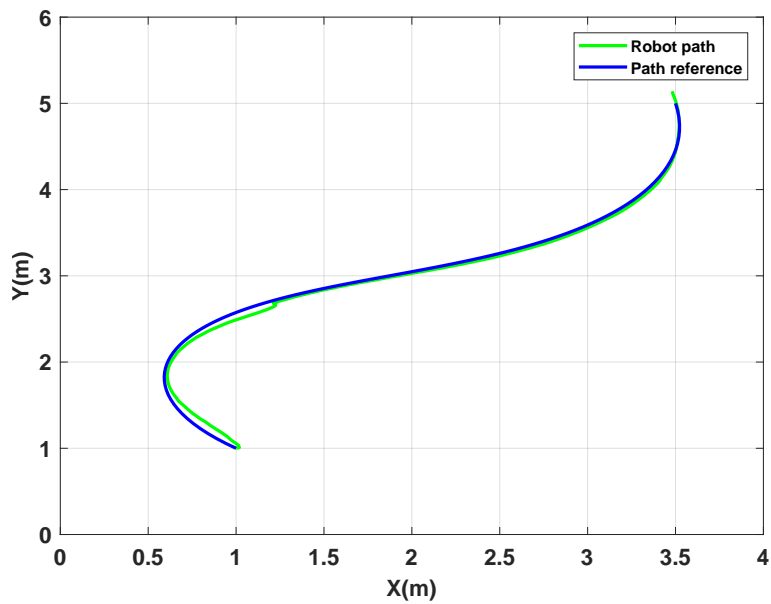


Figure 5.19: Comparison of Robotino path with the reference path

## 5.9 Experimental data-based results for an outdoor over-actuated URV

The following assumptions are considered for the proposed algorithm: i) the elevations in the road profile are neglected, ii) the switching between any two

## 5.9. Experimental data-based results for an outdoor over-actuated URV

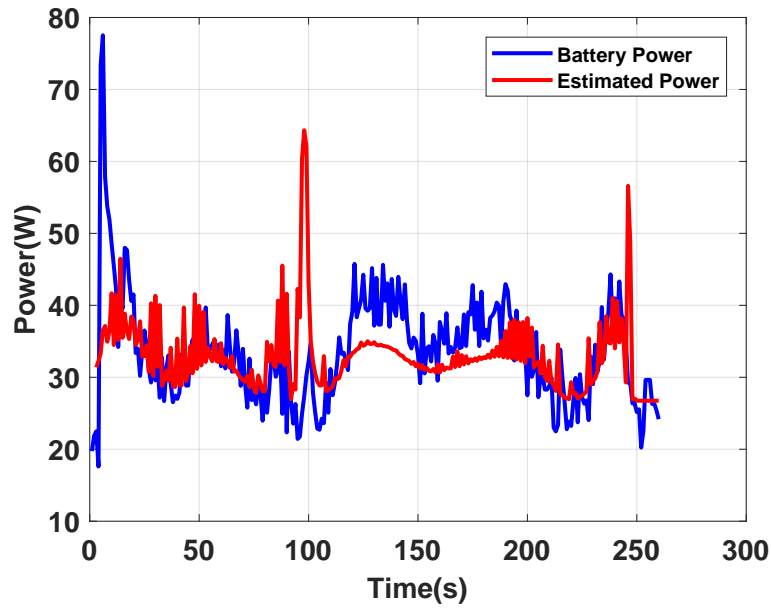


Figure 5.20: Comparison of power consumption of Robotino with the estimated model

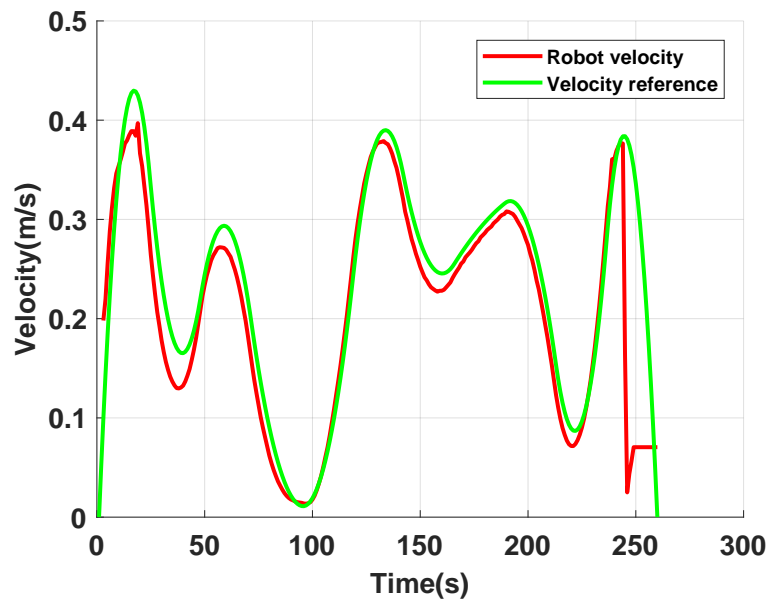


Figure 5.21: Comparison of Robotino velocity with the reference velocity

driving modes is possible, and iii) the maximum velocity of URV is 16km/h which ensures the stability along a given path. The developed algorithm is applied on a real path.

The proposed optimization procedure is applied in the case of four driving

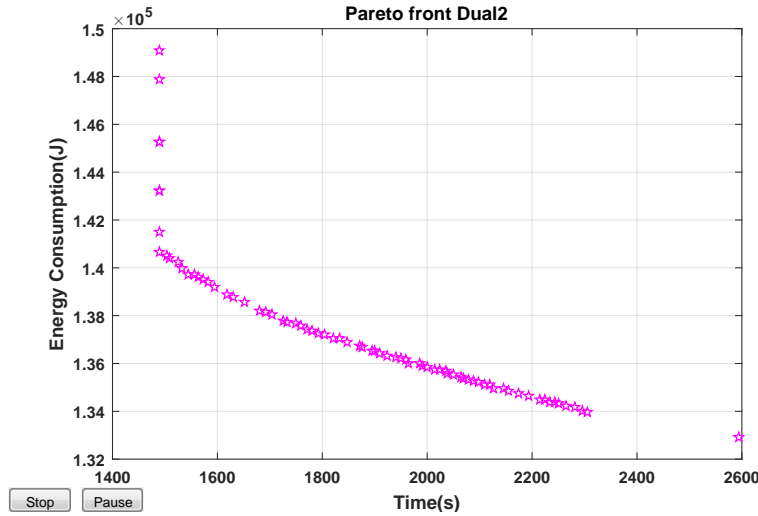


Figure 5.22: Pareto front for method 1 smoothing for Dual2.

modes: Dual2, Dual4, Single2, and Single4. The velocity profile is parameterized using six control points. The population size used in NSGA-II is 60. Fig.5.22, 5.23, Fig.5.24, 5.25 show the Pareto fronts for the different driving modes corresponding to the smoothed paths with method 1. Fig.5.26, 5.27, Fig.5.28, 5.29 show the Pareto fronts for the different driving modes corresponding to the smoothed paths with method 2.

The optimal velocities corresponding to selected compromise points from each Pareto front corresponding to each driving mode are superimposed in Fig.5.30, Fig.5.31 for smoothed paths using method 1 and method 2. The intersection points among different velocity profiles are identified.

Therefore, using these intersection points a digraph is constructed and dynamic programming is applied. In consequence, we obtain the optimal composite velocity profile with the optimal distribution of driving modes for smoothed paths using method 1 and method 2 as shown in Fig.5.32 and 5.33, respectively.

Fig. 5.34 represents the results of optimal velocity profile and optimal driving modes for a discrete energy planning methodology with dynamic programming as discussed in [Bensekrane 2018]. In this figure, we notice that the mode switching and acceleration rate cannot be reasonable for some turns in the path (e.g. turns between arc lengths [1250,1500]). While, using the proposed continuous energy planning methodology, a smooth and reasonable profile of optimal velocity and modes are obtained (Fig. 5.32 and 5.33).

Figures 5.35 and 5.36 shows the comparison of Experimental and ANFIS power consumption for optimal distribution of driving modes for method 1 and method 2 respectively. Refer to Table 5.2, a comparison of energy con-

## 5.9. Experimental data-based results for an outdoor over-actuated UR3

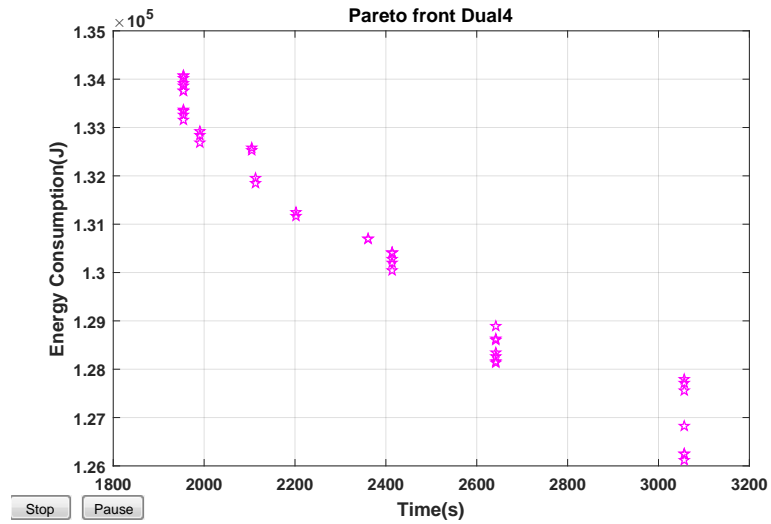


Figure 5.23: Pareto front for method 1 smoothing for Dual4.

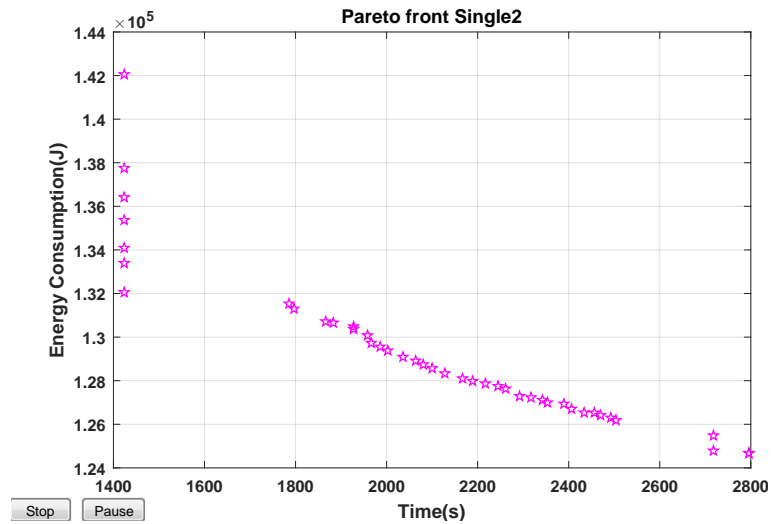


Figure 5.24: Pareto front for method 1 smoothing for Single2.

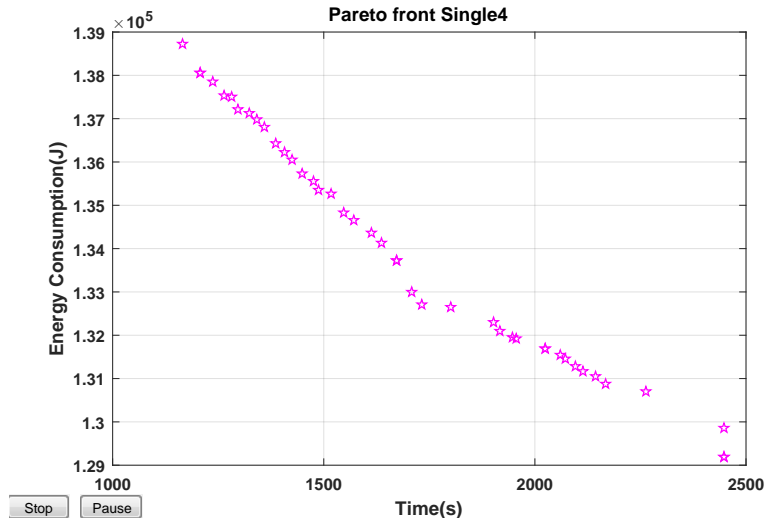


Figure 5.25: Pareto front for method 1 smoothing for Single4.

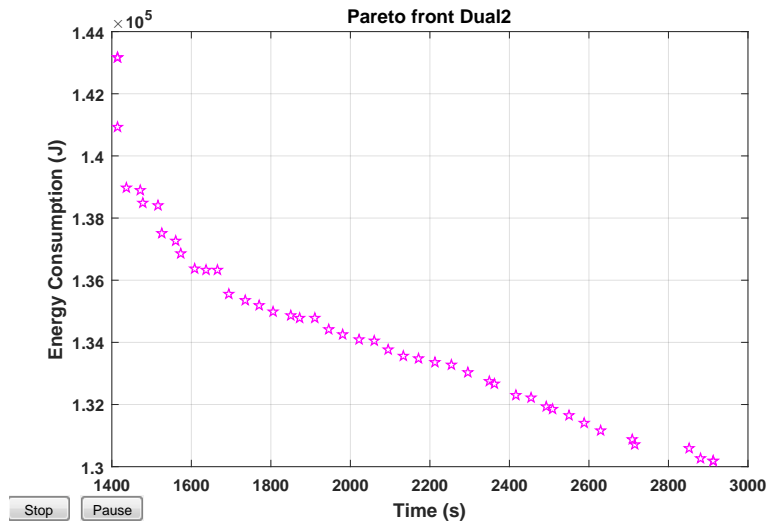


Figure 5.26: Pareto front for method 2 smoothing for Dual2.

## 5.9. Experimental data-based results for an outdoor over-actuated UWB

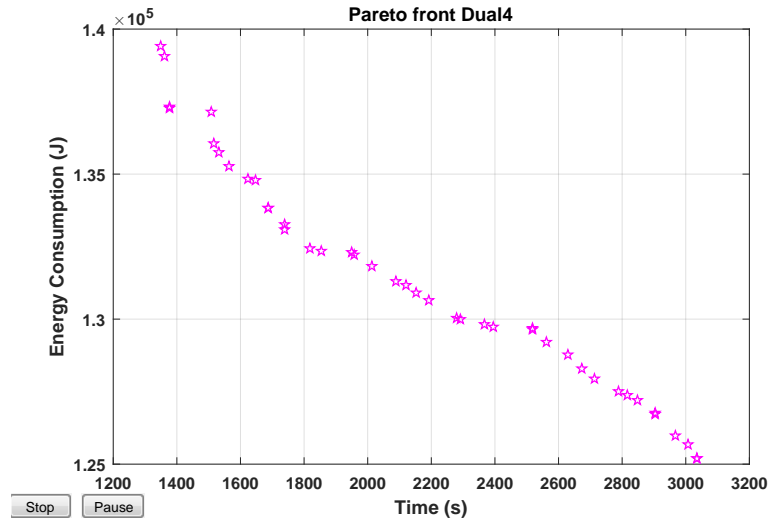


Figure 5.27: Pareto front for method 2 smoothing for Dual4.

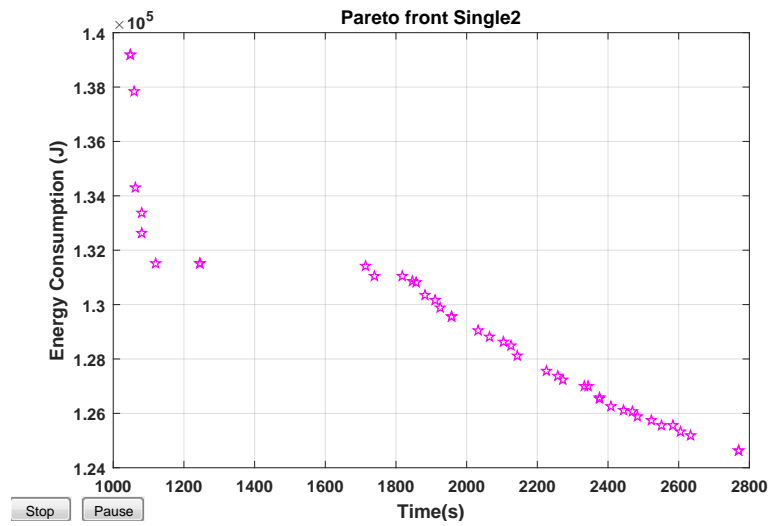


Figure 5.28: Pareto front for method 2 smoothing for Single2.

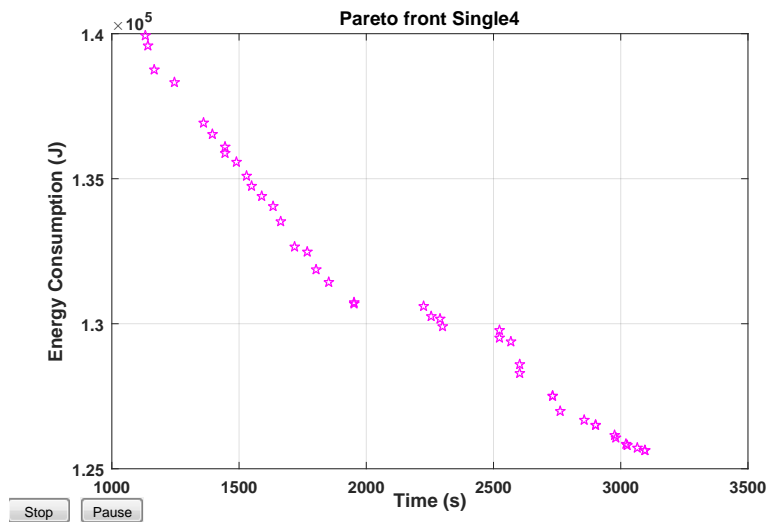


Figure 5.29: Pareto front for method 2 smoothing for Single4.

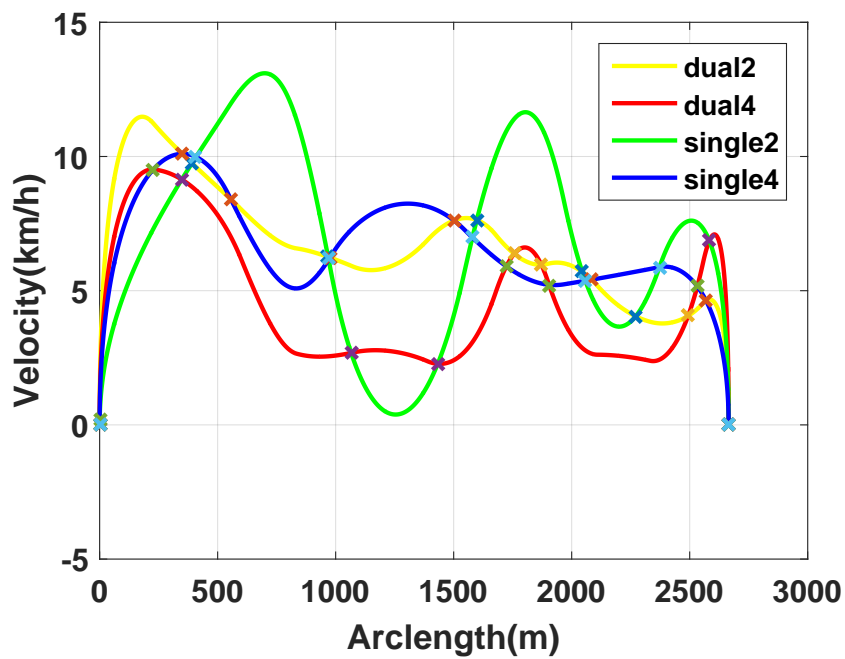


Figure 5.30: Superposition of optimal velocity profiles for different driving modes with smoothing Method 1.

### 5.9. Experimental data-based results for an outdoor over-actuated URV

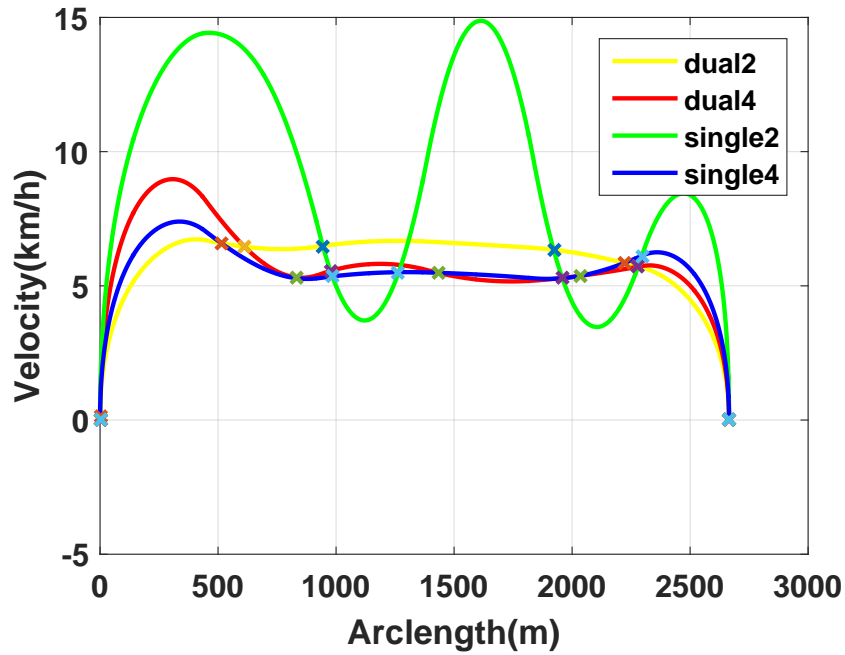


Figure 5.31: Superposition of optimal velocity profiles for different driving modes with smoothing Method 2.

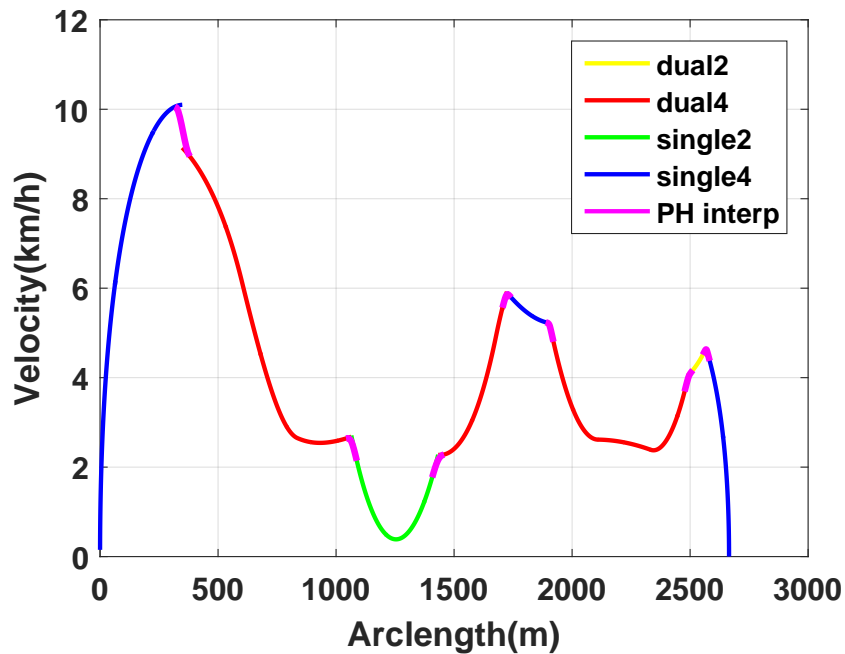


Figure 5.32: Optimal velocity profile and optimal distribution of driving modes for Method 1.



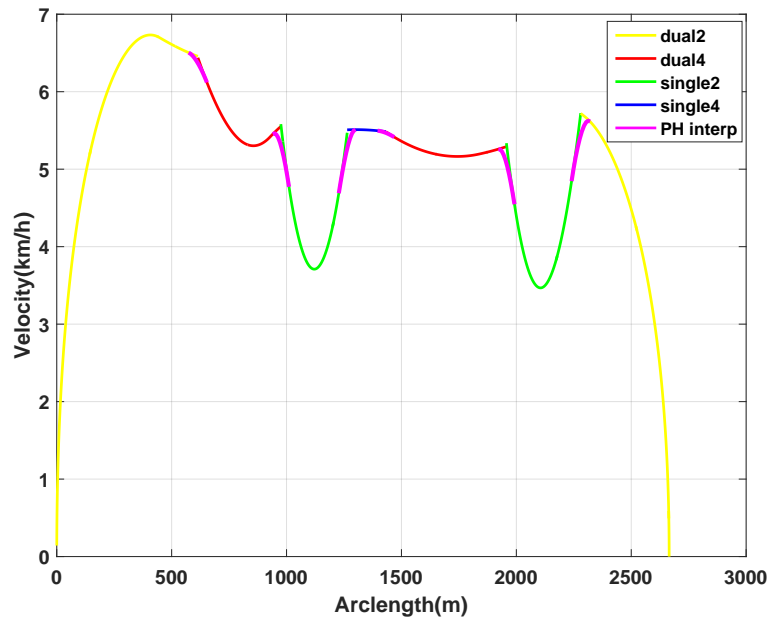


Figure 5.33: Optimal velocity profile and optimal distribution of driving modes for Method 2.

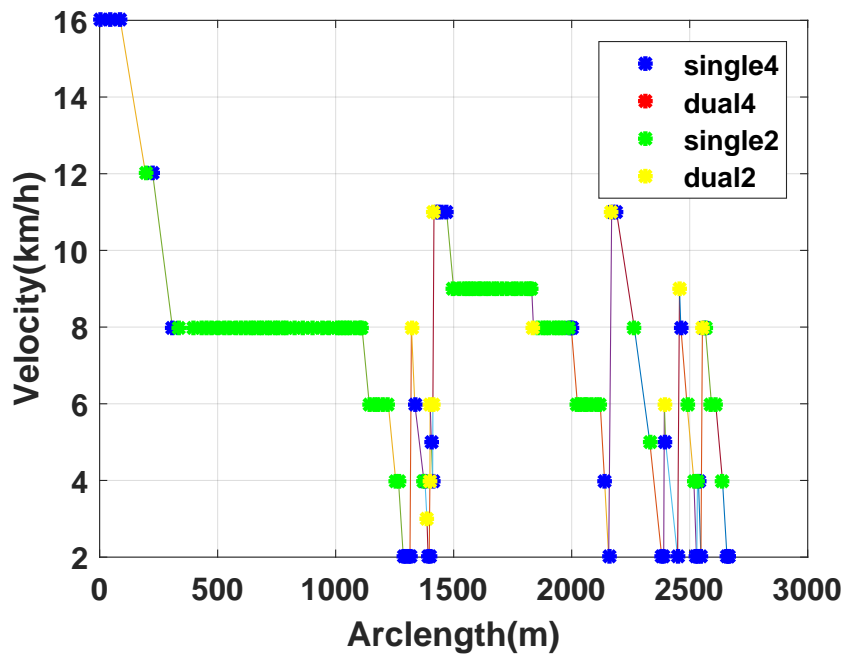


Figure 5.34: Optimal velocity profile and optimal distribution of driving modes for discrete DP method presented in [Bensekrane 2018].

## 5.9. Experimental data-based results for an outdoor over-actuated UR10

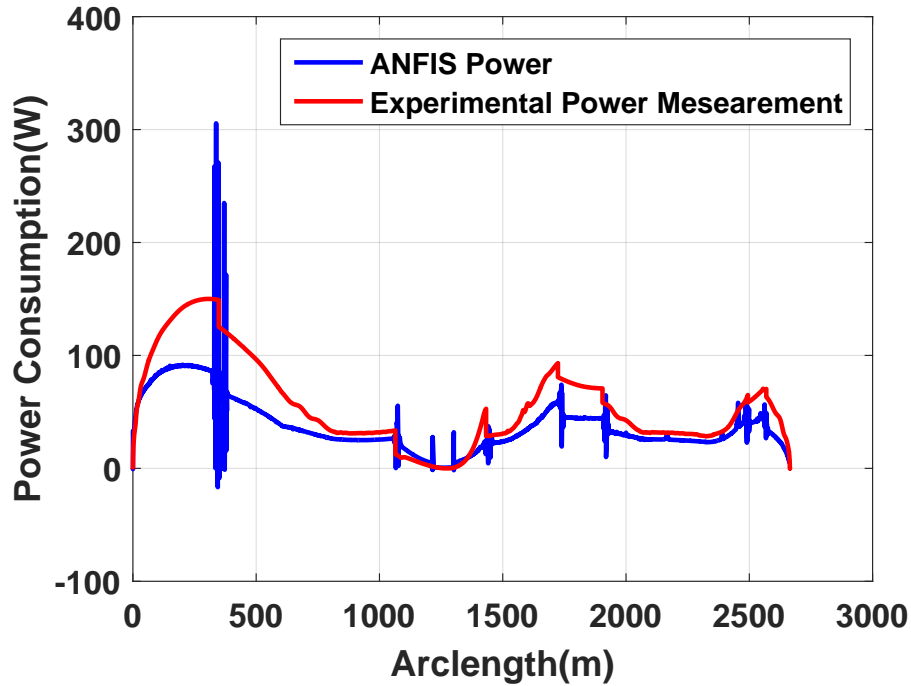


Figure 5.35: Comparison of Experimental and ANFIS power consumption for optimal distribution of driving modes for Method 1.

sumption and travel time for method 1 and method 2 is given for all selected points corresponding to each driving mode and for a combined velocity profile along with the experimental energy and travel time. This comparison is done to show that the methods used to smooth the path effects the energy planning methodology. From a combined velocity profile, it is also noticed that for method 1, the energy consumption is less but the travel time is more important.

Table 5.2: Comparison of energy consumption

Smoothing Method1: Line, Arc, Clothoid					
	Dual2	Dual4	Single2	Single4	Combined
Energy (J)	$1.397e^5$	$1.312e^5$	$1.320e^5$	$1.346e^5$	<b><math>9.4394e^4</math></b>
Time (s)	1543	2203	1423	1571	<b>3953</b>
Smoothing Method 2: Line, PH					
	Dual2	Dual4	Single2	Single4	Combined
Energy (J)	$1.356e^5$	$1.331e^5$	$1.315e^5$	$1.319e^5$	<b><math>1.0333e^5</math></b>
Time (s)	1695	1740	1119	1803	<b>2056</b>

In Table 5.3, a comparison of energy and travel time is shown for the methods presented in this chapter and the discrete method dis-

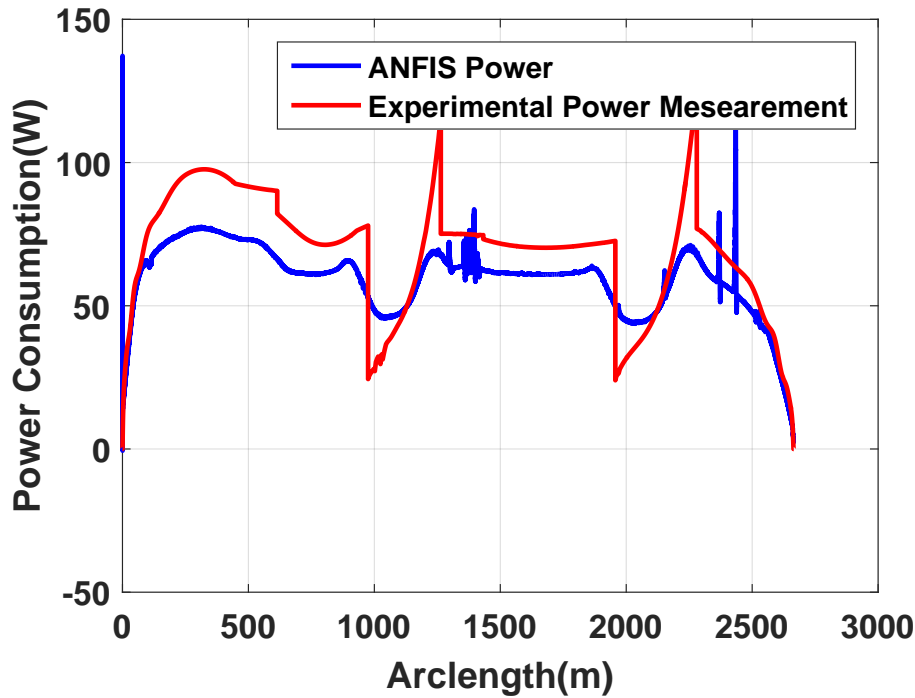


Figure 5.36: Comparison of Experimental and ANFIS power consumption for optimal distribution of driving modes for Method 2.

cussed in [Bensekrane 2018]. It can be observed that the DP method in [Bensekrane 2018] presents only one global solution for energy optimization, unlike the continuous energy planning methodology having multiple optimal solutions with different optimal energy consumption and optimal traveling times.

Table 5.3: Comparison of energy consumption

	Method 1	Method 2	Method in [Bensekrane 2018]
Experimental Energy (J)	<b>9.765e<sup>4</sup></b>	<b>1.0439e<sup>5</sup></b>	<b>7.6589e<sup>4</sup></b>
Experimental Time (s)	<b>3920</b>	<b>2086</b>	<b>1390</b>
Simulated Energy (J)	<b>9.4394e<sup>4</sup></b>	<b>1.0333e<sup>5</sup></b>	<b>1.0426e<sup>5</sup></b>
Simulated Time (s)	<b>3953</b>	<b>2056</b>	<b>1411.9</b>

## 5.10 Conclusion

This chapter presents a continuous energy planning methodology for an over-actuated URV based on power consumption estimation model. The power consumption is estimated using ANFIS model for different driving modes of the URV. The tracked path is generated using two different smoothing meth-

---

ods. Also, NSGA-II algorithm is then applied to generate Pareto fronts regrouping compromise solutions between travel time and the consumed energy, for each driving mode. Finally, a weighted digraph has been made in order to find the optimal velocity profile taking benefit from the various URV driving modes. The obtained results highlighted that the proposed approach is efficient and allows to generate smooth reference velocity profile for the considered URV on the assigned path, that accounts of the over-actuation and the existence of many driving modes. The choice of the smoothing method affected considerably the overall energy consumption and the travel time of a URV. For future work, it is intended to extend the proposed energy planning methodology in case of presence of actuation's faults.

# Conclusion and Prospective

---

## Contents

---

<b>6.1 Summary of Conclusions</b> . . . . .	<b>113</b>
<b>6.2 Future works</b> . . . . .	<b>115</b>

---

The main objective of this thesis is to provide a methodology for energy planning of an autonomous over-actuated URV. Generally, in the literature, the energy management is developed through an optimal control problem. However, the energy planning consists to plan the available energy in an optimal way before the execution of the autonomous navigation algorithms for the URV. In a simple case, energy planning consists of finding an optimal velocity profile. However, in the consideration of the characteristics of an over-actuated vehicle, the problem becomes more complex, where the energy planning needs to find the optimal configuration associated with the velocity profile and the driving modes, along the predefined path. The proposed methodology is validated experimentally on over-actuated URV, and it is also compared with the different methods.

## 6.1 Summary of Conclusions

First, a concise and a complete view of the field of autonomous driving of vehicles is presented, after discussion of the different types of robots according to their kinematic parameters. The main interesting problems addressed in the framework of this PhD thesis are:

1. Power consumption modeling of over-actuated URVs,
2. Energy planning methodology for over-actuated URVs.

Due to the actuation redundancy of over-actuated URVs and the derivatives of the different driving configuration, the modeling of power consumption estimation plays a vital role. The positioning of the energy planning methodology for URVs has been made compared to existing algorithms for autonomous driving. Also, the redundancy in terms of traction or in the steering is optimized along the path as one of the specifications for the proposed contribution.

To reach the global optimization of energy and to plan energy for vehicles for predefined road path, it is essential to have a precise model of energy power consumption estimation, which will allow us to avoid a sudden stop situation or to disrupt vehicle traffic. First, the model of power consumption estimation is formulated for different configuration separately. The total power consumption is decomposed into three elements of power estimation including inertia power, rolling resistance power, gravitational power, and the static power caused by various electrical components. The main consumption power is caused by the rolling resistance which has a relation with the curvature of the trajectory  $C$ , the degree of steerability  $\delta_s$ , and the degree of redundancy  $\delta_R$ .

A generic analytic formulation of power consumption estimation is developed including different kinematic parameters, geometrical parameters, and dynamic parameters for six driving modes of the URV. The different contact forces are estimated by the magic formula of Pacejka and **kept unchangeable for all the offline energy planning**. This generic formulation does not cover all the non-linearities present in the different components of the URV, located at the mechanical chain, the electric chain, and the battery. To overcome these non-linearities in the power consumption modeling estimation, a qualitative model is developed. Thus, an Adaptive Neuro Fuzzy Inference System (ANFIS) is proposed. The inputs of the ANFIS model are the curvature of the path, the velocity and the acceleration of the URV, and the output of the neuronal model is the overall power consumption. ANFIS model was validated experimentally with real URV and it shows a better accuracy for the different driving modes, comparing to the analytic model.

The proposed energy planning is decomposed on three steps:

1. Pre-processing phase: Both quantitative and qualitative models of power consumption estimation are used to find an accurate model of power consumption for the over-actuated URV.
2. Optimization phase: it concerns the use of optimization algorithms to solve a given objective function.
3. Post-processing phase: In this step, a correction of distribution of driving modes is considered for a specific segment of the road path.

In the optimization phase, discrete and continuous optimization algorithms are used. The discrete approach of optimization is based on the discretization (filtering) of the road profile according to geometrical criteria {Lines, Clothoids, and Arcs}. This filtering divides the path into multiple segments according to its geometrical nature. An energy digraph is then constructed, by associating the graph nodes to the starting and ending point of each segment, and the cost value of each vertex in the digraph represents the consumed energy in each segment and for each driving mode. This operation will elabo-

rate on different layers in the digraph, where each layer corresponds to a given driving mode. When the energy digraph is constructed with different driving modes, we use search graph algorithms to find the global optimal solution. The used algorithm in the search graph to find a global solution is Dynamic Programming. The global solution is presented as a couple of velocity profile and the driving mode, associated with each segment of the considered road profile. In terms of the time consuming, Dijkstra and  $A^*$  are compared with dynamic programming. we noticed that  $A^*$  is faster than Dijkstra and dynamic programming in case of discrete optimization. The continuous method was developed to resolve the energy planning problem in the presence of a smooth velocity profile and smooth changes of driving modes. To reach this goal, a multi-objective algorithm based on genetic algorithms (NSGAI) is used. The choice of multi-objective optimization rather than mono-objective algorithms is the importance of the energy and travel time compromise. The path was smoothed using two sets of curves, smooth{Lines, Clothoids, and Arcs} and {Lines, Pythagorean Holograph (PH)}. A Pareto front was developed for each driving mode and for each smoothed path. Finally, a digraph structure is proposed to combine the different optimal velocities obtained from the ideal point from each Pareto front. Our conclusion in terms of discrete and continuous optimizations, used in this work, is that the discrete one is appropriate for short paths, where the time consuming of the algorithm is high, with an accurate discrete road profile. However, the continuous optimization is suitable for long paths, where the time consuming is relatively low and the road profile is continuous and less accurate.

## 6.2 Future works

The possible extensions in the current work regarding the energy planning strategies for URVs are numerous:

1. Doing the online energy planning of the URV, by considering the changes in the environment, in terms of parameters variation of the external efforts of the wheel-ground contacts, as a result of the change of weather for example.
2. According to the planning energy baseline, in case the URV is operating in normal condition, it is important to study the performance of this planning in the case of faults occurrence. The aim is to make the energy planning in critic situations in the case of a fault in actuators or a puncture in the wheel tire,..etc. This allows to make a power planning tolerant to faults.
3. Another prospective of this realized work is to develop coordination between offline energy planning and online energy management. In that

case, it is interesting to make the path planning, the trajectory planning, the task allocation and the routing of the URV, not based only of the short path/trajectory, the optimal velocity,..., but also the optimal energy to be consumed in accordance with specified constraints.



# Experimental Validation

---

## Contents

---

<b>A.1 SCANeR™ Studio</b> . . . . .	<b>117</b>
A.1.1 Massive simulation . . . . .	119
A.1.2 Vehicle Dynamics . . . . .	120
<b>A.2 RobuCAR Motor Characterization</b> . . . . .	<b>120</b>
A.2.1 Technical specifications . . . . .	121
A.2.2 Test bench for motor characterization . . . . .	121

---

## A.1 SCANeR™ Studio

SCANeR™ studio is a comprehensive software dedicated to automotive and transport simulation addressing both testing and driving for Advanced Driver Assistance Systems (ADAS), Autonomous vehicle, Human-Machine Interface (HMI) and headlight use cases. SCANeR™ provides all the tools and models that are necessary to build an ultra-realistic virtual World: road environment, vehicle dynamics, traffic, sensors, real or virtual drivers, headlights, weather conditions and scenario scripting. Far from being a black box tool, it is a genuine modular simulation platform, flexible, expandable and open, meeting the needs of researchers and engineers. Its versatility makes a complete range of setups possible: driving simulators, model-in-the-loop, software-in-the-loop, hardware-in-the-loop.

With realistic models for the vehicle, the sensors and the environment Fig. A.2, SCANeR™ is the central development and testing platform for many ADAS and autonomous vehicle use cases:

- Active & Passive safety systems
- HMI integration / evaluation
- Collision avoidance, Warning, Assistance systems
- Automatic parking
- Validation
- Training

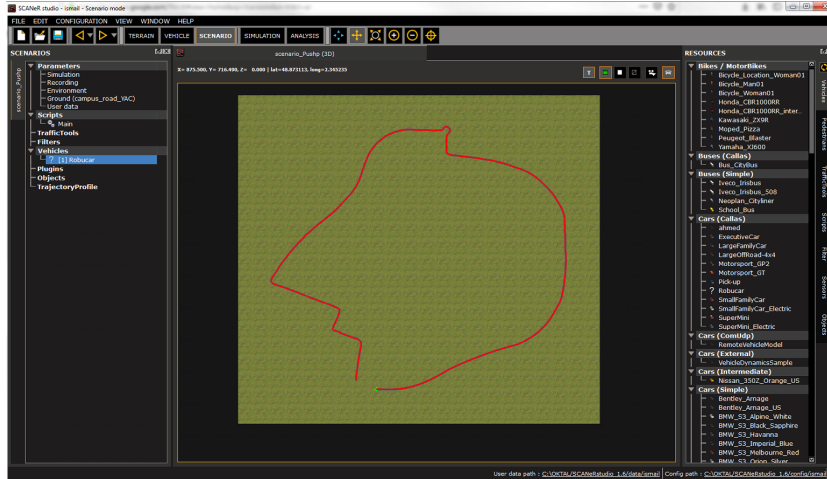


Figure A.1: Simulation of RobuCAR in Campus of Lille University

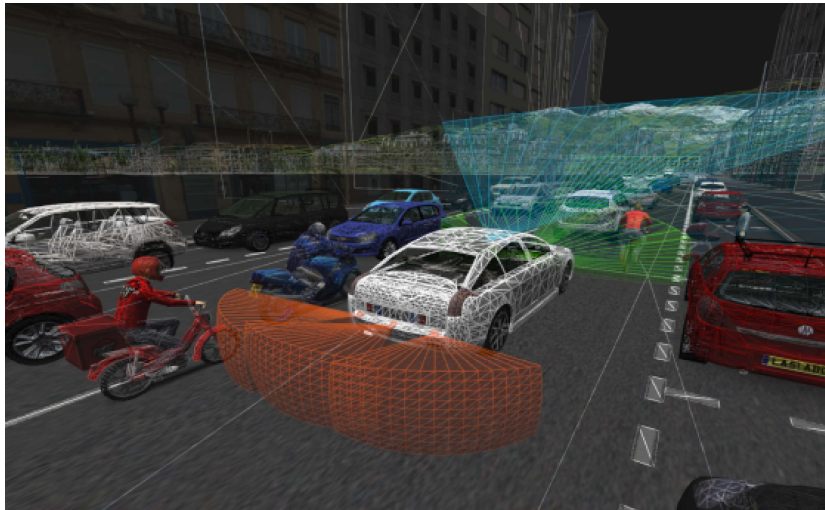


Figure A.2: Environment modeling and vehicle sensing

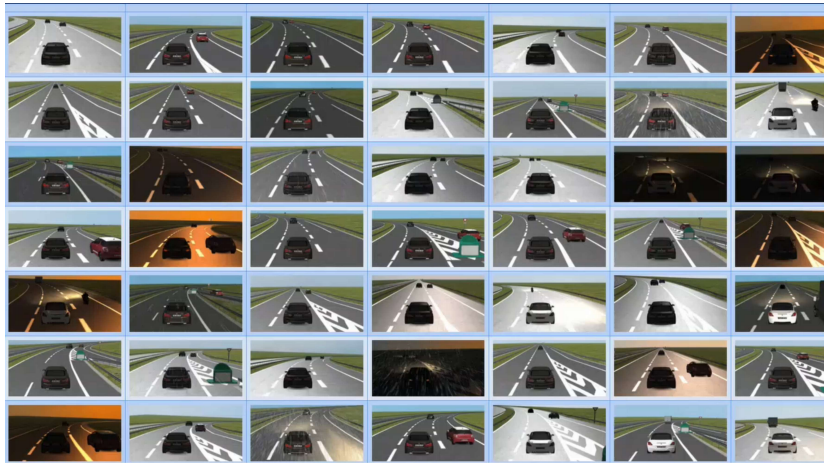


Figure A.3: Different lighting for driving

Well-integrated in the development process, it allows the evaluation of the HMI system at an early stage of development and improves the relevance of Ergonomic Studies Fig. A.3, with respect to the existing tools and methods. Use cases for human factors studies :

- Evaluation of human driver performance and behavior,
- Driver fatigue, sleepiness, Hypo vigilance, drugs and alcohol effects,
- Ergonomics,
- Traffic safety,
- Infrastructure and transportation studies,
- Human Machine Interface (HMI) and ADAS,
- System prototyping and integration.

### A.1.1 Massive simulation

SCANeR™ virtual platform enables driver assistance systems (ADAS) and autonomous driving functions to be endlessly tested and validated. The use of virtual testing to complement track or road testing provides safer test condition and reduced costs and time. This use case relies on exclusive SCANeR™ features:

- Modeling of the vehicle, sensors, driver and environment,
- Complex scenario and critical events representative of real driving situations,
- Automated tests edition program,

- Carrying out Massive and Parallel tests in an efficient way,
- Improve the validation process and tests coverage rate,
- High performance computing on premises or in the cloud,
- Metrics and performance analysis and reports,
- Validate functional safety.

### A.1.2 Vehicle Dynamics

SCANer<sup>TM</sup> includes CALLAS model A.4 and offers a virtual proving ground for various civil, military and motorsport vehicle dynamics applications: vehicles concepts and design, performance, homologation, advanced chassis control, consumption and pollution optimization, etc.



Figure A.4: CALLAS & PROSPER for vehicle dynamics

## A.2 RobuCAR Motor Characterization

The motor of RobuCAR is an electric motor manufactured by MBR company under the reference CFB0.120F1-48V 22 A 3200T/Mn 900W. It has the following characteristics:

## A.2.1 Technical specifications

### A.2.1.1 Motor characteristics

- Power: 900 W
- Voltage: 48 V
- Resistance: 1,6 Ohm
- Induction flow: 180 T
- $K_e$ : 16,2 V
- Motor speed 3200tr/mn
- Protection: IP 44
- Mass: 9,5 kg

### A.2.1.2 Reducer characteristics

- Coaxial reducer: raio 1-29 (RobuCAR AT)
- Nominal torque: 32 Nm
- Radial load: 2040 Nm in the middle of the motor shaft
- Mass: 8 kg

## A.2.2 Test bench for motor characterization

In order to characterize the RobuCAR motor, a test bench is set up as shown in the Fig. A.5. The purpose of this characterization is to plot the motor efficiency map by measuring the ratio of mechanical power and electric power for different loads. The latter is introduced in the specific field of the electric motor in the dynamic model under SCANeR<sup>TM</sup>. This operation is done to guarantee a better representation of the motor and to have a dynamic model of RobuCAR URV very close to real URV.

Fig. A.6 represents the load variation on RobuCAR motor, and Fig.A.7 show the acquisition setup with a real-time embedded industrial controller called CompactRio and voltage and current sensors.

The experimental results for characterization of RobuCAR motor are seved with a frequency of 0.01s. The efficiency maps for free load, 10% of load, 20% of load, 30% of load, 40% of load, 50% of load are presented in Fig. A.8, Fig.A.9, Fig.A.10, Fig.A.11, Fig.A.12, and Fig.A.13 respectively.

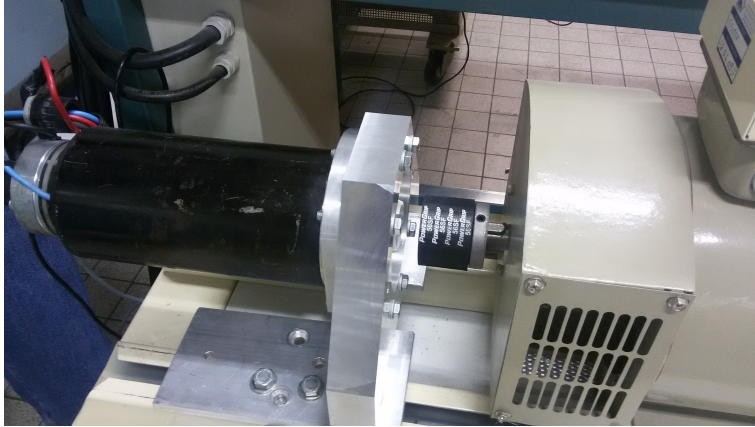


Figure A.5: RobuCAR motor on the test bench

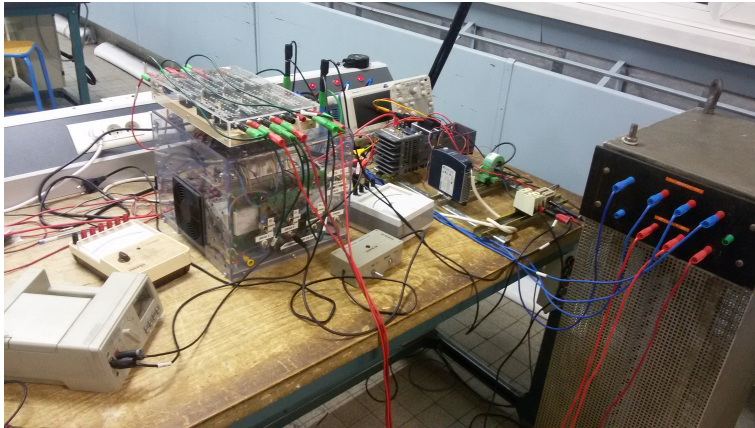


Figure A.6: Load variation test bench

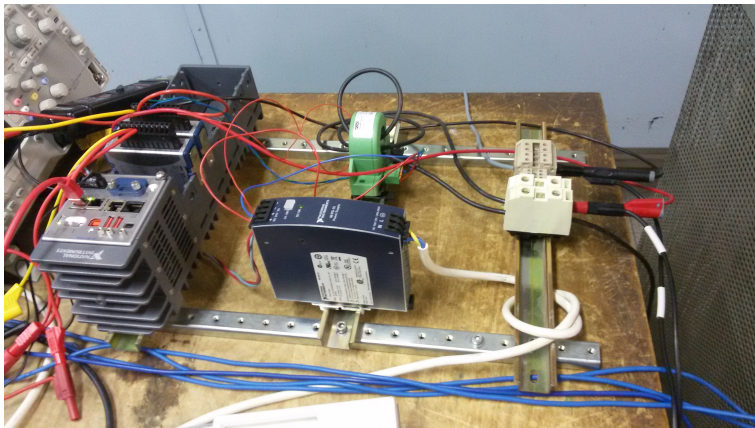


Figure A.7: Acquisition setup for the motor characterization

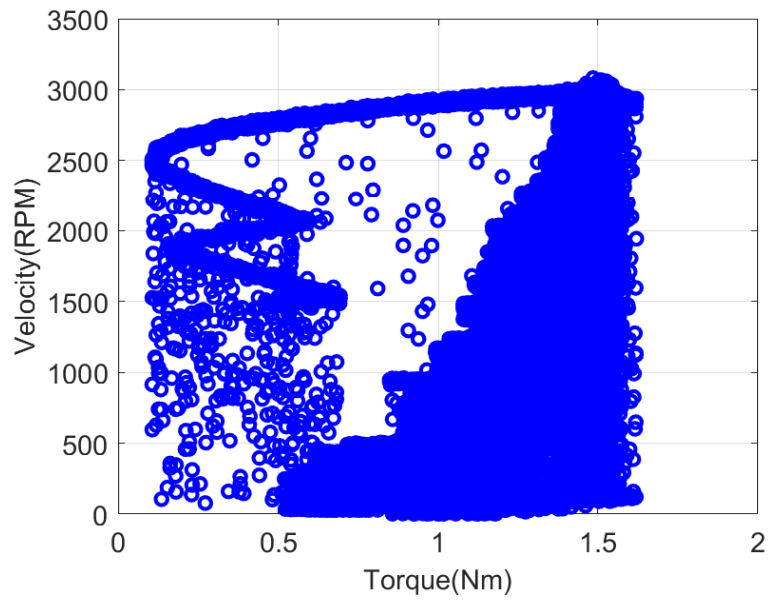


Figure A.8: Map efficiency with free load

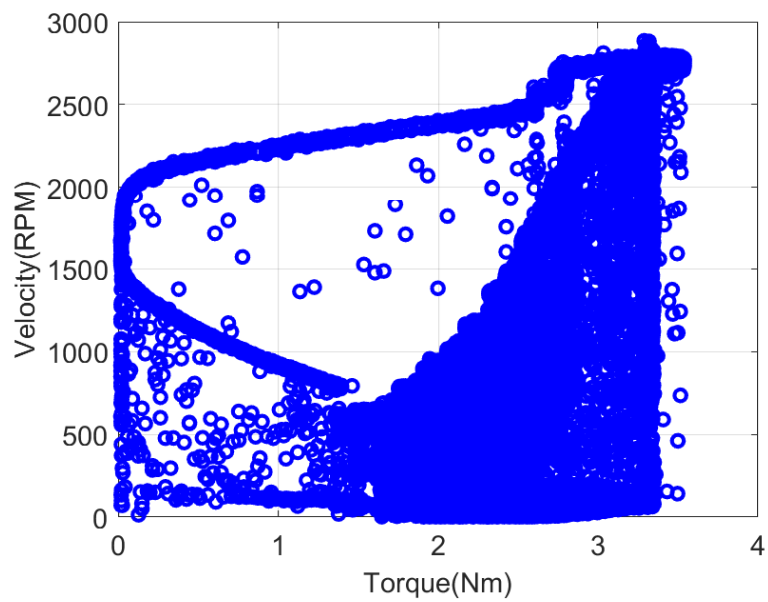


Figure A.9: Map efficiency with 10% load

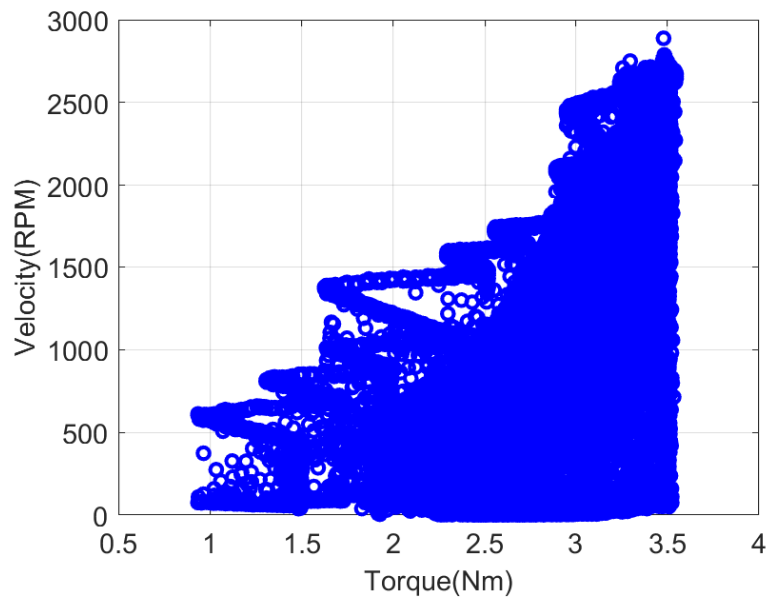


Figure A.10: Map efficiency with 20% load

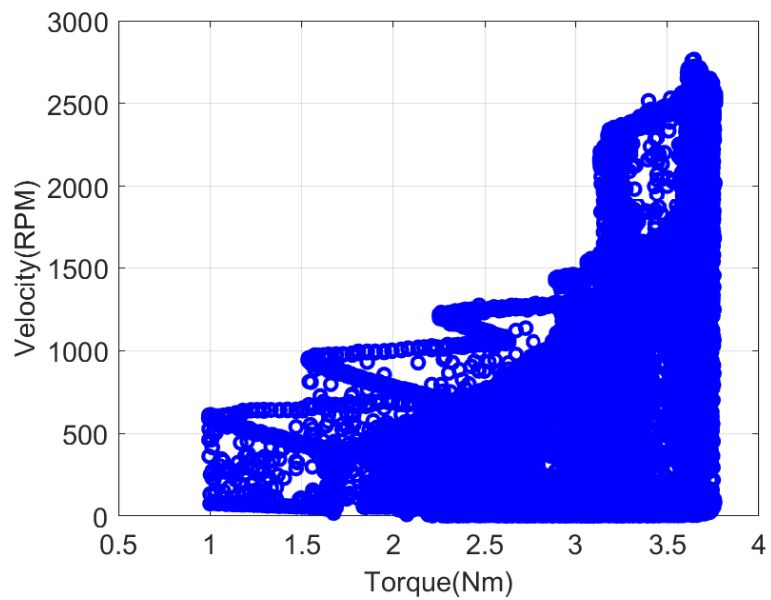


Figure A.11: Map efficiency with 30% load



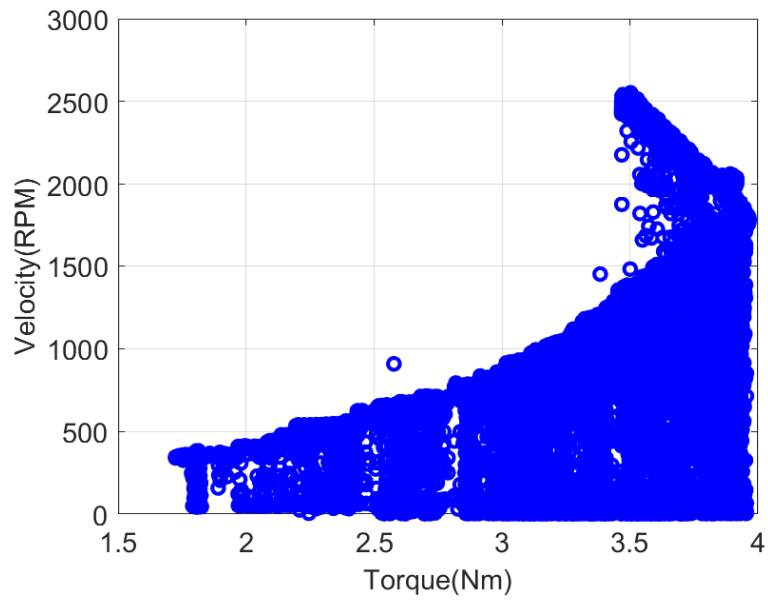


Figure A.12: Map efficiency with 40% load

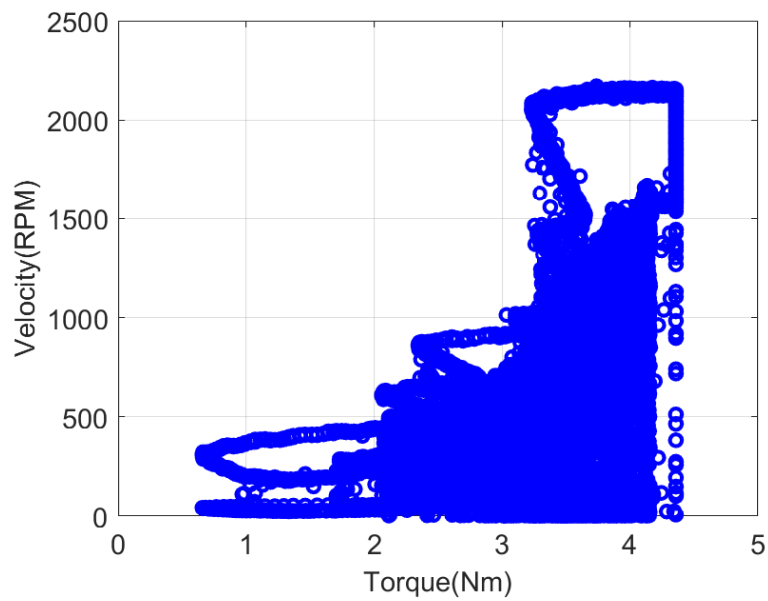


Figure A.13: Map efficiency with 50% load

# Bibliography

- [Aarniovuori 2018] Lassi Aarniovuori, Markku Niemelä, Juha Pyrhönen, Wenping Cao and Emmanuel B Agamloh. *Loss Components and Performance of Modern Induction Motors*. In 2018 XIII International Conference on Electrical Machines (ICEM), pages 1253–1259. IEEE, 2018. (Cited on page 20.)
- [Abousleiman 2016] Rami Abousleiman and Osamah Rawashdeh. *Electric vehicle modelling and energy-efficient routing using particle swarm optimisation*. IET Intelligent Transport Systems, vol. 10, no. 2, pages 65–72, 2016. (Cited on page 43.)
- [Adewumi 2018] Aderemi Oluyinka Adewumi and Olawale Joshua Adeleke. *A survey of recent advances in vehicle routing problems*. International Journal of System Assurance Engineering and Management, vol. 9, no. 1, pages 155–172, 2018. (Cited on page 36.)
- [Ahlberg 1967] J Harold Ahlberg, Edwin Norman Nilson and Joseph Leonard Walsh. *The theory of splines and their application*. 1967. (Cited on pages 54 and 86.)
- [Alidaee 2010] Bahram Alidaee, Hongman Gao and Haibo Wang. *A note on task assignment of several problems*. Computers & Industrial Engineering, vol. 59, no. 4, pages 1015–1018, 2010. (Cited on page 37.)
- [Ao 2007] G-Q Ao, J-X Qiang, H Zhong, L Yang and B Zhuo. *Exploring the fuel economy potential of ISG hybrid electric vehicles through dynamic programming*. International journal of automotive technology, vol. 8, no. 6, pages 781–790, 2007. (Cited on page 42.)
- [Athans 2013] Michael Athans and Peter L Falb. *Optimal control: an introduction to the theory and its applications*. Courier Corporation, 2013. (Cited on page 36.)
- [Avnaim 1988] Francis Avnaim, Jean-Daniel Boissonnat and Bernard Faverjon. *A practical exact motion planning algorithm for polygonal objects amidst polygonal obstacles*. In Proceedings. 1988 IEEE International Conference on Robotics and Automation, pages 1656–1661. IEEE, 1988. (Cited on page 33.)
- [Aylett 1998] R Aylett and D Barnes. *A multi-robot architecture for planetary rovers*. In Proceedings of the 5th ESA Workshop on Advanced Space Technologies for Robotics and Automation, pages 1–3, 1998. (Cited on page 38.)

- [Barraquand 1992] J. Barraquand, B. Langlois and J. . Latombe. *Numerical potential field techniques for robot path planning*. IEEE Transactions on Systems, Man, and Cybernetics, vol. 22, no. 2, pages 224–241, March 1992. (Cited on page 32.)
- [Barthelmes 2017] S. Barthelmes and S. Zehnter. *An all-terrain-controller for over-actuated wheeled mobile robots with feedforward and optimization-based control allocation*. In 2017 IEEE 56th Annual Conference on Decision and Control (CDC), pages 5215–5222, Dec 2017. (Cited on page 65.)
- [Bensekrane 2017] Ismail Bensekrane, Rochdi Merzouki, Kumar Pushpendra and Yacine Amara. *Towards Adaptive Power Consumption Estimation for Over-actuated Unmanned Vehicles*. In IEEE International Conference on Robotics and Biomimetics, 2017. (Cited on pages 48 and 49.)
- [Bensekrane 2018] Ismail Bensekrane, Pushpendra Kumar, Achille Melingui, Vincent Coelen, Yacine Amara and Rochdi Merzouki. *Energy Planning for Unmanned Over-Actuated Road Vehicle*. In 2018 IEEE Vehicle Power and Propulsion Conference (VPPC), pages 1–6. IEEE, 2018. (Cited on pages xi, 44, 82, 102, 108 and 110.)
- [Bertsekas 1995] Dimitri P Bertsekas, Dimitri P Bertsekas, Dimitri P Bertsekas and Dimitri P Bertsekas. *Dynamic programming and optimal control*, volume 1. Athena scientific Belmont, MA, 1995. (Cited on page 72.)
- [Bertsekas 2006] DP Bertsekas. *Nonlinear Programming, Athena Scientific, 1999*. REFER ÈENCIAS BIBLIOGR AFICAS, vol. 89, 2006. (Cited on pages 35 and 36.)
- [Betts 1998] John T Betts. *Survey of numerical methods for trajectory optimization*. Journal of guidance, control, and dynamics, vol. 21, no. 2, pages 193–207, 1998. (Cited on page 30.)
- [Betts 2001] JT Betts. *Practical Methods for Optimal Control Using Nonlinear Programming (2001)*. Society for Industrial and Applied Mathematics, 2001. (Cited on page 36.)
- [Betts 2010] John T Betts. *Practical methods for optimal control and estimation using nonlinear programming*, volume 19. Siam, 2010. (Cited on pages 30, 35 and 36.)
- [Bianchi 2010] Domenico Bianchi, Luciano Rolando, Lorenzo Serrao, Simona Onori, Giorgio Rizzoni, Nazar Al-Khayat, Tung-Ming Hsieh and Pengju Kang. *A rule-based strategy for a series/parallel hybrid electric vehicle: an approach based on dynamic programming*. In ASME 2010 Dynamic Systems and Control Conference, pages 507–514. American Society of Mechanical Engineers, 2010. (Cited on page 42.)

- [Bin 2009] Y Bin, A Reama, A Cela, R Natowicz, H Abderrahmane and Y Li. *On fast dynamic programming for power splitting control of plug-in hybrid electric vehicles*. In ASME 2009 Dynamic Systems and Control Conference, pages 229–236. American Society of Mechanical Engineers, 2009. (Cited on page 42.)
- [Bliss 1946] Gilbert A Bliss. *Lectures on the Calculus of Variations*. 1946. (Cited on page 36.)
- [Boehme 2013] Thomas J Boehme, Markus Schori, Benjamin Frank, Matthias Schultalbers and Wolfgang Drewelow. *A predictive energy management for hybrid vehicles based on optimal control theory*. In 2013 American Control Conference, pages 5984–5989. IEEE, 2013. (Cited on page 42.)
- [Botelho 1999] Sylvia C Botelho and Rachid Alami. *M+: a scheme for multi-robot cooperation through negotiated task allocation and achievement*. In Proceedings 1999 IEEE International Conference on Robotics and Automation (Cat. No. 99CH36288C), volume 2, pages 1234–1239. IEEE, 1999. (Cited on page 38.)
- [Boyali 2010] Ali Boyali and Levent Güvenç. *Real-time controller design for a parallel hybrid electric vehicle using neuro-dynamic programming method*. In 2010 IEEE International Conference on Systems, Man and Cybernetics, pages 4318–4324. IEEE, 2010. (Cited on page 42.)
- [Boyd 2004] Stephen Boyd and Lieven Vandenberghe. *Convex optimization*. Cambridge university press, 2004. (Cited on pages 35 and 36.)
- [Brembeck 2012] J. Brembeck and P. Ritzer. *Energy optimal control of an over actuated Robotic Electric Vehicle using enhanced control allocation approaches*. In 2012 IEEE Intelligent Vehicles Symposium, pages 322–327, June 2012. (Cited on pages ix, 29 and 30.)
- [Brooks 1985] Rodney A Brooks and Tomas Lozano-Perez. *A subdivision algorithm in configuration space for findpath with rotation*. IEEE Transactions on Systems, Man, and Cybernetics, no. 2, pages 224–233, 1985. (Cited on page 32.)
- [Bruyninckx 1997] Herman Bruyninckx and Dominiek Reynaerts. *Path planning for mobile and hyper-redundant robots using Pythagorean hodograph curves*. In Advanced Robotics, 1997. ICAR'97. Proceedings., 8th International Conference on, pages 595–600. IEEE, 1997. (Cited on page 87.)
- [Bryson 1975] A Bryson and Y Ho. *Applied Optimal Control* Hemisphere Publishing. New York, 1975. (Cited on page 36.)

- [Butcher 2008] John Charles Butcher and Nicolette Goodwin. Numerical methods for ordinary differential equations, volume 2. Wiley Online Library, 2008. (Cited on page 35.)
- [Caceres-Cruz 2015] Jose Caceres-Cruz, Pol Arias, Daniel Guimarans, Daniel Riera and Angel A Juan. *Rich vehicle routing problem: Survey*. ACM Computing Surveys (CSUR), vol. 47, no. 2, page 32, 2015. (Cited on page 36.)
- [Campion 1996] G. Campion, G. Bastin and B. Dandrea-Novel. *Structural properties and classification of kinematic and dynamic models of wheeled mobile robots*. IEEE Transactions on Robotics and Automation, vol. 12, no. 1, pages 47–62, Feb 1996. (Cited on page 14.)
- [Cao 2017] Wujun Cao and Wenshui Yang. *A survey of vehicle routing problem*. In MATEC Web of Conferences, volume 100, page 01006. EDP Sciences, 2017. (Cited on page 36.)
- [Chen 1995] Danny Z Chen, Robert J Szczerba and JJ Uhran. *Planning conditional shortest paths through an unknown environment: A framed-quadtree approach*. In Proceedings 1995 IEEE/RSJ International Conference on Intelligent Robots and Systems. Human Robot Interaction and Cooperative Robots, volume 3, pages 33–38. IEEE, 1995. (Cited on page 33.)
- [Chen 2009] Zheng Chen and Chris Chunting Mi. *An adaptive online energy management controller for power-split HEV based on dynamic programming and fuzzy logic*. In 2009 IEEE Vehicle Power and Propulsion Conference, pages 335–339. IEEE, 2009. (Cited on page 40.)
- [Chen 2014] Y. Chen, X. Li, C. Wiet and J. Wang. *Energy Management and Driving Strategy for In-Wheel Motor Electric Ground Vehicles With Terrain Profile Preview*. IEEE Transactions on Industrial Informatics, vol. 10, no. 3, pages 1938–1947, Aug 2014. (Cited on pages 65 and 82.)
- [Chen 2018] L. Chen, Y. Shan, W. Tian, B. Li and D. Cao. *A Fast and Efficient Double-tree RRT\*-like Sampling-based Planner Applying on Mobile Robotic Vehicles*. IEEE/ASME Transactions on Mechatronics, pages 1–1, 2018. (Cited on page 65.)
- [Cheng 2001] Peng Cheng, Zuojun Shen and S La Valle. *RRT-based trajectory design for autonomous automobiles and spacecraft*. Archives of control sciences, vol. 11, no. 3/4, pages 167–194, 2001. (Cited on page 33.)
- [Choset 1996] Howie M Choset and Joel Burdick. *Sensor based motion planning: The hierarchical generalized Voronoi graph*. PhD thesis, Citeseer, 1996. (Cited on page 33.)

- [Coutinho 2018] Walton Pereira Coutinho, Maria Battarra and Jörg Fliege. *The unmanned aerial vehicle routing and trajectory optimisation problem, a taxonomic review*. Computers & Industrial Engineering, vol. 120, pages 116–128, 2018. (Cited on page 30.)
- [Dahlquist 2003] Germund Dahlquist and A Björck. *Numerical methods, Mineola*, 2003. (Cited on page 35.)
- [Dasgupta 2011] Prithviraj Dasgupta. *Multi-robot task allocation for performing cooperative foraging tasks in an initially unknown environment*. In Innovations in Defence Support Systems-2, pages 5–20. Springer, 2011. (Cited on page 37.)
- [Deb 2001] Kalyanmoy Deb. *Multi-Objective Optimization Using Evolutionary Algorithms*. John Wiley & Sons. Inc., New York, NY, 2001. (Cited on page 89.)
- [Dextreit 2013] Clement Dextreit and Ilya V Kolmanovsky. *Game theory controller for hybrid electric vehicles*. IEEE Transactions on Control Systems Technology, vol. 22, no. 2, pages 652–663, 2013. (Cited on page 43.)
- [Diwekar 2008] Urmila Diwekar. Introduction to applied optimization, volume 22. Springer Science & Business Media, 2008. (Cited on page 38.)
- [Dizqah 2016] A. M. Dizqah, B. Lenzo, A. Sorniotti, P. Gruber, S. Fallah and J. De Smet. *A Fast and Parametric Torque Distribution Strategy for Four-Wheel-Drive Energy-Efficient Electric Vehicles*. IEEE Transactions on Industrial Electronics, vol. 63, no. 7, pages 4367–4376, July 2016. (Cited on page 82.)
- [Elbert 2014] P. Elbert, T. N̄<sub>4</sub>esch, A. Ritter, N. Murgovski and L. Guzzella. *EngineOn/OffControl for the Energy Management of a Serial Hybrid Electric Bus via Convex Optimization*. IEEE Transactions on Vehicular Technology, vol. 63, no. 8, pages 3549–3559, Oct 2014. (Cited on page 40.)
- [Fang 2011] Lincun Fang, Shiyin Qin, Gang Xu, Tianli Li and Kemin Zhu. *Simultaneous optimization for hybrid electric vehicle parameters based on multi-objective genetic algorithms*. Energies, vol. 4, no. 3, pages 532–544, 2011. (Cited on page 43.)
- [Farouki 1990] Rida T Farouki and Takis Sakkalis. *Pythagorean hodographs*. IBM Journal of Research and Development, vol. 34, no. 5, pages 736–752, 1990. (Cited on page 86.)
- [Fleming 2012] Wendell H Fleming and Raymond W Rishel. Deterministic and stochastic optimal control, volume 1. Springer Science & Business Media, 2012. (Cited on page 36.)

- [Frazzoli 2001] Emilio Frazzoli. *Robust hybrid control for autonomous vehicle motion planning*. PhD thesis, Massachusetts Institute of Technology, 2001. (Cited on page 33.)
- [Gao 2005] Wenzhong Gao and Sachin Kumar Porandla. *Design optimization of a parallel hybrid electric powertrain*. In 2005 IEEE Vehicle Power and Propulsion Conference, pages 6–pp. IEEE, 2005. (Cited on page 43.)
- [Gasparetto 2015] Alessandro Gasparetto, Paolo Boscarol, Albano Lanzutti and Renato Vidoni. *Path planning and trajectory planning algorithms: A general overview*. In Motion and operation planning of robotic systems, pages 3–27. Springer, 2015. (Cited on page 30.)
- [Gear 1971] C William Gear. Numerical initial value problems in ordinary differential equations. Prentice Hall PTR, 1971. (Cited on page 35.)
- [Gill 1981] Philip E Gill, Walter Murray and Margaret H Wright. *Practical optimization*. 1981. (Cited on page 36.)
- [Gong 2007] Qiuming Gong, Yaoyu Li and Zhong-Ren Peng. *Trip based power management of plug-in hybrid electric vehicle with two-scale dynamic programming*. In 2007 IEEE Vehicle Power and Propulsion Conference, pages 12–19. IEEE, 2007. (Cited on pages 40 and 42.)
- [Goto 2010] K. Goto, K. Kon and F. Matsuno. *Motion planning of an autonomous mobile robot considering regions with velocity constraint*. In 2010 IEEE/RSJ International Conference on Intelligent Robots and Systems, pages 3269–3274, Oct 2010. (Cited on page 65.)
- [Guo 2013] Tianyou Guo and Huei Peng. *A simplified skid-steering model for torque and power analysis of tracked small unmanned ground vehicles*. In 2013 American Control Conference, pages 1106–1111. IEEE, 2013. (Cited on pages 27 and 28.)
- [Haidegger 2012] Tamás Haidegger, Levente Kovács, Radu-Emil Precup, Balázs Benyó, Zoltán Benyó and Stefan Preitl. *Simulation and control for telerobots in space medicine*. Acta Astronautica, vol. 81, no. 1, pages 390–402, 2012. (Cited on page 19.)
- [Harrer 2017] Manfred Harrer and Peter Pfeffer. Steering handbook. Springer, 2017. (Cited on page 20.)
- [Hassan 2012] Mohd Khair Hassan, N Aziah, HMI Nizam, AG A Mutalib, Siti Fauziah Toha and BSKK Ibrahim. *A comparative study of power consumption of electric power steering system*. In 2012 IEEE International Conference on Power and Energy (PECon), pages 178–182. IEEE, 2012. (Cited on page 20.)
- [Hildebrand 2012] Francis B Hildebrand. Methods of applied mathematics. Courier Corporation, 2012. (Cited on page 36.)

- [Horst 2000] Reiner Horst, Panos M Pardalos and Nguyen Van Thoai. Introduction to global optimization. Springer Science & Business Media, 2000. (Cited on page 38.)
- [Hou 2014] Cong Hou, Minggao Ouyang, Liangfei Xu and Hewu Wang. *Approximate Pontryagin's minimum principle applied to the energy management of plug-in hybrid electric vehicles*. Applied Energy, vol. 115, pages 174–189, 2014. (Cited on page 42.)
- [Hou 2019] Linfei Hou, Liang Zhang and Jongwon Kim. *Energy Modeling and Power Measurement for Mobile Robots*. Energies, vol. 12, no. 1, page 27, 2019. (Cited on pages ix, 24 and 25.)
- [Hucho 1993] Wolf Hucho and Gino Sovran. *Aerodynamics of road vehicles*. Annual review of fluid mechanics, vol. 25, no. 1, pages 485–537, 1993. (Cited on page 20.)
- [Hull 2013] David G Hull. Optimal control theory for applications. Springer Science & Business Media, 2013. (Cited on page 36.)
- [Jakkula 2007] SK Jakkula, Y Shen and J Sokolowski. *Extraction of road network topology for transportation and GIS applications*. In MODSIM World Conference & Expo Virginia Beach, VA, 2007. (Cited on pages 54 and 85.)
- [Jang 1993] J-SR Jang. *ANFIS: adaptive-network-based fuzzy inference system*. IEEE transactions on systems, man, and cybernetics, vol. 23, no. 3, pages 665–685, 1993. (Cited on pages 51 and 53.)
- [Jazar 2017] Reza N Jazar. Vehicle dynamics: theory and application. Springer, 2017. (Cited on pages ix, 20, 22 and 47.)
- [Jeong 2011] Jongryeol Jeong, Daeheung Lee, Namwook Kim, Yeong-il Park and Suk Won Cha. *Fuel economy analysis of a parallel hybrid bus using the optimal control theory*. In 2011 IEEE Vehicle Power and Propulsion Conference, pages 1–5. IEEE, 2011. (Cited on page 42.)
- [Johri 2013] Rajit Johri, Wei Liang and Ryan McGee. *Hybrid electric vehicle energy management with battery thermal considerations using multi-rate dynamic programming*. In ASME 2013 Dynamic Systems and Control Conference, pages V001T05A003–V001T05A003. American Society of Mechanical Engineers, 2013. (Cited on page 42.)
- [Kavraki 1994] Lydia Kavraki, Petr Svestka and Mark H Overmars. Probabilistic roadmaps for path planning in high-dimensional configuration spaces, volume 1994. Unknown Publisher, 1994. (Cited on page 33.)



- [Kessels 2007] JTBA Kessels and PPJ van den Bosch. *Electronic horizon: Energy management using telematics information*. In 2007 IEEE Vehicle Power and Propulsion Conference, pages 581–586. IEEE, 2007. (Cited on page 40.)
- [Khamis 2011] Alaa M Khamis, Ahmed M Elmogy and Fakhri O Karray. *Complex task allocation in mobile surveillance systems*. Journal of Intelligent & Robotic Systems, vol. 64, no. 1, pages 33–55, 2011. (Cited on page 38.)
- [Khamis 2015] Alaa Khamis, Ahmed Hussein and Ahmed Elmogy. *Multi-robot task allocation: A review of the state-of-the-art*. In Cooperative Robots and Sensor Networks 2015, pages 31–51. Springer, 2015. (Cited on pages 37 and 38.)
- [Khatib 1985] Oussama Khatib. *Real-time obstacle avoidance for manipulators and mobile robots*. In Proceedings. 1985 IEEE International Conference on Robotics and Automation, volume 2, pages 500–505. IEEE, 1985. (Cited on page 33.)
- [Kim 2008] Chong Hui Kim and Byung Kook Kim. *Minimum-energy motion planning for differential-driven wheeled mobile robots*. In Motion Planning. IntechOpen, 2008. (Cited on page 20.)
- [Kim 2011] Namwook Kim, Suk Won Cha and Huei Peng. *Optimal equivalent fuel consumption for hybrid electric vehicles*. IEEE Transactions on Control Systems Technology, vol. 20, no. 3, pages 817–825, 2011. (Cited on page 42.)
- [Kolmanovsky 2008] Ilya V Kolmanovsky, L Lezhnev and Tatiana L Maizenberg. *Discrete-time drift counteraction stochastic optimal control: Theory and application-motivated examples*. Automatica, vol. 44, no. 1, pages 177–184, 2008. (Cited on page 43.)
- [Kuffner Jr 2000] James J Kuffner Jr and Steven M LaValle. *RRT-connect: An efficient approach to single-query path planning*. In ICRA, volume 2, 2000. (Cited on page 33.)
- [Kumar 2012] Suresh Nanda Kumar and Ramasamy Panneerselvam. *A survey on the vehicle routing problem and its variants*. Intelligent Information Management, vol. 4, no. 03, page 66, 2012. (Cited on page 36.)
- [Kumar 2014] P. Kumar, R. Merzouki, B. Conrard, V. Coelen and B. Ould Bouamama. *Multilevel Modeling of the Traffic Dynamic*. IEEE Transactions on Intelligent Transportation Systems, vol. 15, no. 3, pages 1066–1082, June 2014. (Cited on page 65.)

- [Kunchev 2006] Voemir Kunchev, Lakhmi Jain, Vladimir Ivancevic and Anthony Finn. *Path planning and obstacle avoidance for autonomous mobile robots: A review*. In International Conference on Knowledge-Based and Intelligent Information and Engineering Systems, pages 537–544. Springer, 2006. (Cited on page 30.)
- [Latombe 2012] Jean-Claude Latombe. Robot motion planning, volume 124. Springer Science & Business Media, 2012. (Cited on pages 30 and 33.)
- [LaValle 2001] Steven M LaValle and James J Kuffner Jr. *Randomized kinodynamic planning*. The international journal of robotics research, vol. 20, no. 5, pages 378–400, 2001. (Cited on page 33.)
- [LaValle 2006] Steven M LaValle. Planning algorithms. Cambridge university press, 2006. (Cited on page 73.)
- [Leitmann 2013] George Leitmann. The calculus of variations and optimal control: an introduction, volume 24. Springer Science & Business Media, 2013. (Cited on page 36.)
- [Lenagh 2013] William H Lenagh. Multi-robot task allocation: a spatial queuing approach. University of Nebraska at Omaha, 2013. (Cited on page 38.)
- [Li 2012] Weimin Li, Guoqing Xu and Yangsheng Xu. *Online learning control for hybrid electric vehicle*. Chinese Journal of Mechanical Engineering, vol. 25, no. 1, pages 98–106, 2012. (Cited on page 42.)
- [Liang 2009] Zhang Liang, Zhang Xin, Tian Yi and Zhang Xinn. *Intelligent energy management for parallel HEV based on driving cycle identification using SVM*. parameters, vol. 6, no. 5, page 4, 2009. (Cited on page 43.)
- [Lin 2003] Chan-Chiao Lin, Huei Peng, Jessy W Grizzle and Jun-Mo Kang. *Power management strategy for a parallel hybrid electric truck*. IEEE transactions on control systems technology, vol. 11, no. 6, pages 839–849, 2003. (Cited on page 40.)
- [Lin 2004] Chan-Chiao Lin, Huei Peng and JW Grizzle. *A stochastic control strategy for hybrid electric vehicles*. In Proceedings of the 2004 American control conference, volume 5, pages 4710–4715. IEEE, 2004. (Cited on page 42.)
- [Liu 2012] S. Liu and D. Sun. *Modeling and experimental study for minimization of energy consumption of a mobile robot*. In 2012 IEEE/ASME International Conference on Advanced Intelligent Mechatronics (AIM), pages 708–713, July 2012. (Cited on page 19.)

- [Liu 2013] Shuang Liu and Dong Sun. *Minimizing energy consumption of wheeled mobile robots via optimal motion planning*. IEEE/ASME Transactions on Mechatronics, vol. 19, no. 2, pages 401–411, 2013. (Cited on page 97.)
- [Liu 2017] W. Liu, A. Khajepour, H. He, H. Wang and Y. Huang. *Integrated torque vectoring control for a three-axle electric bus based on holistic cornering control method*. IEEE Transactions on Vehicular Technology, vol. PP, no. 99, pages 1–1, 2017. (Cited on page 82.)
- [Long 2012] VT Long and NV Nhan. *Bees-algorithm-based optimization of component size and control strategy parameters for parallel hybrid electric vehicles*. International journal of automotive technology, vol. 13, no. 7, pages 1177–1183, 2012. (Cited on page 43.)
- [Lu 2000] Bingwei Lu, Lily Jan and Yuh-Nung Jan. *Control of cell divisions in the nervous system: symmetry and asymmetry*. Annual review of neuroscience, vol. 23, no. 1, pages 531–556, 2000. (Cited on page 19.)
- [Lyshevski 1998] Sergey Edward Lyshevski and Charles Yokomoto. *Control of hybrid-electric vehicles*. In Proceedings of the 1998 American Control Conference. ACC (IEEE Cat. No. 98CH36207), volume 4, pages 2148–2149. IEEE, 1998. (Cited on page 40.)
- [Maclaurin 2008] Bruce Maclaurin. *Comparing the steering performances of skid-and Ackermann-steered vehicles*. Proceedings of the Institution of Mechanical Engineers, Part D: Journal of Automobile Engineering, vol. 222, no. 5, pages 739–756, 2008. (Cited on pages ix, 27 and 29.)
- [Martan 2008] Diego Martan, Bruno Caballero and Rodolfo Haber. *Optimal tuning of a networked linear controller using a multi-objective genetic algorithm. Application to a complex electromechanical process*. In 2008 3rd International Conference on Innovative Computing Information and Control, pages 91–91. IEEE, 2008. (Cited on page 19.)
- [Merzouki 2006] Rochdi Merzouki, B Ould Bouamama, Mohand Arab Djeziri and Mohamed Bouteldja. *Modelling and estimation for tire-road system using bond graph approach*. In 2006 IEEE/RSJ International Conference on Intelligent Robots and Systems, pages 3785–3790. IEEE, 2006. (Cited on page 20.)
- [Montazeri-Gh 2006] Morteza Montazeri-Gh, Amir Poursamad and Babak Ghalichi. *Application of genetic algorithm for optimization of control strategy in parallel hybrid electric vehicles*. Journal of the Franklin Institute, vol. 343, no. 4-5, pages 420–435, 2006. (Cited on page 43.)
- [Morales 2009] J. Morales, J. L. Martinez, A. Mandow, A. J. Garcia-Cerezo and S. Pedraza. *Power Consumption Modeling of Skid-Steer Tracked*

- Mobile Robots on Rigid Terrain*. IEEE Transactions on Robotics, vol. 25, no. 5, pages 1098–1108, Oct 2009. (Cited on pages 27 and 28.)
- [Morales 2010] J. Morales, J. L. Martinez, A. Mandow, A. Pequeno-Boyer and A. Garcia-Cerezo. *Simplified power consumption modeling and identification for wheeled skid-steer robotic vehicles on hard horizontal ground*. In 2010 IEEE/RSJ International Conference on Intelligent Robots and Systems, pages 4769–4774, Oct 2010. (Cited on pages 27 and 28.)
- [Ngo 2010] Dac Viet Ngo, Theo Hofman, Maarten Steinbuch and Alex FA Serrears. *An optimal control-based algorithm for hybrid electric vehicle using preview route information*. In Proceedings of the 2010 American Control Conference, pages 5818–5823. IEEE, 2010. (Cited on page 42.)
- [Nilsson 1984] Nils J Nilsson. *Shakey the robot*. Technical report, SRI INTERNATIONAL MENLO PARK CA, 1984. (Cited on page 33.)
- [Niu 2013] Ji Gao Niu, Feng Lai Pei, Su Zhou and Tong Zhang. *Multi-objective optimization study of energy management strategy for extended-range electric vehicle*. In Advanced Materials Research, volume 694, pages 2704–2709. Trans Tech Publ, 2013. (Cited on page 43.)
- [Noborio 1990] Hiroshi Noborio, Tomohide Naniwa and Suguru Arimoto. *A quadtree-based path-planning algorithm for a mobile robot*. Journal of Robotic Systems, vol. 7, no. 4, pages 555–574, 1990. (Cited on page 33.)
- [Oh 2007] Kyoungcheol Oh, Junhong Min, Donghoon Choi and Hyunsoo Kim. *Optimization of control strategy for a single-shaft parallel hybrid electric vehicle*. Proceedings of the Institution of Mechanical Engineers, Part D: Journal of Automobile Engineering, vol. 221, no. 5, pages 555–565, 2007. (Cited on page 43.)
- [Okt ] *Oktal website for SCANer studio*. <http://www.oktal.fr/en/>. (Cited on page 54.)
- [Olver 2010] Frank WJ Olver, Daniel W Lozier, Ronald F Boisvert and Charles W Clark. *Nist handbook of mathematical functions* hardback and cd-rom. Cambridge University Press, 2010. (Cited on page 69.)
- [Opila 2011] Daniel F Opila, Xiaoyong Wang, Ryan McGee, R Brent Gillespie, Jeffrey A Cook and Jessy W Grizzle. *An energy management controller to optimally trade off fuel economy and drivability for hybrid vehicles*. IEEE Transactions on Control Systems Technology, vol. 20, no. 6, pages 1490–1505, 2011. (Cited on page 42.)
- [Opila 2013] Daniel F Opila, Xiaoyong Wang, Ryan McGee and JW Grizzle. *Real-time implementation and hardware testing of a hybrid vehicle energy management controller based on stochastic dynamic programming*.

- Journal of dynamic systems, measurement, and control, vol. 135, no. 2, page 021002, 2013. (Cited on page 42.)
- [Ousingsawat 2004] Jarurat Ousingsawat and Mark E Campbell. *Multiple vehicle team tasking for cooperative estimation*. In American Control Conference, 2004. (Cited on page 36.)
- [Ozatay 2014] E. Ozatay, S. Onori, J. Wollaeger, U. Ozguner, G. Rizzoni, D. Filev, J. Michelini and S. Di Cairano. *Cloud-Based Velocity Profile Optimization for Everyday Driving: A Dynamic-Programming-Based Solution*. IEEE Transactions on Intelligent Transportation Systems, vol. 15, no. 6, pages 2491–2505, Dec 2014. (Cited on page 82.)
- [Pacejka 2005] Hans Pacejka. *Tire and vehicle dynamics*. Elsevier, 2005. (Cited on page 49.)
- [Parasuraman 2014] R. Parasuraman, K. Kershaw, P. Pagala and M. Ferre. *Model Based On-Line Energy Prediction System for Semi-autonomous Mobile Robots*. In 2014 5th International Conference on Intelligent Systems, Modelling and Simulation, pages 411–416, Jan 2014. (Cited on pages ix and 27.)
- [Pérez 2010] LV Pérez and GO García. *State constrained optimal control applied to supervisory control in HEVs*. Oil & Gas Science and Technology—Revue de l’Institut Français du Pétrole, vol. 65, no. 1, pages 191–201, 2010. (Cited on page 43.)
- [Quaglia 2016] Davide Quaglia and Riccardo Muradore. *Communication-aware bandwidth-optimized predictive control of motor drives in electric vehicles*. IEEE Transactions on Industrial Electronics, vol. 63, no. 9, pages 5602–5611, 2016. (Cited on page 82.)
- [Rao 2014] Anil V Rao. *Trajectory optimization: a survey*. In Optimization and optimal control in automotive systems, pages 3–21. Springer, 2014. (Cited on page 36.)
- [Razavian 2012] Reza Razavian, Nasser L Azad and John McPhee. *On real-time optimal control of a series hybrid electric vehicle with an ultra-capacitor*. In 2012 American Control Conference (ACC), pages 547–552. IEEE, 2012. (Cited on page 42.)
- [Reif 1994] John Reif, John Reif and Micha Sharir. *Motion planning in the presence of moving obstacles*. Journal of the ACM (JACM), vol. 41, no. 4, pages 764–790, 1994. (Cited on page 30.)
- [Salman 2005] Mutasim Salman, Man-Feng Chang and Jyh-Shin Chen. *Predictive energy management strategies for hybrid vehicles*. In 2005 IEEE Vehicle Power and Propulsion Conference, pages 21–25. IEEE, 2005. (Cited on page 40.)

- [Samet 1988] Hanan Samet. *An overview of quadtrees, octrees, and related hierarchical data structures*. In Theoretical Foundations of Computer Graphics and CAD, pages 51–68. Springer, 1988. (Cited on page 33.)
- [Sampathnarayanan 2014] Balaji Sampathnarayanan, Simona Onori and Stephen Yurkovich. *An optimal regulation strategy with disturbance rejection for energy management of hybrid electric vehicles*. *Automatica*, vol. 50, no. 1, pages 128–140, 2014. (Cited on page 43.)
- [Schwartz 1983] Jacob T Schwartz and Micha Sharir. *On the  $\hat{a}$ piano movers’ $\hat{a}$  problem I. The case of a two-dimensional rigid polygonal body moving amidst polygonal barriers*. *Communications on pure and applied mathematics*, vol. 36, no. 3, pages 345–398, 1983. (Cited on page 33.)
- [Shah 2010] MA Shah and N Aouf. *3d cooperative pythagorean hodograph path planning and obstacle avoidance for multiple uavs*. In Cybernetic Intelligent Systems (CIS), 2010 IEEE 9th International Conference on, pages 1–6. IEEE, 2010. (Cited on page 86.)
- [Shamah 1999] Benjamin Shamah. *Experimental Comparison of Skid Steering vs. Explicit Steering for Wheeled Mobile Robot*, M. Sc. 1999. (Cited on pages ix, 24, 26 and 27.)
- [Shanmugavel 2007] Madhavan Shanmugavel, Antonios Tsourdos, Rafal Zbikowski and Brian White. *3D path planning for multiple UAVs using Pythagorean hodograph curves*. In AIAA Guidance, navigation and control conference and exhibit, page 6455, 2007. (Cited on page 86.)
- [Sherali 2006] Hanif D Sherali and CM Shetty. *Nonlinear programming: Theory and algorithms*. Wiley-Interscience, 2006. (Cited on pages 35 and 36.)
- [Shuaiyu 2007] Wang Shuaiyu, Huang Kaisheng, Jin Zhenhua and Peng Yuanyuan. *Parameter optimization of control strategy for parallel hybrid electric vehicle*. In 2007 2nd IEEE Conference on Industrial Electronics and Applications, pages 2010–2012. IEEE, 2007. (Cited on page 43.)
- [Siegwart 2011] Roland Siegwart, Illah Reza Nourbakhsh, Davide Scaramuzza and Ronald C Arkin. *Introduction to autonomous mobile robots*. MIT press, 2011. (Cited on pages 14 and 16.)
- [Sleumer 1999] Nora Sleumer and Nadine Tschichold-Gürmann. *Exact cell decomposition of arrangements used for path planning in robotics*. Technical report/ETH Zürich, Department of Computer Science, vol. 329, 1999. (Cited on page 33.)
- [Spall 2012] James C Spall. *Stochastic optimization*. In Handbook of computational statistics, pages 173–201. Springer, 2012. (Cited on page 38.)

- [Sundström 2010] Olle Sundström, Daniel Ambühl and Lino Guzzella. *On implementation of dynamic programming for optimal control problems with final state constraints*. Oil & Gas Science and Technology—Revue de l’Institut Français du Pétrole, vol. 65, no. 1, pages 91–102, 2010. (Cited on page 42.)
- [Takeda 2011] Kazuya Takeda, John HL Hansen, Pinar Boyraz, Lucas Malta, Chiyomi Miyajima and Hüseyin Abut. *International large-scale vehicle corpora for research on driver behavior on the road*. IEEE Transactions on Intelligent Transportation Systems, vol. 12, no. 4, pages 1609–1623, 2011. (Cited on pages ix and 23.)
- [Thibault 2018] Laurent Thibault, Giovanni De Nunzio and Antonio Sciarretta. *A Unified Approach for Electric Vehicles Range Maximization via Eco-Routing, Eco-Driving, and Energy Consumption Prediction*. IEEE Transactions on Intelligent Vehicles, vol. 3, no. 4, pages 463–475, 2018. (Cited on page 43.)
- [Tokekar 2011] Pratap Tokekar, Nikhil Karnad and Volkan Isler. *Energy-optimal velocity profiles for car-like robots*. In 2011 IEEE International Conference on Robotics and Automation, pages 1457–1462. IEEE, 2011. (Cited on pages 27 and 28.)
- [Tseng 2008] Chyuan-Yow Tseng, Yi-Hsuan Hung, Chien-Hsiung Tsai and Yu-Jen Huang. *Parameters optimization for the energy management system of hybrid electric vehicle*. In ICMIT 2007: Mechatronics, MEMS, and Smart Materials, volume 6794, page 67940I. International Society for Optics and Photonics, 2008. (Cited on page 43.)
- [Vantsevich 2007] Vladimir V Vantsevich. *Multi-wheel drive vehicle energy/fuel efficiency and traction performance: objective function analysis*. Journal of Terramechanics, vol. 44, no. 3, pages 239–253, 2007. (Cited on page 20.)
- [Verstraten 2016] Tom Verstraten, Raphael Furnémont, Glenn Mathijssen, Bram Vanderborght and Dirk Lefeber. *Energy consumption of geared DC motors in dynamic applications: Comparing modeling approaches*. IEEE Robotics and Automation Letters, vol. 1, no. 1, pages 524–530, 2016. (Cited on page 19.)
- [Vintner 2000] R Vintner. *Optimal Control (Systems & Control: Foundations and Applications)*, 2000. (Cited on page 36.)
- [Vrkalovic 2017] Sasa Vrkalovic, Teodor-Adrian Teban and Ioan-Daniel Borlea. *Stable Takagi-Sugeno fuzzy control designed by optimization*. Int. J. Artif. Intell, vol. 15, no. 2, pages 17–29, 2017. (Cited on page 19.)

- [Wang 2007] Zhancheng Wang, Bufu Huang, Yangsheng Xu and Weimin Li. *Optimization of series hybrid electric vehicle operational parameters by simulated annealing algorithm*. In 2007 IEEE international conference on control and automation, pages 1536–1541. IEEE, 2007. (Cited on page 43.)
- [Wang 2009] Junmin Wang and Raul G Longoria. *Coordinated and reconfigurable vehicle dynamics control*. IEEE Transactions on Control Systems Technology, vol. 17, no. 3, pages 723–732, 2009. (Cited on page 47.)
- [Wang 2012] Lei Wang, Yong Zhang, Chengliang Yin, Hu Zhang and Cunlei Wang. *Hardware-in-the-loop simulation for the design and verification of the control system of a series-parallel hybrid electric city-bus*. Simulation Modelling Practice and Theory, vol. 25, pages 148–162, 2012. (Cited on page 42.)
- [Wang 2014] Weida Wang, Lijin Han, Changle Xiang, Yue Ma and Hui Liu. *Synthetical efficiency-based optimization for the power distribution of power-split hybrid electric vehicles*. Chinese Journal of Mechanical Engineering, vol. 27, no. 1, pages 58–68, 2014. (Cited on page 43.)
- [West 2001] Douglas Brent West *et al.* Introduction to graph theory, volume 2. Prentice hall Upper Saddle River, 2001. (Cited on pages 69 and 91.)
- [Wu 2008] Jian Wu, C-H Zhang and N-X Cui. *PSO algorithm-based parameter optimization for HEV powertrain and its control strategy*. International Journal of Automotive Technology, vol. 9, no. 1, pages 53–59, 2008. (Cited on page 43.)
- [Wu 2011] Lianghong Wu, Yaonan Wang, Xiaofang Yuan and Zhenlong Chen. *Multiobjective optimization of HEV fuel economy and emissions using the self-adaptive differential evolution algorithm*. IEEE Transactions on vehicular technology, vol. 60, no. 6, pages 2458–2470, 2011. (Cited on page 43.)
- [Wu 2014a] Guoyuan Wu, Kanok Boriboonsomsin and Matthew J Barth. *Development and evaluation of an intelligent energy-management strategy for plug-in hybrid electric vehicles*. IEEE Transactions on Intelligent Transportation Systems, vol. 15, no. 3, pages 1091–1100, 2014. (Cited on pages 40 and 43.)
- [Wu 2014b] Xiaolan Wu, Guifang Guo, Jun Xu and Binggang Cao. *Application of parallel chaos optimization algorithm for plug-in hybrid electric vehicle design*. International Journal of Bifurcation and Chaos, vol. 24, no. 01, page 1450001, 2014. (Cited on page 43.)



- [Xiao 2014] Xuesu Xiao and William (Red) L. Whittaker. *Energy Considerations for Wheeled Mobile Robots Operating on a Single Battery Discharge*. Technical report CMU-RI-TR-14-16, Carnegie Mellon University, Pittsburgh, PA, August 2014. (Cited on pages ix, 20, 21, 22 and 24.)
- [Xiong 2009] Weiwei Xiong, Chengliang Yin, Yong Zhang and Jianlong Zhang. *Series-parallel hybrid vehicle control strategy design and optimization using real-valued genetic algorithm*. CHINESE JOURNAL OF MECHANICAL ENGINEERING-ENGLISH EDITION-, vol. 22, no. 6, pages 862–868, 2009. (Cited on page 43.)
- [Xu 2016] Wenjun Xu, Huan Liu, Jiayi Liu, Zude Zhou and Duc Truong Pham. *A practical energy modeling method for industrial robots in manufacturing*. In Monterey Workshop, pages 25–36. Springer, 2016. (Cited on page 19.)
- [Younis 2011] Adel Younis, Leon Zhou and Zuomin Dong. *Application of the new SEUMRE global optimisation tool in high efficiency EV/PHEV/EREV electric mode operations*. International Journal of Electric and Hybrid Vehicles, vol. 3, no. 2, pages 176–190, 2011. (Cited on page 43.)
- [Yu 2009] Yuan-bin Yu, Qing-nian Wang, Yong-jiu Chen, Chang-jian Hu and Bo-shi Wang. *Control strategy optimization research using Dynamic Programming method for Synergic Electric System on HEV*. In 2009 IEEE Intelligent Vehicles Symposium, pages 770–774. IEEE, 2009. (Cited on page 42.)
- [Yu 2010] Wei Yu, Oscar Ylaya Chuy Jr, Emmanuel G Collins Jr and Patrick Hollis. *Analysis and experimental verification for dynamic modeling of a skid-steered wheeled vehicle*. IEEE transactions on robotics, vol. 26, no. 2, pages 340–353, 2010. (Cited on pages 26 and 28.)
- [Zhang 2001] Rongjun Zhang and Yaobin Chen. *Control of hybrid dynamical systems for electric vehicles*. In Proceedings of the 2001 American Control Conference.(Cat. No. 01CH37148), volume 4, pages 2884–2889. IEEE, 2001. (Cited on pages 40 and 43.)
- [Zhang 2009] Lipeng Zhang, Cheng Lin and Xiang Niu. *Optimization of control strategy for plug-in hybrid electric vehicle based on differential evolution algorithm*. In 2009 Asia-Pacific Power and Energy Engineering Conference, pages 1–5. IEEE, 2009. (Cited on page 43.)
- [Zhang 2010] C. Zhang, A. Vahidi, P. Pisu, X. Li and K. Tennant. *Role of Terrain Preview in Energy Management of Hybrid Electric Vehicles*. IEEE Transactions on Vehicular Technology, vol. 59, no. 3, pages 1139–1147, March 2010. (Cited on page 82.)

- [Zhang 2014] Yi Zhang, Heping Liu and Qiang Guo. *Varying-domain optimal management strategy for parallel hybrid electric vehicles*. IEEE Transactions on Vehicular Technology, vol. 63, no. 2, pages 603–616, 2014. (Cited on page 43.)
- [Zhang 2015] Pei Zhang, Fuwu Yan and Changqing Du. *A comprehensive analysis of energy management strategies for hybrid electric vehicles based on bibliometrics*. Renewable and Sustainable Energy Reviews, vol. 48, pages 88–104, 2015. (Cited on pages ix, 40 and 41.)
- [Zhang 2017] C. Zhang, S. Zhang, G. Han and H. Liu. *Power Management Comparison for a Dual-Motor-Propulsion System Used in a Battery Electric Bus*. IEEE Transactions on Industrial Electronics, vol. 64, no. 5, pages 3873–3882, May 2017. (Cited on page 82.)
- [Zhu 1990] D Zhu and J-C Latombe. *Constraint reformulation in a hierarchical path planner*. In Proceedings., IEEE International Conference on Robotics and Automation, pages 1918–1923. IEEE, 1990. (Cited on page 33.)
- [Zirour 2008] Mourad Zirour. *Vehicle routing problem: models and solutions*. Journal of Quality Measurement and Analysis JQMA, vol. 4, no. 1, pages 205–218, 2008. (Cited on page 36.)

# Vers une Stratégie de Planification Énergétique pour la Conduite Autonome d'un Véhicule Routier Sur-actionné

## Résumé

Dans cette thèse, une planification énergétique pour les véhicules routiers sans conducteur (URV), suractionnés avec une direction redondante est proposée. En effet, des indicateurs sur la géométrie de la route, la redondance des actionnements, le profil de la vitesse optimale et le mode de conduite sont identifiés pour chaque segment de la trajectoire de l'URV. Ainsi, un modèle d'estimation de la consommation d'énergie d'un URV sur-actionné est développé. Deux méthodes de modélisation de la consommation d'énergie sont considérées. La première méthode est basée sur un modèle analytique de consommation d'énergie prenant en compte le degré de steerabilité, le degré de mobilité et le degré de redondance dans l'actionnement. La deuxième méthode utilisée pour la modélisation de la consommation d'énergie repose sur la méthode qualitative d'apprentissage des données, à savoir: le système d'inférence neuro-floue adaptatif (ANFIS). Cette dernière a été considérée pour répondre à la présence des incertitudes paramétriques de l'URV et aux incertitudes sur son interaction avec l'environnement. La validation de l'estimation de la consommation énergétique a été appliquée à un véhicule autonome réel appelé RobuCar. La stratégie de la planification énergétique a été élaborée selon deux approches: discrète et continue. L'approche discrète repose sur la construction d'un digraphe d'énergie avec toutes les configurations possibles, tenant compte des contraintes cinématiques et dynamiques basées sur une grille 3D, selon: la vitesse, la longueur de l'arc, le mode de conduite. Dans ce graphe orienté et pondéré, les arêtes décrivent l'énergie consommée par l'URV le long d'un segment de la trajectoire. Un algorithme d'optimisation est appliqué sur le digraphe pour obtenir une solution globale optimale combinant le mode de conduite, la consommation électrique et le profil de vitesse de l'URV. L'approche continue repose sur une stratégie d'optimisation multicritères utilisant des algorithmes génétiques (NSGA-II). Ensuite, un chemin réel est considéré et modélisé, en utilisant deux types de courbes constituée d'un ensemble de géométries lisses: la première est lignes, clothoïdes et arcs, et la seconde regroupe des lignes et courbes de Hodograph de Pythagore. La stratégie de planification énergétique est ensuite appliquée aux chemins générés. En outre, un graph orienté est construit pour synthétiser le profil de vitesse optimale qui minimise la consommation énergétique globale tout en prenant en compte tous les modes de conduite. Les résultats sont comparés à ceux donnés par la méthode de programmation dynamique pour une optimisation globale hors ligne.

**Mots clés:** Panification énergétique, Consommation d'énergie, Redondance, Sur-actionné, Conduite autonome.

---

# Towards an Energy Planning Strategy for Autonomous Driving of an Over-actuated Road Vehicle

## Abstract

In this thesis, an energy planning for over-actuated unmanned road vehicles (URVs) with redundant steering configurations is proposed. In fact, indicators on the road profile geometry, the redundancy of actuation, the optimal velocity profile and the driving modes are identified for each segment of the URV's trajectory. Thus, a power consumption estimation model of an over-actuated autonomous driving vehicle is developed. Two methods for power consumption modeling are considered. The first method is based on an analytic model of power consumption, taking into account the degree of steerability, the degree of mobility and the degree of actuation redundancy. The second method used for power consumption modeling is based on data-learning qualitative method, namely: Adaptive Neuro Fuzzy Inference System (ANFIS). The latter has been considered in case of the presence of unknown dynamic parameters of the URV and uncertainties of interaction with the environment. Validation of the estimation of the power consumption has been applied on a real autonomous vehicle called RobuCar. Energy planning strategy has been built using two approaches, discrete and continuous. The discrete approach depends on the construction of an energy digraph with all feasible configurations taking into account kinematic and dynamic constraints based on a 3D grid map setup, according to the velocity, the arc-length, and the driving mode. In this weighted directed graph, the edges describe the consumed energy by the URV along a segment of a trajectory. An optimization algorithm is applied on the digraph to get a global optimal solution combining the driving mode, the power consumption and the velocity profile of the URV. The continuous approach is based on a multi-criteria optimization strategy using genetic algorithms (NSGA-II). Then a real road path is considered and modelled by using two smooth geometrical combinations: the first one uses lines, clothoids and arcs, and the second one uses lines and Pythagorean Hodograph (PH) curves. The energy planning strategy is then applied to the generated paths. Also, a directed graph is built to synthesis the optimal velocity profile that minimizes the overall energy consumption while accounting for all driving modes. Results are compared with those given by the dynamic programming method for global offline optimization.

**Keywords:** Energy Planning, Power consumption, Redundancy, Over-actuated, Autonomous driving.

---